Universidade de São Paulo
Instituto de Física

Modelo duplo quântico de grupo

Marzia Petrucci

Orientador: Prof. Dr. Paulo Teotônio Sobrinho

Tese de doutorado apresentada ao Instituto de Física da Universidade de São Paulo, como requisito parcial para a obtenção do título de Doutora em Ciências.

Banca Examinadora:
Prof. Dr. Paulo Teotônio Sobrinho - Orientador (IFUSP)
Prof. Dr. João C. A. Barata (IFUSP)
Prof. Dr. Hugo Luiz Mariano (IME-USP)
Prof. Dr. Eliezer Batista (UFSC)
Prof. Dr. Valdecir Marvulle (UFABC)

São Paulo
2020

FICHA CATALOGRÁFICA
Preparada pelo Serviço de Biblioteca e Informação
do Instituto de Física da Universidade de São Paulo

Petrucci, Marzia

Modelo duplo quântico de grupo / Group quantum double model. São Paulo, 2020.

Tese (Doutorado) – Universidade de São Paulo. Instituto de Física. Depto. de Física Matemática.

Orientador: Prof. Dr. Paulo Teotônio Sobrinho
Área de Concentração: Física

Unitermos: 1.Ordem topológico; 2. Teoria de gauge; 3. Álgebra de Hopf; 4. Hopf group coálgebra.

USP/IF/SBI-061/2020

University of São Paulo
Physics Institute

Group Quantum Double Model

Marzia Petrucci

Supervisor: Prof. Dr. Paulo Teotônio Sobrinho

Thesis submitted to the Physics Institute of the University of São Paulo in partial fulfillment of the requirements for the degree of Doctor of Science.

Examining Committee:
Prof. Dr. Paulo Teotônio Sobrinho - Supervisor (IFUSP)
Prof. Dr. João C. A. Barata (IFUSP)
Prof. Dr. Hugo Luiz Mariano (IME-USP)
Prof. Dr. Eliezer Batista (UFSC)
Prof. Dr. Valdecir Marvulle (UFABC)

São Paulo
2020

…My apologies to great questions for small answers. …

Under One Small Star, Wislawa Szymborska

Acknowledgment

I would like to thank my supervisor for the possibility to engage in this path, for the patient presence and professional assistance. I deeply enjoyed the journey. Journey worth pursuing even more for the companions I met in my research group, especially Pablo.

I am grateful to Stuart, Ciça, Carlos, Kris and Jenifer for assistance in my inner work.

I owe to the love found here in Brazil: Marcinha and Roba, Renata and Ananda, Cata, as Gumietes, Marcos, Rubens. To the strong family that made this possible. And finally to my chosen family, my friends spread all over. All of you make my life truly rich and prosperous.

I dedicate this work to Rossella: *"Domani é un altro giorno."*

This study was financed in part by the Coordenação de Aperfeiçoamento de Pessoal de Nível Superior - Brasil (CAPES) -Finance Code 001. I would like to thank the CPG and FISMAT secretary, all the caretakers and workers at USP.

Abstract

This thesis introduces a generalization of the Quantum Double Model (QDM) using an algebraic structure called Hopf group coalgebra. We called the new class of models Group Quantum Double Model (G-QDM).

The QDM is an exactly solvable model realized on a 2D lattice, made by discretizing an oriented surface. The Hilbert space expresses a quantum many body system, with independent degrees of freedom associated to the links of the lattice. The dynamics, given by a Hamiltonian, is constructed from operators acting on first neighbors. One important quantity of the QDM is the ground state degeneracy (GSD), which depends on the topology of the surface. In other words, for the QDM the GSD is a topological quantum invariant. We show a new proof of the invariant using a new diagrammatic formalism.

In the G-QDM we generalize the theory by adding to the links of the lattice non-dynamical elements of a finite group G. This is interpreted as an external gauge field defined on the surface. Contrary to the QDM, the GSD of the G-QDM depends on more data than the topology of the surface. In this case the GSD is sensible to the external gauge field applied to the lattice. Therefore GSD is no longer a topological invariant of the surface.

In the present work we achieved to show that the GSD in the G-QDM is invariant under local transformations of the external gauge field and under diffeomorphisms of the surface. We calculate the numerical invariant for specific examples.

Keywords: topological order; gauge theory; Hopf algebra; Hopf group coalgebra

Resumo

A tese introduz uma generalização do Modelo Duplo Quântico (QDM) utilizando uma estrutura algébrica chamada de Hopf group coálgebra. A nova classe de modelos é chamada de Modelo de Duplo Quântico de Grupo (G-QDM).

O modelo QDM é um modelo exatamente solúvel realizado sobre uma rede 2D, obtida discretizando uma superfície orientada. O espaço de Hilbert é expresso por um sistema à muitos corpos, com grãus de liberdade associados às arestas da rede. A dinâmica, dada por um Hamiltoniano local, é construída por operadores agindo sobre primeiros vizinhos. Uma quantidade importante do QDM é a degenerescência do estado fundamental (GSD), que depende da topologia da superfície. Em outras palavras, para o QDM a GSD é um invariante quântico topológico. Mostramos uma nova prova do invariante introduzindo um novo formalismo com diagramas.

No G-QDM generalizamos a teoria acrescentando elementos de um grupo finito G às arestas da rede. Isso pode ser interpretado como um campo de gauge externo definido sobre a rede. Ao contrario do QDM, o GSD do G-QDM depende de mais informação que só da topologia da superfície. Nsse caso o GSD é sensível ao campo de gauge externo aplicado na rede. Consequentemente o GSD não é mais um invariante topológico da superfície.

No presente trabalho conseguimos demonstrar que o GSD é invariante por transformações locais do campo externo e por difeomorfismos da superfície. Calculamos o invariante numérico em exemplos específicos.

Palavras-chaves: ordem topológico; teoria de gauge; álgebra de Hopf; Hopf group coálgebra

Contents

1 Introduction 1

1.1 Further achievements 6

2 The Invariant K_H 7

3 Preliminaries: QDM 11

3.1 The Manifold 12

3.2 Hopf Algebra 14

3.2.1 Tensors 14

3.3 Hopf Algebra with Kuperberg diagrams 16

3.3.1 Algebra 16

3.3.2 Coalgebra 17

3.3.3 Bialgebra 18

3.3.4 Hopf Algebra 19

3.3.5 Group Algebra 21

3.4 Quantum Double Model Reviewed 23

3.4.1 The Operators 24

3.4.2 Kuperberg Diagram for QDM 26

3.4.3 Orientation 35

3.4.4 Ground State 35

3.4.5 Projector Operator 36

3.4.6 Curves Diagrams 37

3.4.7 Transformation of the Tensor Network 42

4 Group Quantum Double Model 51

4.1 Hopf G-Coalgebra 51

4.1.1 Algebra 52

4.1.2 Homormophism between Algebras 53

4.1.3 Compatibility Axioms 54

4.1.4 Antipode 54

4.1.5 Integrals 55

4.1.6 Hopf Algebra 58

4.2 Hamiltonian Model 58
4.2.1 Vertex Operator A_v 59
4.2.2 Plaquette Operator B_p 62
4.2.3 Unitary Equivalence 65
4.2.4 Curves Diagrams with External Gauge Parameter 66
4.3 Gauge Transformation in the Parameters 67
4.4 Transformation of the Tensor Network with the External Gauge Parameter 68
4.4.1 Flip Move 69
4.4.2 Subdivision Move 72
4.4.3 Cancellation Move 73
4.5 Example 78

5 Conclusions 87
5.1 Publications 88

1 Introduction

In the recent years in the field of condensed matter we have discovered new phenomena which cannot be understood by Landau's theory for the classification of phases of matter. Landau's classification differentiates between phases characterized in the disposition of its elements by invariance under translation and under rotation. The two transformations can be linked to a symmetry group. The characterization of the phase only needs a local order parameter. A phase transition breaks the symmetry to reach a new phase of matter [1, 2]. Yet this classification following Landau's theory of symmetry breaking with local order parameters does not cover all possibilities.

In the 1980s Thouless and Haldane developed theoretical methods to describe phases of matter with topological concepts. In 1982 Thouless and collaborators explained the quantization of the quantum Hall conductance in 2 dimensional electron gases involving topology [4]. A class of new phenomena can be interpreted by quantum field theory depending on the topology [3]. The new phenomena were classified as topological states of matter [5]. Witten introduced a QFT depending only on the topology of the 3D-manifold underneath, where the partition function of the theory is a topological invariant [7, 8]. This new perspective led to the study of many other quantum invariants (of knots and 3D-manifolds) [9, 10, 11, 12, 13].

The existence of topological states of matter fueled researches in many directions, for example: materials for quantum computation, quantum devices. In this effort topological properties are helpful in the implementation of quantum memory robust to local perturbations as they encode the q-bit within global features of the material. An example of this approach is *topological order*, where we can differentiate between different ground states only with global operators [14, 15, 16, 17, 18].

What is Topological Order? What does characterize this new type of classification of matter? Few properties are common to this class of new phenomena. Generally the scientific community agrees that indicators are: the presence of a gap between the ground state and the excited states, quasi-particles with fractional statistic and the degeneracy of the ground state, robust to perturbations [14, 19, 20].

To gain a better perspective on the subject it is certainly a good start to build models with the characteristics listed above and understand what are the implications. This study is related to the areas of quantum groups and quantum invariants, of low dimensional topology and gauge theory on the lattice. We will introduce a family of such models generalizing the ideas of Alexei Kitaev on the *Quantum Double Model*

(QDM) [21, 22].

The QDM is an exactly solvable model which presents topological order and non-Abelian anyons. The later are quasi-particles excitations of fractional statistic at low energies [23, 24]. The QDM is a quantum system of spins (generalized spins) built on a 2D lattice. The lattice Σ we consider is a discretization of a compact surface Λ. The discretization is a triangular lattice (sometimes we will refer to a squared one for toric surfaces).

We illustrate the most simple example of topologically ordered theories: the *toric code*. It is a QDM with a $\mathbb{Z}_2$ degree of freedom associated to each link of a 2D squared lattice Σ. The lattice discretizes a torus T.

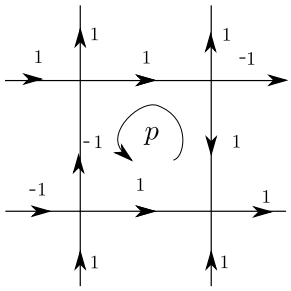

Figure 1.1: A configuration for the toric code on a squared lattice.

Let us define a state $|\psi\rangle$ of the toric code as a map which associates an element of $\mathbb{Z}_2$ to every link, $\psi : \Sigma \to \mathbb{Z}_2$. Note that $|\psi\rangle$ can be thought of as a gauge $\mathbb{Z}_2$ connection on the lattice. Two states are gauge equivalent if along each loop the product is the same. In that case the states can be obtained from each other by gauge transformations. An elementary gauge transformation is associated to each vertex v; its operator A_v acts on the links around the vertex. It create a superposition of states normalized: it copies the original and adds one state with the links in v flipped. We can define the holonomy of a plaquette p as the product along the edges of its boundary. The plaquette operator B_p acts on the links around a plaquette and annihilates the states whose holonomy is not the identity. The two operators commute between each other and are projectors. The Hamiltonian is

$$\mathbb{H} = -\sum_v A_v - \sum_p B_p$$

We say that a state $|\psi\rangle$ has trivial holonomy if all plaquettes have holonomy 1. States with trivial holonomy are ground states. However there can be multiple states with the minimum energy. We can project to the ground states space with a projector operator. The projector operator is $P_0 = \prod_v A_v \prod_p B_p$. Its trace is the dimension of the subspace, it is the degeneracy of the model.

The degeneracy depends on the topology of the surface and on the group $\mathbb{Z}_2$. Its states are different phases, which differ for global features: configurations which can present non-contractible loops. One can prove that the trace of P_0 calculates the number of homomorphisms $\pi_1(T) \to \mathbb{Z}_2$. The same result holds in the QDM where $\mathbb{Z}_2$ is generalized by a finite involutory Hopf algebra [25].

In the thesis we start presenting the QDM. As a warm up exercise we show that its ground state degeneracy is a topological invariant. We do so by using a method that will be adapted to treat the G-QDM. In these paragraphs we explain the steps followed in the thesis.

In Chapter 2 we explain the invariant used in the G-QDM. In the G-QDM we add another label to every link of the lattice with elements of a group G, this labeling fixes a G-connection. It can be considered as an external gauge field that is coloring the lattice. For loops in the dual lattice the product of the G-labels along the curve is called monodromy. We have a compatibility condition imposing that colors around a vertex when multiplied are equal to the trivial element. This condition implies a flatness conditions for the parallel transport of the G-connection. However the condition is applied locally, while non-contractible loops can have different values as monodromy. We have lattices whose colorings define the same monodromy and, consequently, are in the same equivalence class. The invariant is equal to the ground state degeneracy of the model defined by the G-labels. It is invariant under local changes of the G-connections, which do not change the monodromy.

In Chapter 3 we present in a pedagogical way all the ingredients for the construction of the invariant for the QDM. This invariant was originally introduced by Kuperberg as a topological invariant of 3D-manifold [26, 27, 28]. The proof of the topological invariance involves a tensor network that involves the Hopf algebra maps related to the operators in the Hamiltonian and the geometrical information of the lattice [29, 30, 31, 32]. The tensor network is an operator projecting to the ground state subspace. The trace of the operator is computed by contracting the input arrows of the tensor network with the output ones. This operation is adding a circle S^1 to the topology of the tensor network. This implies that the degeneracy of the model built over Σ is equal to the Kuperberg invariant of $\Sigma \times S^1$.

Let us describe in more detail the QDM, its lattice and algebra content. We discretize a closed surface into a simplicial complex, thus the faces of the lattice are triangles. In section 3.1 we explain more about simplicial complexes. In some cases we will use instead a squared lattice, since this is more frequent in the literature (the toric code was built on a squared lattice) and, due to its symmetry, it is easier to visualize. We describe a lattice state model with independent degrees of freedom on the links. In the QDM the states of each link l are elements of a finite Hopf algebra A. This defines the local Hilbert space $\mathcal{H}_l$. The Hilbert space is then the tensor product over all the links $\mathcal{H} = \otimes_l \mathcal{H}_l$. The maps for the Hopf algebra are presented in a diagrammatic way,

known as Kuperberg diagram, in 3.3. The local operators for the Hamiltonian $\mathbb{H}$ are expressed as tensor networks of the maps in the Kuperberg diagrams formalism, this is explained in section 3.4.1. They are the plaquette operator B_p, which affects only the links around the plaquette p. And the vertex operator A_v, which acts non-trivially on the links around the vertex v (and is therefore sometimes called star operator). We further justify the operator representations with the Hopf algebra maps. We proceed by steps showing them first in the case that A is a group algebra. The Hamiltonian is of the form

$$\mathbb{H} = -\sum_v A_v - \sum_p B_p.$$

Both A_v and B_p commute with each other and squared are equal to themselves, in other words they are projector operators.

We can see how to construct the tensor network associated to the ground state projector $P_0 = \prod_v A_v \prod_p B_p$, as shown in section 3.4.5. The degeneracy of the ground state is equal to the trace of the projector, which is

$$tr(P_0) = GSD.$$

To handle the tensor network associated to the trace we introduce another formalism. In the new formalism we associate the maps of the tensor network to an alphabet of circles, inspired by the Heegaard decomposition. This decomposition allows us to perform simplifications in a easier way, explained in section 3.4.6. We introduce the decomposition and its simplifications: the sliding and the two point move. The simplifications do not alter the topology of the network.

We are ready to prove that the invariant does not depend on the specifics of the lattice, we introduce the Pachner moves. These moves change the interior of one or few triangles leaving unaltered their boundaries [6]. The moves also transform the tensor network, acting non trivially only on the operators of the portion of the lattice considered. One result of this thesis, presented in 3.4.7, is the diagrammatic expression for the transformations of the tensor network. With these diagrams we prove a relation of equivalence between the tensor networks of the projector operators in the different triangulations. This implies that the ground state degeneracy is a topological invariant of the surface.

The main chapter is Chapter 4, where we give an overview of the algebraic framework of the G-QDM. The model is a QDM with an additional labeling of the links by elements of a finite group G; this labeling can be considered as an external gauge field. The labels are not dynamical and can be interpreted as a G-connection on the triangulation. Although not all labelings are allowed, only the ones that satisfy the flatness of the G-connection. The flatness condition is imposed locally around each vertex of the lattice: the product of the labels around a vertex needs to be equal to 1, the

identity in G. Additionally we show a local transformation in the external gauge field which connects different lattices with the same monodromy. We have lattices with transformations between them, which define Hamiltonians equivalent to one another.

The relation of equivalence determines classes of equivalent Hamiltonians with different flat G-connection locally but with the same monodromy globally. In the same class it is possible to switch the model modifying the G-labels around a plaquette. This is a transformation in the external gauge field, which does not change the invariant we are calculating. The invariant was presented by Vladimir Turaev and discussed in details by Alexis Virelizier in [33, 34, 35]. The new class of models proposed is not topological in the usual sense because it also takes into account the external gauge field. The analysis shows that the invariant only depend on the topology of the manifold and the monodromy of the connection.

Let us describe in more detail the algebraic and geometric parameters of the G-QDM. The algebraic content is a finite Hopf group coalgebra H, which is a family of finite dimensional algebras H_a over the complex field: $H = \{H_a\}_{a\in G}$ with G a finite group, equipped with homorphism maps between the algebras [34]. We propose the Hopf group coalgebra with diagrams altering the language of the Kuperberg diagram. Therefore the arrows acquire labels belonging to the group G to specify the algebra. We check the axioms for a Hopf group coalgebra, and their compatibility conditions between the algebras in section 4.1.

The geometrical information is simply a surface divided as a simplices. Each links carries a label $a \in G$, and the possible states of the link are elements of H_a, thus the local Hilbert space $\mathcal{H}_l$ is H_a. Note that the label of each link is fixed not dynamical.

The global Hilbert space is, as before, the tensor product of the local Hilbert spaces. The new Hamiltonian model has the deformed versions of the local operators A_v and B_p, described in section 4.2. The deformed operators take into account the additional information of the external gauge field parameters. The Hamiltonian looks exactly as in the QDM; it is the sum of the operators over all the vertices and plaquettes.

A particularity of the Hopf group coalgebra is that the integral only exists in the algebra labeled by the identity element. [†] This fact forces a compatibility condition of the algebras around a vertex imposed by the vertex operator. This condition is equivalent to the requirement of a flat G-connection, i.e. it forces the parallel transport around a contractible dual loop to be trivial. A trivial G-connection can be achieved by multiple colorings of the lattice. The latter allows the existence of different Hamiltonians with the same ground space and same monodromy. To switch between Hamiltonians we can perform a transformation in the external parameters, involving only the links around a plaquette as explained in 4.3. However, the important information is the monodromy, which is not affected by the local transformations. We can divide the Hamiltonians into equivalence classes by the monodromy. The invariant K_H is the same within a class, being invariant under the local parameters transformations.

[†] An integral is an element of an algebra which multiplied by whatever element of the algebra is proportional to the integral itself. We will be more precise in the next chapter.

To calculate the invariant we can then present the projector P_0; as before its trace is the degeneracy of the ground state. To simplify the network we present the transformation of the labeled lattice. It is only allowed to transform links labeled by the identity element in G, therefore we transform the parameters before applying the moves, the details are given in 4.4. Finally we have all the instruments to calculate the invariant K_H.

We propose then a realization of the model with the Hopf group coalgebra $H = \{H_g\}_{g\in G}$, where the algebras H_g are copies of the same Hopf algebra A, considered as subspaces of the product $H = \mathbb{C}[G]^* \otimes A$. The product results in a non trivial action by the elements of the group algebra on the elements of the Hopf algebra. We illustrate the properties the action has to satisfy to fully describe a Hopf group coalgebra in section 4.5. We are ready to calculate the invariant in two concrete examples living on a torus: one with Abelian groups, the other non-Abelian. The invariant calculates the degeneracy of the ground state, beyond the topology it depends on the monodromy of the surface.

1.1 Further achievements

During the doctoral period the studies of models with topological order opened up many topics for research. One path followed was the characterization of the topological entanglement entropy of the models generated by the Abelian higher gauge theory [36]. The AHGT are higher dimensional generalizations of the QDM. The generalization was obtained by encoding the geometrical and gauge information into a cohomological formalism. The theory allows in this way to explore topological order in d-dimension in a generic way. In Prof. Teotonio's group we have explored the entanglement entropy for this theories, extracting the topological information for the models in n-dimensions, in a paper published in JHEP [36].

In the quest of topological phases beyond topological order in the last few years fracton phases of matter were discovered. Fractons are lattice models with excitations with restricted mobility and highly entangled ground state. We built a class of models within this framework in 2 and 3 dimensions. This work is to be published on PRLB [37].

2 The Invariant K_H

In the introduction we have talked about the importance of models with topological order. In specific about how models with finitely degenerate and highly entangled ground state are interesting for the scientific community. The purpose of this thesis is to present a model which has the desired properties but characterizes a new type of order beyond the topological one. It has as novelty the dependence on the monodromy over the surface, beyond the invariance under small deformations of the surface. We associate a scalar invariant K_H equal to the degeneracy of the ground state of the Hamiltonian model in the G-QDM.

To show the topological invariance, therefore an invariance under small deformations, i.e. diffeomorphisms, of the surface, we present the discretized version of them. On the lattice we build the Hamiltonian model, whose constituents are commuting operators. The operators are realized with a tensor network associated to the triangulation. To different lattices we associate different tensor networks. However the tensor networks can be related with local transformations. The local transformations act on the operators of few triangles leaving unaltered the rest of tensor network. These local transformations are derived from the Pachner moves, which relate different triangulations. We first introduce them in the QDM, proving its invariance under transformations of the lattice.

To explain the dependence on the monodromy we need the introduce more details. We endow the surface Λ with an additional structure of a G-bundle. Every link in the lattice Σ is labeled by an element of a finite group G as a local fiber. Therefore each link is associated to an algebra indexed by an element of G, its orientation is depicted in figure 2.1. This coloring is fixed with the lattice. Locally we have $\Sigma \times G$ as principal G-bundle. The G-bundle is equipped with an action $(x, g)h = (x, gh)$ for $x \in \Sigma$ and $g \in G$, as the multiplication in G, and a projection $(x, g) \to x$. For each point $x \in \Lambda$ we can associate a piecewise smooth loop in the dual lattice $\gamma : [0, 1] \to \Sigma^*$. To every dual loop we relate the monodromy, which is the product of the elements of the fibers encountered along the loop. Therefore a loop collects the values according to the relative orientation in the monodromy. Note that we follow the right-hand rule for the orientation of the G labels: the thumb parallel to the link's orientation, the index results as the orientation of the G label. In Fig. 2.1(b) the links exiting the vertex v result in the clockwise orientation, therefore they appear in the monodromy unaltered (like χ and ϵ). For the links entering the vertex v, in the monodromy they appear with the

opposite parameter (like β and α).

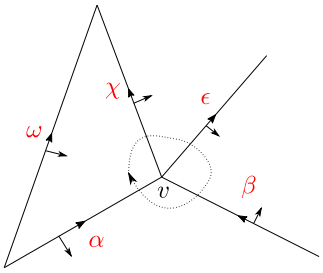

(a) The monodromy is $\chi\epsilon\beta^{-1}\alpha^{-1}$.

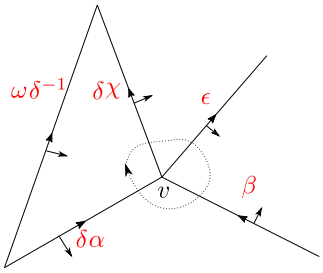

(b) After the transformation of the parameters in one triangle, the monodromy is $\delta\chi\epsilon\beta^{-1}\alpha^{-1}\delta^{-1}$.

Figure 2.1: Dual path around vertex v.

We require to satisfy the notion of trivial monodromy for the trivial loop, so we associate the identity element of G for all contractible loops, i.e. loops homotopic to a point. This is ensured by the compatibility condition imposed on the elements of the fibers. This condition imposes that the product of the elements in G around each vertex equals the identity in G. In our example in figure Fig. 2.1(a) that would be $\chi\epsilon\beta^{-1}\alpha^{-1} = 1$. This local condition is equivalent to impose the flatness condition of the G-connection on the lattice.

The loops on the lattice are divided into classes, which are comprehensive of the possible deformations of the loops. Loops that can be continuously deformed into one another belong to the same class. This classes are related to the homotopy classes of the surface Λ. The homotopy classes of the initial surface Λ are in correspondence with the fundamental group $\pi_1(\Lambda, x)$. The compatibility condition induces a homomorphism $\phi : \pi_1(\Lambda, x) \longrightarrow G$. If the surface is simply connected the homotopy classes do not depend on the point x, although the loops' monodromy can be conjugated, being in the same class for the relation of conjugation. The monodromy for the loops characterizes a class, being a global information, not affected by the compatibility condition, which acts locally. The global information encoded in the monodromy is associated to the lattice. The same classes divide the Hamiltonians, defined by the G-coloring of the lattice.

The classes for the Hamiltonians are differentiated by the monodromy associated to the lattice. Within a class we can shift from one lattice to another with a transformation of the elements of the fiber for the links around a plaquette. The transformation multiplies the elements with the same element in G respecting their orientations, as depicted in figure Fig. 2.1(b). All plaquettes are in the clockwise orientation, so for links

following the plaquette's orientation we multiply on the left for the element in G (in the Fig.2.1(b), the element is δ). Otherwise we multiply the parameter's link on the right with the opposite element (in Fig.2.1(b) the opposite element is δ^{-1}). The transformation preserve the compatibility condition for each vertex. The monodromy calculated around each vertex remains equal to the identity. Therefore, the transformation does not change the class of Hamiltonians.

Equipped with the transformations presented we proved the invariance of K_H under small deformations and under transformations in the external gauge field. The invariant is a refined version of the topological quantum invariant of the QDM. As in the QDM the ground state of the G-QDM is highly entangled and finitely degenerate. The invariant K_H is sensible to the topology of the surface and to the monodromy.

3 Preliminaries: QDM

In this chapter we review the basic notions for the Quantum Double Model (QDM), although in a different way as presented by Alexei Kitaev in [16]. We represent the operators of the Hamiltonian using diagrams. For this purpose we associate to operators tensors characterizing the Hopf algebra content of the Kitaev model. We present the invariant linked to the ground state degeneracy in a diagrammatic way. Its proof is valid for finite semi-simple involutory Hopf algebras. The material of this chapter will be used to define the generalization of the QDM presented in Chapter 4. Our intent is to be self contained and didactic, so the mathematical content is presented in steps to gain an intuition first.

Diagrammatic languages are powerful and useful in Physics. Feynman diagrams are the most famous example: they provide the working physicist a tool for hard mathematical calculations. In Quantum many-body systems tensor networks and their corresponding diagrams are used to manage the enormous amount of degrees of freedom of the Hilbert space [38, 39]. Another example are the graphical notation of Roger Penrose for spin networks, where we have tensor algebra networks associated to simplify the calculations [40].

The last example of tensor networks concerns more the diagrammatic notation we are presenting here. They were introduced by Greg Kuperberg in relation with the definition of invariants of a closed oriented 3-manifold. His proof for the invariant involved Heegaard splitting of the surface and its tensor networks [26]. We are not using the splitting; instead, we will discretize the manifold using triangulations. We will demonstrate the invariant using curves diagrams representing a tensor network. The tensor network we build corresponds to the projector operator to the ground state. For the construction of the network we use Hopf algebra maps associated to geometric objects of the triangulation. In this way we build a Hamiltonian model over the surface, with first neighbors interactions.

The main result we are presenting relates the ground state degeneracy of the Quantum Double Model, living on a $2D$ lattice Σ, to the Kuperberg invariant. To calculate the degeneracy we define a diagrammatic version for the Hamiltonian model and its operators.

In the following section we describe the basic ingredients to present the invariant: the triangulation and the algebra.

- We consider a $2D$ surface discretized by a simplicial triangulation. The constituents are vertices, links and triangles, also called plaquettes or faces. We consider a certain triangulation as the initial data. In some cases we refer to a squared lattice, as it is easier to visualize.

- Elements of a finite Hopf algebra are assigned to the links. We describe the Hopf algebra content diagrammatically.

We introduce the constituents for the general theory step by step in the following. We quickly introduce the basic geometrical knowledge necessary to tackle the present work. We are dealing with a topological space: a surface and its discretization.

3.1 The Manifold

In 1952 Edwin E. Moise proved the 3D version for the main conjecture of geometric topology, Hauptvermutung. He showed that any topological 3-manifold is triangularizable: it has a unique piece wise linear structure. This is true for dimensions equal or less than three,[41, 42]. A triangulation is a homeomorphism from the topological manifold to a simplicial complex. A simplicial complex $\mathcal{K}$ is specified by a finite set of vertices V and a finite set of simplices S. The most powerful invariant in algebraic topology to distinguish between 3-manifolds is the fundamental group, π_1, as it determines all the homology group of a closed 3-manifold. We only consider closed, simply connected, oriented manifolds.

Earlier in 1925 Tibor Radò proved the Hauptvermutung version for Riemann surfaces [43]. Thus they are homeomorphic to simplicial complexes. The model proposed lives on an oriented surface Λ, discretized by triangles, which is homeomorphic to a homogeneous simplicial complex, $\mathcal{K}$. In other words we decompose the surface into a lattice made of triangles, with no disconnected points or links. We consider a given orientation for all links and faces, as in Fig. 3.1.

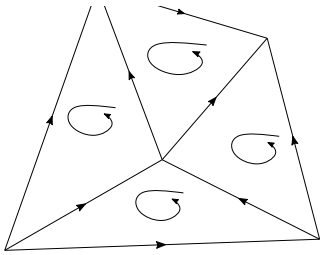

Figure 3.1: Triangulation with oriented links and faces

.

Consequently every closed surface can be decomposed into a polygon, which can be further divided in triangles. In figure Fig. 3.2 we show realizations for the torus T, for the projective plane $\mathbb{R}P^2$ and the Klein bottle K. Note the identification of the edges with the same letter, please look at [44] for further details. We consider only oriented surfaces, therefore non orientable surfaces such as $\mathbb{R}P^2$, the Klein bottle K will not be used.

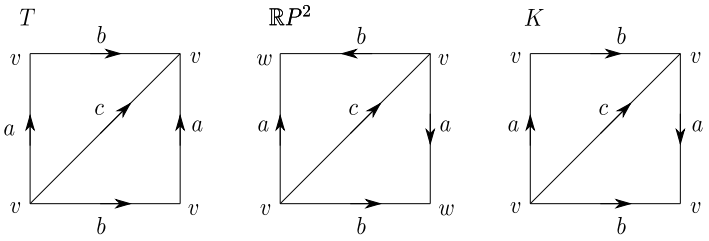

Figure 3.2: Examples of simplicial complexes of known surfaces, from [44].

We have shown examples of the discretization on various surfaces. More over we know that every surface can be subdivided into a simplicial complex made of triangles, their links and vertices.

As an example $\mathcal{K}_3$, a three dimensional elementary simplex is a tetrahedron labeled by the list of ordered vertices $[v_0, v_1, v_2, v_3]$. The notation made by the ordered list of vertices shows the boundaries of every simplex in a straightforward way, thanks to the boundary maps. The boundary map $\partial : \mathcal{K}_n \to \mathcal{K}_{(n-1)}$ determines the orientation of the faces of the boundary of the simplex, with the formula

$$\partial([v_0, \ldots, v_n]) = \sum_i (-1)^i [v_0, \ldots, \hat{v}_i, \ldots, v_n],$$

where the $\hat{v}_i$ element has been removed.

On a 3-simplex $\mathcal{K}_3$ the boundary map is $\partial([v_0, v_1, v_2, v_3]) = [v_1, v_2, v_3] - [v_0, v_2, v_3] + [v_0, v_1, v_3] - [v_0, v_1, v_2]\}$. A 2-simplex is an oriented surface with three vertices $[v_0, v_1, v_2]$, whose boundaries are 1-simplices $[v_0, v_1]$, $[v_0, v_2]$, $[v_1, v_2]$, oriented links. A 0-simplex is made by one vertex $[v_0]$. In figure Fig. 3.3 there is a representation of some components of a 3-simplex described in this paragraph.

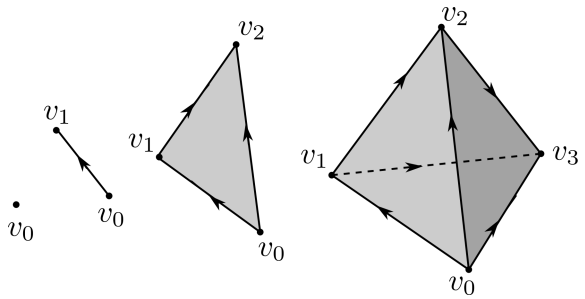

Figure 3.3: 0-simplex, 1-simplex, 2-simplex and 3-simplex

Every 0-simplex is boundary of at least three 1-simples. Every 1-simplex is boundary of 2-simplexes in a homogeneous simplicial complex of dimension 2.

The triangulation registers the geometric information, encoded in the connectivity of the links. But there are many possibilities in building a triangulation, changing the number of vertices and the connections between them. We are going to prove that our invariant do not depend on the triangulation.

3.2 Hopf Algebra

We are now presenting the tensor networks associated to the lattice, but first we introduce how we represent tensors.

3.2.1 Tensors

To have a better understanding of the model we propose we start by introducing tensors in a diagrammatic language. Diagrammatic notations are not new, but in this review we use a notation first introduced by Greg Kuperberg in [26].

Let's begin defining tensor product between spaces: let us consider a pair of vector spaces V and W with basis $\{e_i\}_{i=1\ldots dimV}$ and $\{f_j\}_{j=1\ldots dimW}$ respectively. We can define the tensor product of $V \otimes W$ as the vector space spanned by the set of ordered couples $\{e_i \otimes f_j\}_{i=1\ldots dimV,\, j=1\ldots dimW}$. We obtain elements of the form $v \otimes w = v^i w^j e_i \otimes f_j$, for every pair $v = v^i e_i \ \in V$ and $w = w^j f_j \ \in W$. We use the Einstein's summation convention.

We can now introduce the dual space V^* as the space of linear maps ϕ from the vector space V to the complex numbers $\mathbb{C}$, $\phi : V \to \mathbb{C}$. It is a vector space when equipped with operations: a sum between two maps $(\phi + \psi)(v) = \phi(v) + \psi(v), \quad v \in V$, and the multiplication with a scalar $(\lambda\phi)(v) = \lambda(\phi(v))$, $\lambda \in \mathbb{C}$. We introduce the dual basis for V^*: $\{e^j\}_{j=1\ldots dimV^*}$, defined by the action on the basis element of V, $e^i(e_j) = \delta^i_j$. It is worth to note that V and V^* have the same dimension.

In a consequent way we have the tensor product $V \otimes V^*$ with basis $\{e_i \otimes e^j\}_{i,j=1\ldots dimV}$. An element of this vector space is $T = T^b_a e_b \otimes e^a$. We define tensors by representations of the tensor product of a vector space and its dual space. In other words, we associate with a bijection a tensor T living in $V^* \otimes V$. The elements of the dual space are represented in diagram by arrows going in the tensor, and for V by arrows pointing out, as in

$$T^b_a \equiv \xrightarrow{a} T \xrightarrow{b} \quad .$$

The tensor associated to the identity map, $1_V : V \to V$, is $1 = e^a \otimes e_a$, it belongs to $V^* \otimes V$. In this language it is pictured just as a continuous arrow,

$$\mathbb{1} \equiv \longrightarrow \quad .$$

We can extend the same reasoning for diagrams with multiple tensor products. Let us consider a tensor $T \in \underbrace{V^* \otimes \ldots \otimes V^*}_{\text{n}} \otimes \underbrace{V \otimes \ldots \otimes V}_{\text{m}}$, represented in components as $T = T^{b_1 \ldots b_m}_{a_1 \ldots a_n}\ e^{a_1} \otimes \ldots \otimes e^{a_n} \otimes e_{b_1} \otimes \ldots \otimes e_{b_m}$. The corresponding diagram has n arrows coming in and m arrows going out. In diagrammatic notation to have a faithful representation it is important to pay attention to the legs labeling. In the image below for elements belonging to V on the right the order is clockwise and for the dual space on the left it goes counterclockwise,

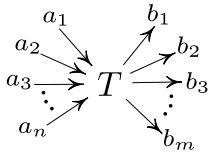

.

When working with tensors an important operation is the contraction of indices. We can perform it for example between tensors $A = A^k_{ij}\, e_k \otimes e^i \otimes e^j$ and $B = B^{ai}_k\, e_a \otimes e_i \otimes e^k$, which results in the formula $A^k_{ij}\, B^{ai}_k\, e_a \otimes e^j$. The diagrammatic representation of the contraction is realized by the connection of the corresponding arrows. The i index in A is the first entry and for B is the second leg out, looking like

$$\xrightarrow{j} A \overset{i}{\leftarrow}\!\!\times\!\!\overset{k}{\rightarrow} B \xrightarrow{a}$$

.

The reduced tensor shown in the picture has a smaller number of free legs, therefore a full contraction has no free legs at all and results in a number. A net of tensors and contractions forms a tensor network.

3.3 Hopf Algebra with Kuperberg diagrams

Now that we have familiarized ourselves with the Kuperberg notation for tensors and contractions we would like to introduce its full expression with the tensor network associated to a Hopf algebra of finite dimension.

A Hopf algebra is a self-dual structure which is an algebra and a coalgebra at the same time. The two 'sectors' satisfy compatibility conditions, giving an extra structure called a bialgebra. With an additional anti-homomorphism we have what is called a Hopf algebra. To know more on Hopf algebra the best reference you can look at is the book of Dascalescu [45].

A Hopf algebra is constructed with the following ingredients $(A, m, \eta, \Delta, \epsilon, S)$. We have to specify the vector space A, and a series of maps: the multiplication $m : A \otimes A \longrightarrow A$ and the unit $\eta : \mathbb{C} \longrightarrow A$ for the algebra sector. The dual space A^* is isomorphic to A, we have the maps coproduct $\Delta : A \longrightarrow A \otimes A$ and counit $\epsilon : A \longrightarrow \mathbb{C}$. Finally we define the antipode $S : A \longrightarrow A$. We are ready now to introduce the structure of a finite dimensional Hopf algebra using the diagrammatic language. The diagrammatic expression for the tensors associated to the maps are presented in figure Fig. 3.4.

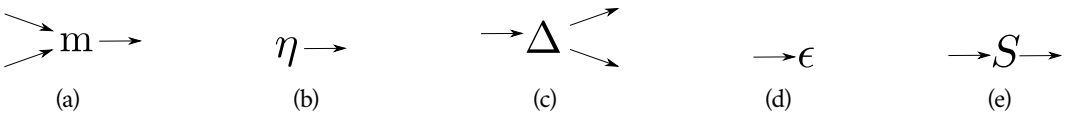

(a) (b) (c) (d) (e)

Figure 3.4: Diagrams for Hopf algebra

3.3.1 Algebra

An algebra is a vector space equipped with an associative product and a unit. The multiplication, acting on elements of the basis $\{e_i\}_{i=1...dimA}$, is $m(e_i \otimes e_j) = m_{ij}^k e_k$, where the coefficients belong to $\mathbb{C}$ and are also called structure constants. The product belongs to $A^* \otimes A^* \otimes A$, defined by $m \equiv m_{ij}^k e_k \otimes e^i \otimes e^j$. The associativity fixes the structure constants of the product to satisfy $m_{ab}^k m_{kc}^l = m_{bc}^k m_{ak}^l$. This property is pictured with the equivalence of diagrams

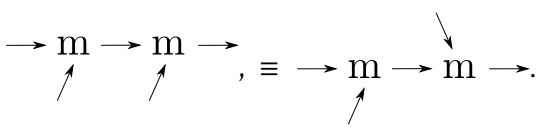

The unit is $1 \mapsto \eta^i\, e_i$ in the chosen basis. It is simultaneously a left and right unit, as demonstrated in equations:

$$\begin{aligned} m(\eta \otimes e_j) &= m(\eta^i\, e_i \otimes e_j) = \eta^i\, m_{ij}^k\, e_k = \delta_j^k\, e_k = e_j \ \text{ left unit} \\ m(e_i \otimes \eta) &= m(e_i \otimes \eta^j\, e_j) = m_{ij}^k\, \eta^j e_k = \delta_i^k\, e_k = e_i \ \text{ right unit.} \end{aligned}$$

Both these equations are equal to the identity map $1_A : A \longrightarrow A$, the equivalence is pictured by

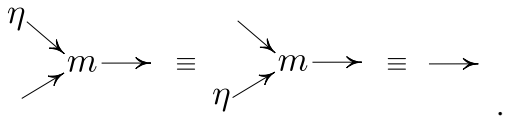

.

In this little examples of the use of diagram, it is self evident the power and utility of the Kuperberg realization for algebraic properties respects to the calculations.

3.3.2 Coalgebra

We can dualize the maps reversing the direction of the arrows and creating a coassociative coproduct and a counit. The coproduct in the basis elements reads $\Delta(e_i) = \Delta_i^{jk}\, e_j \otimes e_k$, with coefficients in $\mathbb{C}$. We associate a tensor Δ which belongs to $A^* \otimes A \otimes A$. The structure constants have to attend the following requirement for the coassociativity $\Delta_i^{ja}\, \Delta_j^{cb} = \Delta_i^{cj}\, \Delta_j^{ba}$, shown by:

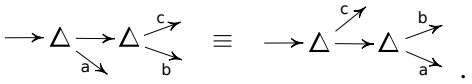

.

The counit is represented in elements by $\epsilon(e_i) = c^i$, resulting in numbers belonging to $\mathbb{C}$. Similarly it is a left and right counit; so when it is applied to the coproduct it is equal to the identity tensor. Therefore it satisfies two equations:

$$\begin{aligned} (\epsilon \otimes 1_A) \circ \Delta(e_i) = \Delta_i^{jk}\, \epsilon(e_j) e_k = \Delta_i^{jk}\, c^j\, \delta_i^k\, e_k = e_i \quad \text{left counit,} \\ (1_A \otimes \epsilon) \circ \Delta(e_j) = \Delta_j^{ik}\, e_i \epsilon(e_k) = \Delta_j^{ik}\, c^k\, \delta_j^i\, e_i = e_j \quad \text{right counit.} \end{aligned}$$

We give the same information with the diagrammatic expression

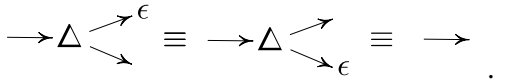

.

3.3.3 Bialgebra

In general an algebra and its dual, the coalgebra, are independent. But when they satisfy properties of compatibility, the new structure achieved is a bialgebra. These properties dictate how the two algebras act on each other. We have to specify the contractions of the maps of the algebra on the dual parts and vice versa.

In the literature the first relation is known as the bialgebra axiom which is the equivalence of diagrams

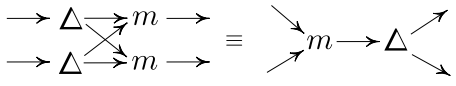

. (3.1)

The diagrams are related to two different equation, we show the realization in components. The left diagram is equation 3.2 and the right one corresponds to 3.3. To write the equation with maps we introduce the map $\tau : A \otimes A \longrightarrow A \otimes A$, doing a flip $\tau(a \otimes b) = b \otimes a$. The formulas are

$$\begin{aligned}
&\Big((m \otimes m) \circ (1_A \otimes \tau \otimes 1_A) \circ (\Delta \otimes \Delta)\Big)(e_i \otimes e_j) = \\
&= \Big((m \otimes m) \circ (1_A \otimes \tau \otimes 1_A)\Big)\big((\Delta_i^{pq}\, e_p \otimes e_q) \otimes (\Delta_j^{st}\, e_s \otimes e_t)\big) = \\
&= (m \otimes m)\big(\Delta_i^{pq}\, \Delta_j^{st} (e_p \otimes e_s) \otimes (e_q \otimes e_t)\big) = \Delta_i^{pq}\, m_{ps}^{l}\, \Delta_j^{st}\, m_{qt}^{n}\; e_l \otimes e_n \; ;
\end{aligned} \tag{3.2}$$

$$(\Delta \circ m)(e_i \otimes e_j) = \Delta(m_{ij}^{k}\, e_k) = \Delta_k^{ln}\, m_{ij}^{k}\; e_l \otimes e_n \; . \tag{3.3}$$

The equivalence of the two equations is granted when the structure constants satisfy $\Delta_k^{ln}\, m_{ij}^{k} = \Delta_i^{pq}\, m_{ps}^{l}\, \Delta_j^{st} m_{qt}^{n}$. We underline the elegance of the diagrammatic representation over the intricate realization with maps and their structure constants. When ever it is possible we are going to work just on the diagrammatic representation of the algebra content.

We have another relation of the bialgebra: we have the contraction between the unit and counit which is equal to 1. In components it is $\epsilon(\eta) = \epsilon(\eta^i e_i) = c^i \eta^i = 1$. The diagram results in

.

The other properties are the interplay between the multiplications and the dual units. The application of the counit to the product is $\epsilon\big(m(e_i \otimes e_j)\big) = \epsilon(m_{ij}^{k}\, e_k) = \epsilon(e_i) \otimes \epsilon(e_j)$, in diagram is

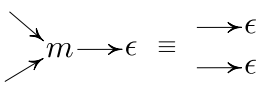

. (3.4)

Dualizing the relation, we feed the coproduct with the unit to have $\Delta(\eta) = \eta \otimes \eta = \eta^i \eta^j e_i \otimes e_j$. We explicit it in figure

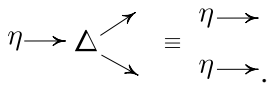

(3.5)

Another way of interpreting these properties is that we are giving $A \otimes A$ an algebra structure. We must define a product between two elements, in a intuitive way this is defined by the relation

$$(a_1 \otimes b_1)(a_2 \otimes b_2) = (a_1 a_2 \otimes b_1 b_2).$$

The equivalence defined in 3.4 and 3.5 are creating the unit and counit for the structure $A \otimes A$. We then define a homomorphism between algebras $A \longrightarrow A \otimes A$ by imposing the equivalence

$$\Delta(ab) = \Delta(a)\Delta(b)\,,$$

where on the left side we have the product $m \in A$ and on the right side the new product defined. We find in this way the bialgebra axiom of diagram 3.1 in a more intuitive way.

3.3.4 Hopf Algebra

A bialgebra with a map generalizing of the inverse element is a Hopf algebra [47]. The last ingredient is the antipode, an anti-morphism, explicitly it is $S(e_i) = s_i^j e_j$. We note the antipode is an involution $S^2 = \mathbb{1}$, as proved by a theorem, which states that a Hopf algebra is involutive when is finite dimensional and semi-simple[†], as in our case. Involution means we have the following properties for $x, y \in A$

$$\begin{cases} S(xy) = S(y)S(x) & \text{anti-automorphism} \\ S(S(x)) = x & \text{involution.} \end{cases}$$

[†] A semi-simple algebra can be decomposed in a direct sum of simple subalgebras. Or equivalently, every homomorphism with the algebra as domain is either injective or constant.

We present the behavior of the antipode in relation to the product and coproduct in figure Fig. 3.5. The relation with the product is presented by the first equivalence of diagrams corresponding to the equations left side (L.S.) and the right one (R.S.).

$$\begin{cases} \big(S \circ m\big)(e_i \otimes e_j) = S(m_{ij}^k\, e_k) = s_k^l\, m_{ij}^k\, e_l & \text{L.S.} \\ \big(m \circ \tau\big)(S(e_i) \otimes S(e_j)) = \big(m \circ \tau\big)(s_i^k\, e_k \otimes s_j^n\, e_n) = m(s_i^k\, s_j^n\, e_n \otimes e_k) = s_i^k\, s_j^n\, m_{nk}^l\, e_l & \text{R.S.} \end{cases}$$

For the R.S. we can use the definition of the opposite product $m^{opp} = m \circ \tau$, therefore we flip the order of legs for the m. The property imposes the equivalence of the

constants $s^l_k\, m^k_{ij} = s^k_i\, s^n_j\, m^l_{nk}$. The second equality diagrams relates to the behavior of the coproduct, the two side are expanded:

$$\begin{cases} \big(\tau \circ (S \otimes S) \circ \Delta\big)(e_i) = \tau((S \otimes S)(\Delta^{jk}_i\, e_j \otimes e_k)) = \tau(\Delta^{jk}_i\, s^l_j\, s^n_k\, e_l \otimes e_n) = \Delta^{jk}_i\, s^l_j\, s^n_k\, e_n \otimes e_l & \text{R.S.} \\ \big(\Delta \circ S\big)(e_i) = \Delta(s^j_i\, e_j) = \Delta^{nl}_j\, s^j_i\, e_n \otimes e_l & \text{L.S.} \end{cases}$$

Imposing the equivalence results in the constraints for the coproduct constants: $\Delta^{jk}_i\, s^l_j\, s^n_k = \Delta^{nl}_j\, s^j_i$. The diagram for the relations are

Figure 3.5: Antipode identities

A really important and useful property is the equivalence called the antipode axiom. The antipode axiom is the definition of the antipode as a anti-morphism map. Expressed by maps it corresponds to the equivalences of equations:

$$m \circ (1_A \otimes S) \circ \Delta = \epsilon\eta$$
$$m \circ (S \otimes 1_A) \circ \Delta = \epsilon\eta\ .$$

When we expand the calculation into the structure constants we have for the left sides, respectively:

$$\big(m \circ (1_A \otimes S) \circ \Delta\big)(e_i) = m\big((1_A \otimes S)(\Delta^{jk}_i\, e_j \otimes e_k)\big) = m(\Delta^{jk}_i\, s^l_k\, e_j \otimes e_l) = \Delta^{jk}_i\, s^l_k\, m^n_{jl}\, e_n$$
$$\big(m \circ (S \otimes 1_A) \circ \Delta\big)(e_i) = m\big((S \otimes 1_A)(\Delta^{jk}_i\, e_j \otimes e_k)\big) = m(\Delta^{jk}_i\, s^l_j\, e_l \otimes e_k) = \Delta^{jk}_i\, s^l_j\, m^n_{lk}\, e_n.$$

While the maps on the right side, expressed in the constants, are $\epsilon(e_i)\eta = c^i\eta^p\, e_p$. We can then impose the equality $\Delta^{jk}_i\, s^l_k\, m^n_{jl} = c^i\eta^p$ and simultaneously $\Delta^{jk}_i\, s^l_j\, m^n_{lk} = c^i\eta^p$. T his relation is expressed in a compact and clean way by the diagram below:

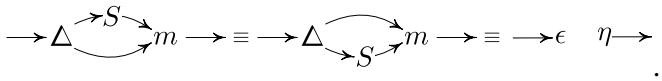

Finally we can introduce the trace element 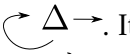 . It is proportional to the integral element $\lambda \longrightarrow$, which is defined by the property 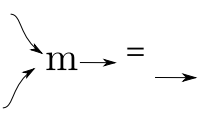 .

In addition we define the cotrace 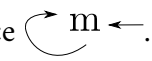 . It is proportional to the cointegral functional , satisfying the relation 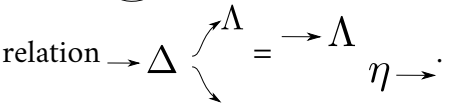 .

The simplest examples of the Hopf algebra structure are realized with elements of a finite group $\mathbb{G}$. When we consider the vector space spanned by the linear combination of the elements of a group $\mathbb{G}$, we have the identification $A = \mathbb{C}[\mathbb{G}]$, called a Group Algebra. Another fundamental example is the generalization of the Group Algebra known as the Quantum Double. The reader can find a good summary on the subject in [29].

3.3.5 Group Algebra

To define the structure of the group algebra we choose a set of elements of the group $\mathbb{G}$ given by $\{\phi_g : g \in \mathbb{G}\}$. Linear combinations of them gives it the structure of a vector space. The ingredients of the Group Algebra are listed in the table 3.1, with e the identity element of $\mathbb{G}$.

Table 3.1: Group algebra structure

(a) product	$m(\phi_g \otimes \phi_h) = \phi_{gh}$
(b) unit	$\eta(1) = \phi_e$
(c) coproduct	$\Delta(\phi_g) = \phi_g \otimes \phi_g$
(d) counit	$\epsilon(\phi_g) = 1 \ \forall g$
(e) antipode	$S(\phi_g) = \phi_{g^{-1}}$

The product is associative and a useful notation for it is $m(\phi_g \otimes \phi_h) = \phi_g\phi_h = \phi_{gh}$. With this notation we can easily prove the associativity given by

$$(\phi_g\phi_h)\phi_l = \phi_{gh}\phi_l = \phi_{(gh)l} = \phi_{g(hl)} = \phi_g\phi_{hl} = \phi_g(\phi_h\phi_l).$$

The coproduct is coassociative and the proof is straightforward, as the final states are exact replicas of the input:

$$\big((1_A \otimes \Delta) \circ \Delta\big)(\phi_g) = (1_A \otimes \Delta)(\phi_g \otimes \phi_g) = \phi_g \otimes \phi_g \otimes \phi_g$$
$$\big((\Delta \otimes 1_A) \circ \Delta\big)(\phi_g) = (\Delta \otimes 1_A)(\phi_g \otimes \phi_g) = \phi_g \otimes \phi_g \otimes \phi_g \ .$$

The same presentation of the components of the group algebra in the table 3.1 are expressed by diagrams as

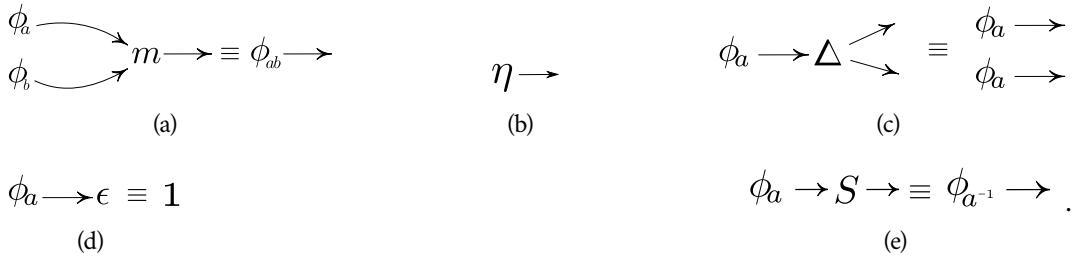

Figure 3.6: Diagrams for Group Algebra

We show the realization in diagrams of the proofs of the important properties of the bialgebra axiom and the antipode axiom. Likewise all the other properties of the Hopf algebra are satisfied by $\mathbb{C}[\mathbb{G}]$, [48]. The algebra and coalgebra do realize the bialgebra axiom satisfying the homomorphism $\Delta(\phi_a\phi_b) = \Delta(\phi_a)\Delta(\phi_b)$. We show the steps in the verification in the equality of the initial and final states of two line of the following diagrams:

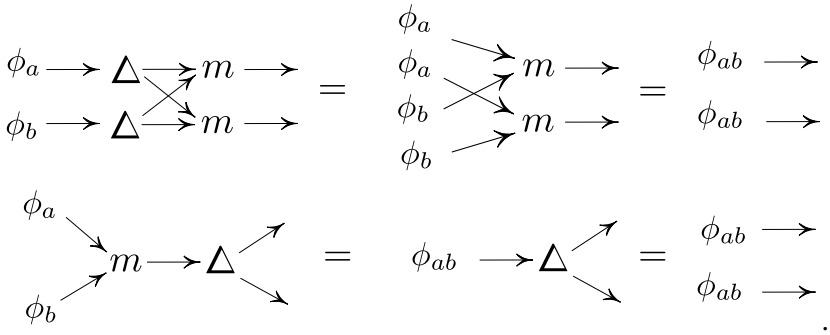

We present the proof of the antipode axiom shown in the series of diagrams. Remember the counit ϵ applied to every vector is equal to one. The proof expression is:

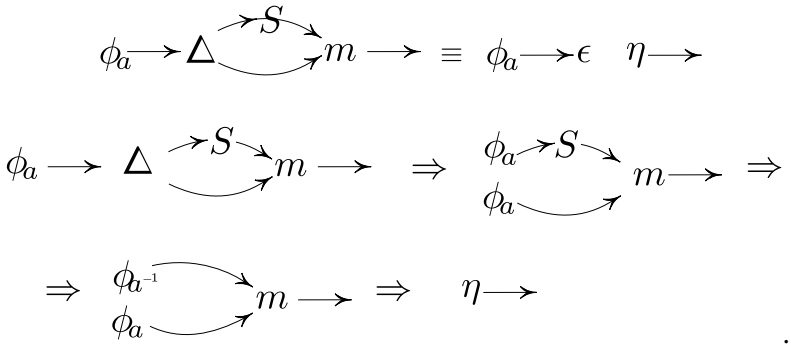

3.4 Quantum Double Model Reviewed

After we have given the tools of the diagrammatic realization of the Hopf algebra, we introduce the relevant tensor networks for the definition and study of the Hamiltonian model. The ingredients needed to discuss the Hamiltonian are a lattice, an orientation and a Hilbert space.

We begin by defining over an oriented surface Λ a lattice Σ defined by a simplicial complex. We choose an orientation for every link, and for convenience we choose the same orientation for all plaquettes, as in 3.1. For every link we associate a $\mathbb{G}$-spin, an element of a finite group $\mathbb{G}$. We have build a net of $\mathbb{G}$-spin similar to the spin network introduced by Penrose. The total Hilbert space over Σ is a tensor product of local vector spaces. We have a many body theory of independent degrees of freedom.

We specify the local vector space with an orthonormal basis indexed by a configuration. A configuration is a choice of elements of the finite group $\mathbb{G}$ for every link, chosen in the basis $\{|g\rangle\}_{g\in\mathbb{G}}$. This set generates a free vector space, the local Hilbert space $\mathcal{H}_l$. The elements of the basis of $\mathcal{H}_l$ are realized diagrammatically by $|g\rangle = |\overset{g}{\longrightarrow}\rangle = |\overset{g^{-1}}{\longleftarrow}\rangle$. A generic element associated to a single link is a linear combination

$$|w\rangle = \sum_g w_g \, |g\rangle$$

with coefficients in the complex numbers. The local state will be pictured by an arrow pointing out:

$$|w\rangle \simeq w \longrightarrow .$$

Elements $|g\rangle$, $|h\rangle$ satisfy the orthogonality condition $\langle h|g\rangle = \delta(h,g)$ as internal product. We have therefore specified the local Hilbert space $\mathcal{H}_l \simeq \mathbb{C}[\mathbb{G}]$, associated to the link l, isomorphic to a group algebra over $\mathbb{G}$.

The total vector space $\mathcal{H}$ is defined by the tensor product of all local Hilbert spaces:

$$\mathcal{H} = \bigotimes_l \mathcal{H}_l.$$

On the total space $\mathcal{H}$ we can define maps $\phi : \Sigma \longrightarrow \mathbb{G}$, where the set $\{|\phi\rangle\}$ is a basis for $\mathcal{H}$. To picture a generic global state $|\psi\rangle$ we will have an arrow pointing out from every link, as independent degrees of freedom. Between elements $|\phi\rangle$, $|\psi\rangle$ we have the usual product $\langle\phi|\psi\rangle = \delta(\phi,\psi)$, where they have to match every local $\mathbb{G}$-spin. In this Hilbert space we have local operators acting just on few edges introducing the dynamics, elsewhere they are the identity operators. The interaction relates just first neighbors.

3.4.1 The Operators

The dynamics is described by a Hamiltonian made by a sum of local operators. The Hamiltonian depends on the triangulation and its orientation. We will see that different orientations give Hamiltonians that are unitary equivalent to one another. We will introduce two sets of operators. One is indexed by a vertex v and act on the adjacent links. Another set of operators is indexed by a plaquette p and act on the links around a plaquette. Both operators apply the identity map on the links unaffected by their action. The vertex operator acting on vertex v is denoted by A_v and the plaquette operator acting on plaquette p is denoted by B_p. The Hamiltonian $\mathbb{H}$ is

$$\mathbb{H} = -\sum_v A_v - \sum_p B_p \,.$$

We are going to look in details the operators in the sections below.

The Vertex Operator A_v

The local operator realizes a gauge transformation on the vertex. We define the operator A_v as the sum over all the possible actions on the adjacent links. In other words

$$A_v = \sum_{g\in\mathbb{G}} \frac{A_v^g}{|\mathbb{G}|}.$$

As you can see, the operator is a sum over all the possible gauge transformations, normalized by the dimension of $\mathbb{G}$. A_v is a unitary operator and is self-adjoint

$$A_v^\dagger = \sum_{g\in\mathbb{G}} \frac{A_v^{-g}}{|\mathbb{G}|} = A_v \,.$$

We can see this by the definition of adjoint taking y, w states in $\mathcal{H}$ we can write $(A_v^g\, y, A_v^g\, w) = (y, w)$, with the important relation $A_v^{g^{-1}}\, A_v^g = \mathbb{1}$. The vertex operator A_v is idempotent, not diagonal, we will proof this using diagrams later.

The operator A_v^g is indexed by a generic element $g \in \mathbb{G}$. Its action can be depicted by

A_v^g 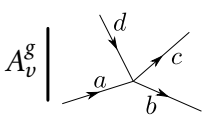

$=$ 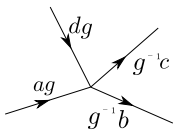

.

A single transformation A_v^g acts on the cone of links around a vertex. It multiplies the states associated to the links by an element $g \in \mathbb{G}$, but we have to distinguish between

the right and left multiplication. A right multiplication is performed for the links oriented towards the vertex and a left multiplication of the inverse element happens for the links pointing out. Let us investigate how a different orientation of the links will affect the action of A_v^g, the diagram is going to differ as shown in

$$A_v^g \left| \right\rangle = \left| \right\rangle . \tag{3.6}$$

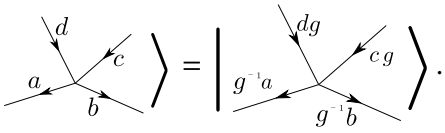

The Plaquette Operator B_p

For every tile of the lattice Σ we act considering the links along the perimeter. For a triangulation on a generic oriented plaquette p the operator is

$$B_p \left| \right\rangle = \delta(cba^{-1}, e) \left| \right\rangle . \tag{3.7}$$

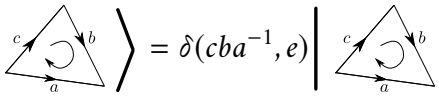

The operator is obviously idempotent and diagonal, it gives back the same state. It calculates the product of the elements along the edges of the surface p, respecting the orientation of the link. It is equal to one just when the product is equal to the identity element of the group.

The operator B_p calculates the holonomy around a plaquette, projecting it to a configuration of flat connection.

Algebra of Operators

With this operators we have an exactly solvable theory as the two operators commute between each other $A_v B_p = B_p A_v \quad \forall v,\ p \in \Sigma$, as the two lines prove

$$A_v B_p \left| \right\rangle = \delta(cba^{-1}, e) A_v \left| \right\rangle = \frac{\sum_g}{|G|} \delta(cba^{-1}, e) \left| \right\rangle,$$

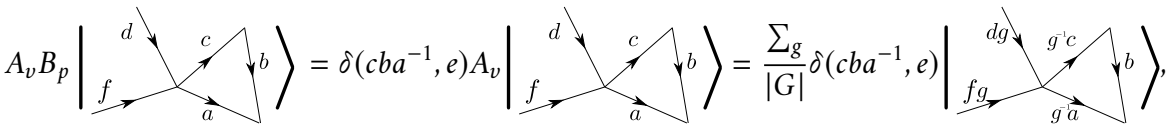

$$B_p A_v \left| \right\rangle = \frac{\sum_g}{|G|} B_p \left| \right\rangle = \frac{\sum_g}{|G|} \delta\left((g^{-1}c)b(g^{-1}a)^{-1}, e\right) \left| \right\rangle.$$

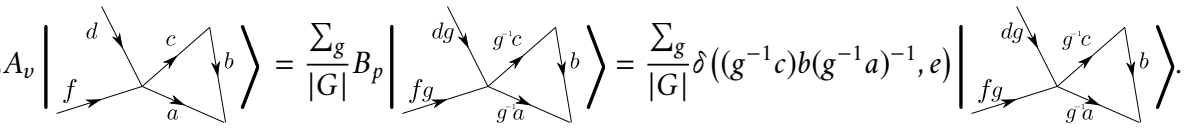

We show the relation for the holomy:

$$cba^{-1} = e \Leftrightarrow (g^{-1}c)b(g^{-1}a)^{-1} = g^{-1}cba^{-1}g = e.$$

The gauge transformations commute with each other when acting on different vertices. $A_{v_1}A_{v_2} = A_{v_2}A_{v_1}\ \forall v_1 \neq v_2 \in \Sigma$, detailed proof is sketched in formula 3.8. In order to see that, we just show that the single operators $A^g_{v_1}$ and $A^h_{v_2}$ already commute:

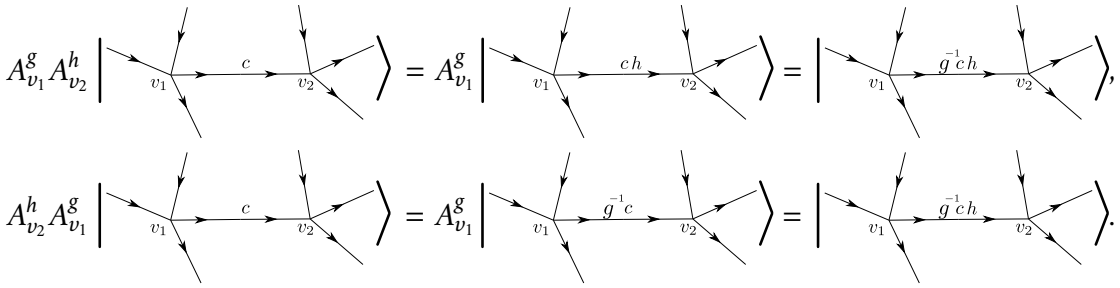

(3.8)

Likewise the holonomy operator satisfies the following algebra for every plaquettes p_1, p_2 in the lattice Σ: $B_{p_1}B_{p_2} = B_{p_2}B_{p_1}$. The result is easily proved, as they act on different spaces.

Both operators are idempotents, in other words they satisfy the following algebra:

$$A_v A_v = A_v \ , \ B_p B_p = B_p \ \ \forall p, v \in \mathcal{K} \ .$$

We are going to prove these relations with Kuperberg diagram in the following section.

3.4.2 Kuperberg Diagram for QDM

We now introduce the same operators in Kuperberg diagrams. The motivation is that we gain generality, as the proofs are valid for every finite Hopf algebra. Nevertheless we recover easily the Group Algebra already presented.

We associate to every face a tensor m given by the multiplication structure and to every link a tensor Δ defined by the comultiplication structure. Both of them will be multi-arrowed, using a notation derived from the associations. For the multiplication the expression into the algebraic formalism would be $tr\Big(m(a_1 \otimes m(a_2 \otimes m(a_3 \otimes a_4)))\Big)$. Below we introduce an example of the new notation:

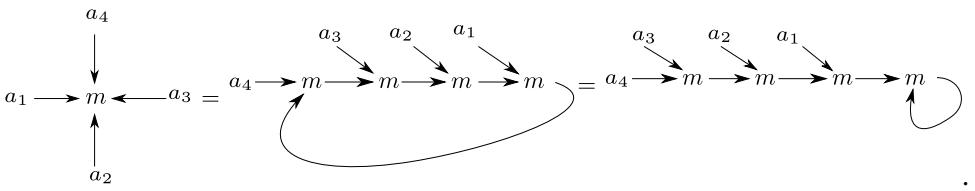

.

For the coproduct we have a dual representation reversing the arrows,

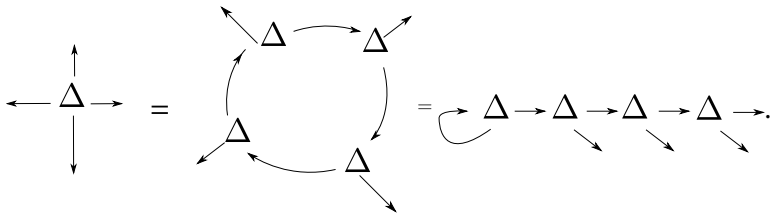

While using the algebraic maps is $(\Delta\otimes\mathbb{1}\otimes\mathbb{1})\circ(\Delta\otimes\mathbb{1})\circ(\Delta(\Lambda))$, where Λ is the cotrace of the Hopf algebra. Let us now introduce the plaquette operator for a given orientation of the plaquette and links. We are giving the recipe to construct the diagram given an oriented lattice. We contract the m on the center of the face with the second leg of the Δ: directly if the orientations agree, otherwise we contract with the first leg and we insert an antipode. Remember the legs for the coproduct are numbered clockwise. For the following plaquette 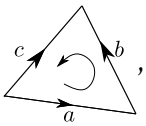 , the plaquette operator is in algebraic maps

$$(\mathbb{1}\otimes\mathbb{1}\otimes m\otimes\mathbb{1})\circ(\mathbb{1}\otimes\tau\otimes\mathbb{1}\otimes\mathbb{1})\circ(\mathbb{1}\otimes\mathbb{1}\otimes\mathbb{1}\otimes m\otimes\mathbb{1})\circ(\mathbb{1}\otimes\mathbb{1}\otimes\mathbb{1}\otimes\mathbb{1}\otimes S\otimes\mathbb{1})\circ(\Delta(a)\otimes\Delta(b)\otimes\Delta(c)),$$

while graphically it is

$$B_p^{\triangle} = \quad (3.9)$$

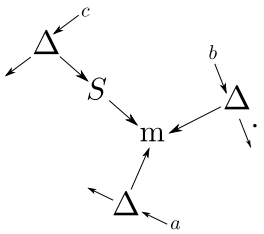

Let us recover the $\mathbb{C}[\mathbb{G}]$ version, to check if we have a coherent definition of the B_p operator. We star from the graphical definition of the operator in 3.9. In the following we apply the definition of the coproduct first, then we expand the multiplication to inspect the order of the elements:

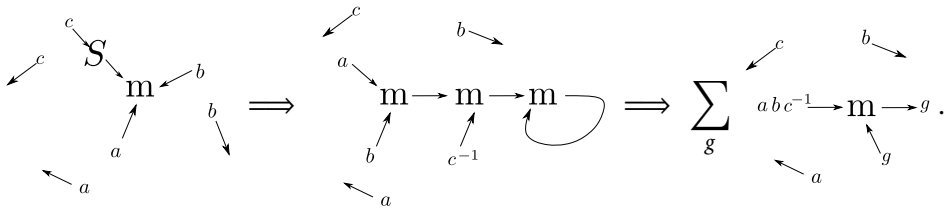

Notice that the rule for the product is to read the legs counterclockwise. We have the identity

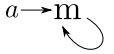

$$= \delta(a, e).$$

You can see we return to the operator in the definition 3.7, when we normalize our definition of the product introducing a new notation, $m_{new} = \frac{m_{old}}{|\mathbb{G}|}$.

We now show the vertex operator with Kuperberg diagram, with the lattice being 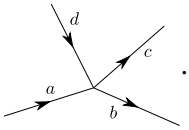

. For the same vertex operator presented before the convention is to set a coproduct Δ in the center of the vertex and for every link a multiplication. We contract the tensors straight on the second leg of the m if the link is towards the vertex, on the contrary we contract on the first leg of m with the addition of an antipode. The vertex operator is

$A_v^{\Delta} =$ 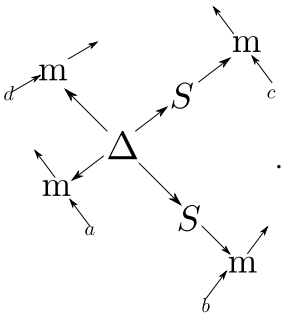

.

We use the definitions for group algebra to verify the operator previously set in 3.4.1 in

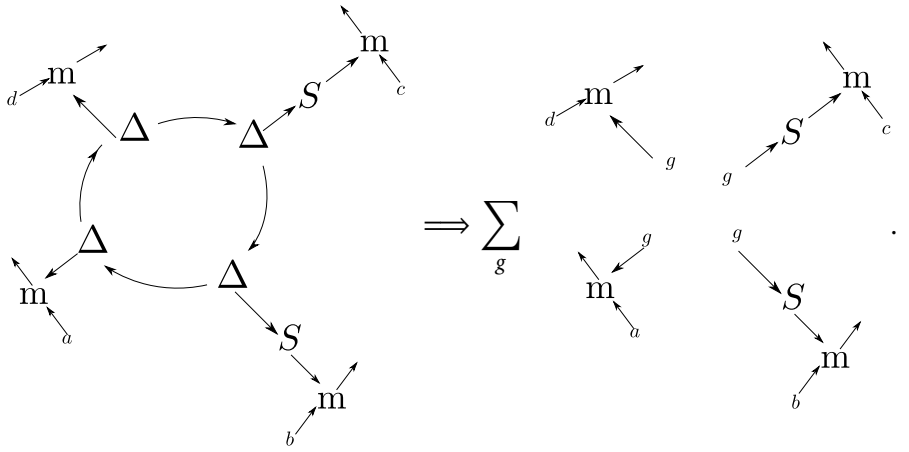

.

Since the coproduct in group algebra just repeats the initial state, the identity is true for every value of g, this is taken care of by the sum. It is now evident that we recover the operator $\sum_g A_v^g$ defined in 3.6 therefore we have to normalize the Δ by a factor $|\mathbb{G}|$, $\Delta_{new} = \frac{\Delta_{old}}{|\mathbb{G}|}$.

Given the rules for setting the operators we now give the proofs of the operators algebra. We switch to a discretization of Σ by a squared lattice, its regularity allows us

to have a definition for the vertex and plaquette operators valid for the entire lattice. We chose the convention to orient all links and plaquettes in the same way. With this setting for the orientation of the lattice 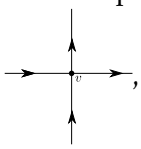

, we can associate a tensor for the A_v operator as in

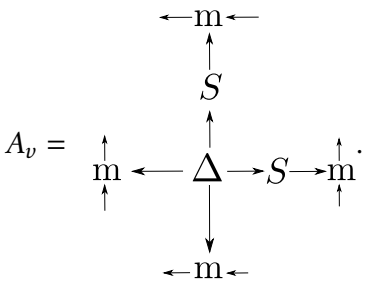

Please note, we have embedded the normalization into the tensor. Every vertex has a factor $|A|$, the dimension of the algebra. This factor corresponds to the normalization for a finite Hopf algebra. Another relevant fact is that we place the antipode when the link is oriented outward the vertex.

We can now include the diagrammatic representation of the product A_vA_v on the same vertex v. In diagram 3.10 we have put subscripts a, d just to distinguish between the two coproducts while we thread our tensors. In the following we apply the initial state to the operator labeled by a, and then to the d operator for every link, it results in

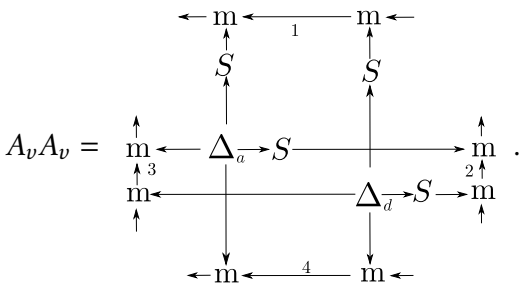

(3.10)

The property of associativity compacts the notation of the products. Then we use the property of the antipode with m to switch the legs order and move the antipodes on

the external arrows,

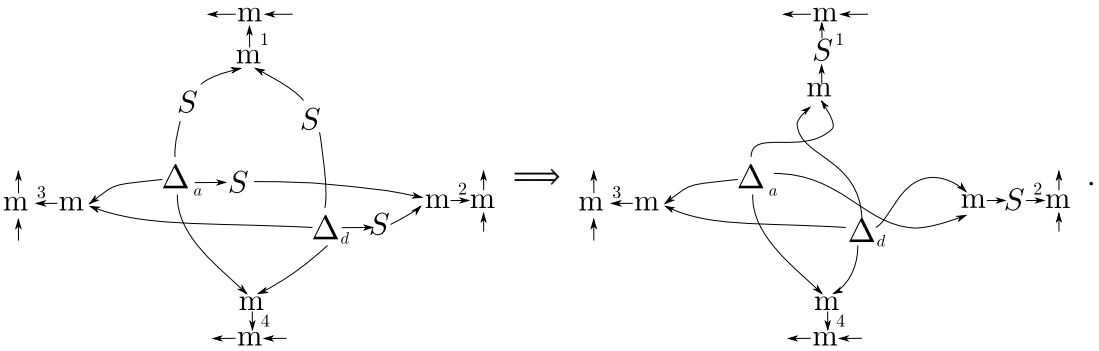

Now we want to use the bialgebra axiom, to do so we rearrange the graphic to make the axiom more visible. Please note that every m has the first leg coming in from the coproduct d, while the second from a. This fact allows us to rearrange the diagram into a bialgebra axiom setting. The bialgebra axiom is more evident if we rearrange the various parts in a horizontal way as shown below. We perform the bialgebra axiom three times, to finally arrive at the last line of calculus where we recover two cotraces multiplied. the product equal to is equal to the dimension of A and the cotrace applied to the series of coproducts. The factor cancels out with the extra factor $\frac{1}{|A|}$ of one Δ. The Δs fuse together, and as final result, we recover a A_v operator.

Graphically it is performed as

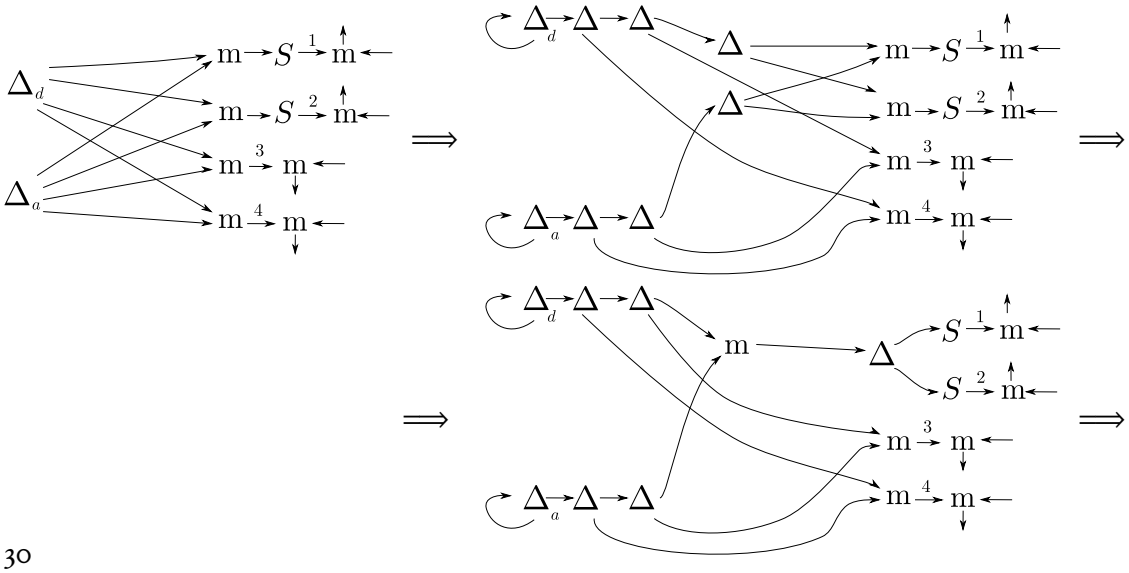

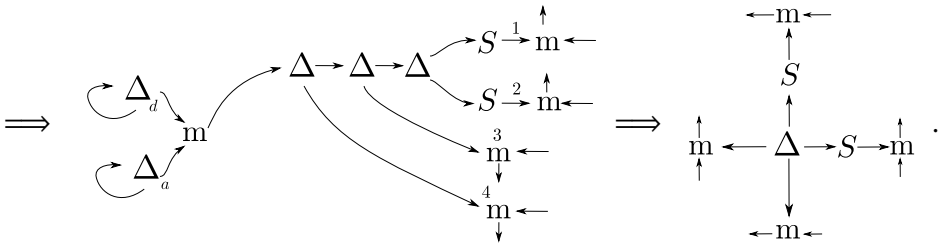

We now show how two vertex operators acting on adjacent vertices commute: $A_{v_1} A_{v_2} = A_{v_2} A_{v_1}$. We have two operators acting on adjacent vertices v_1, v_2 , sharing link 3 in common 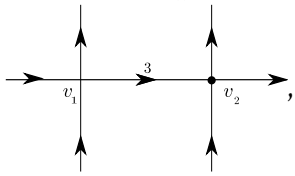 , as in

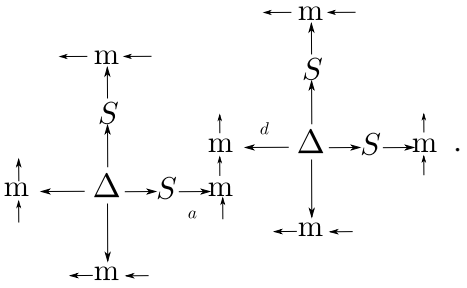

The diagrammatic proof utilizes the notation due to the associativity of the product. The result is straightforward

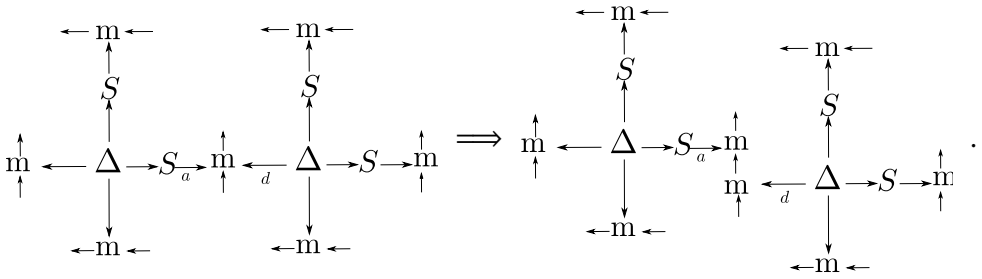

We introduce the realization for the B_p operator for the squared lattice 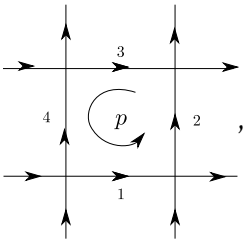 ,

we use the same rules given in the triangular setting, it results in

$B_p =$ 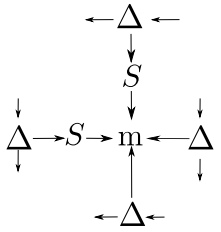 . (3.11)

For the plaquette operator the definition is in 3.11, we position the antipode when the orientation of the link disagree with the orientation of the plaquette, like for links 3 and 4.

We prove that the plaquette operator when two operators act on the same plaquette p results in itself, $B_p B_p = B_p$. As before the subscript $a,\ d$ are just to distinguish between two identical operators,

$B_p B_p =$ 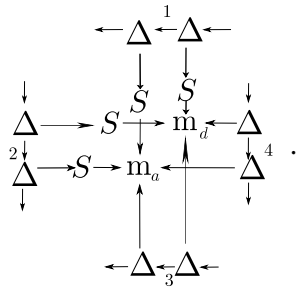 .

Using the coassociativity we first compact the Δs and use the property of the antipode to move them outside the core of the diagram. We see that we have all the multiplications entering first in the d coproduct and then in the a one, so we recognize the bialgebra axiom setting again. The passages are

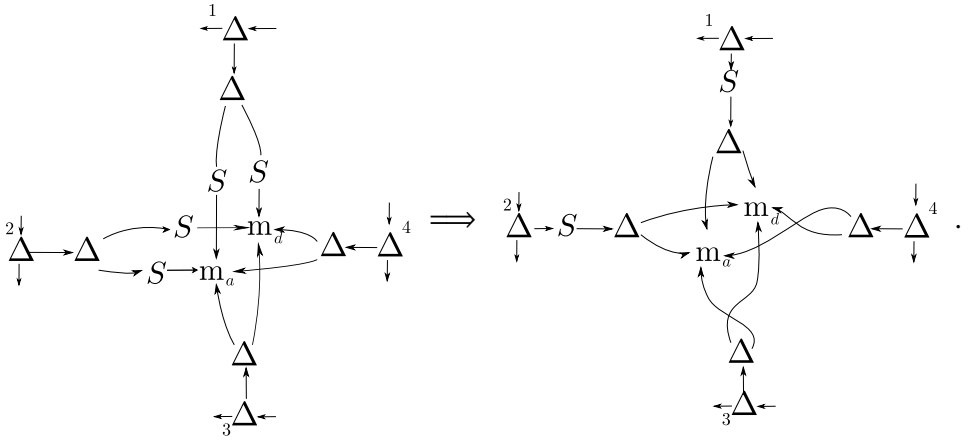

Therefore the last line has two traces applied on a Δ. It is equal the trace applied to the m and a factor equals to the dimension of A. The factor cancels with one extra factor $\frac{1}{|A|}$ embedded in both A_vs at the begging of the calculation. So we recover simply one vertex operator. It is

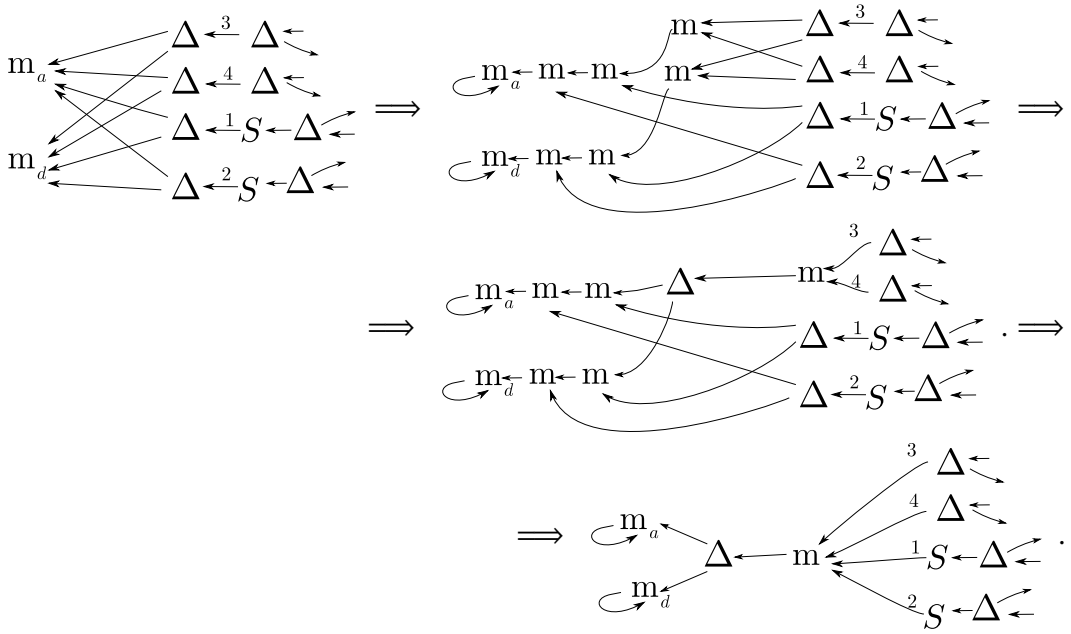

The proof is really equivalent to the previous one for the vertex operators.

We present the relation $B_pA_v = A_vB_p$ using the diagrammatic notation. We consider a plaquette and a vertex positioned as 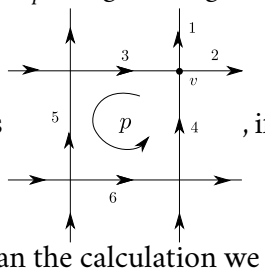 , if v is not a vertex of plaquette p, they commute effortlessly. To clean the calculation we isolate the sole components which interact in diagrams below. All the other tensors are compactified in elements M and D respectively:

$B_p =$ 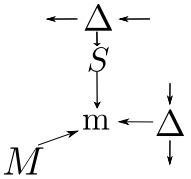 , $A_v =$ 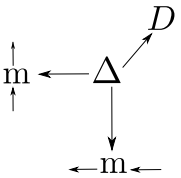 .

For our purpose we set a initial state going in the A_v and after into the plaquette operator, so we stretch both of them in a consequent order. To be compatible with the

entries in the plaquette operator, we need to rotate the order of the entries for m in the A_v. The operation of switching legs of the multiplication is mathematically expressed by the multiplication in the opposite algebra. In our case the Hopf algebra A and the opposite A^{opp} coincide, but we specify the use of m or m^{opp} when switching legs, as in the follow

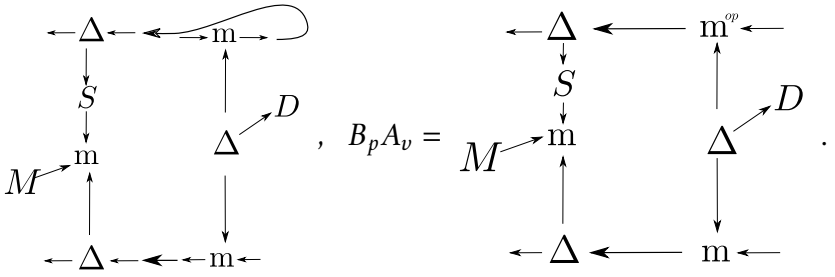

The next steps are to apply the bialgebra axioms and the property of the antipode for the product. We have then a series of products on the left and of coproducts on the right, using the associativity we collapse the notations. The sequence of relations is shown below in a line of diagrams

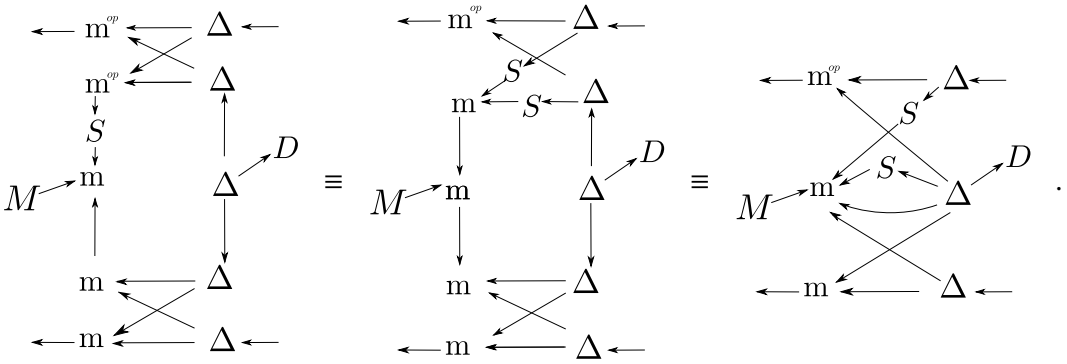

In the next diagram we have used the antipode axiom to uncouple the core of the diagram. In the following diagram we have simply put in plain sight the operators inverted.

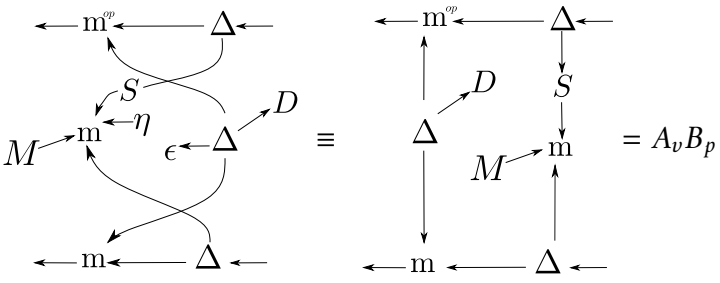

3.4.3 Orientation

Now let's see how a different choice of the orientation in the lattice would have bring us to a different operator and so a different Hamiltonian. We first show the mechanism involving one link in the lattice and how this would change the related plaquette operator. We invert the orientation of link number 4, as in 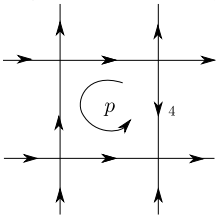

resulting in a different plaquette operator $\widetilde{B}_p$:

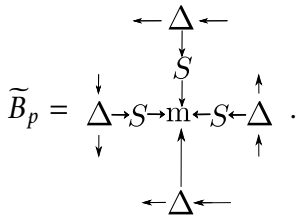

We use simple properties of Hopf algebra to switch to the new orientation from the original operator. We can insert a S^2, which is equal to the identity, to have the new operator conjugated by the antipode $B_p = S\widetilde{B}_p S$. Remember the application of the antipode to the coproduct inverts the legs order, as shown in

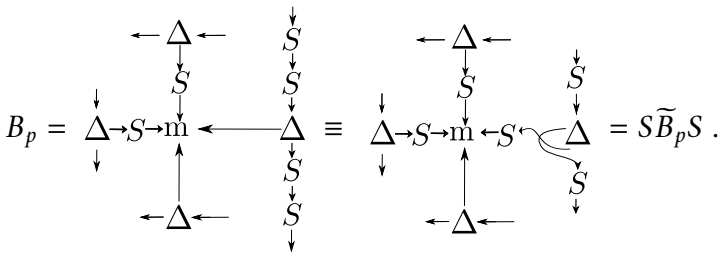

This new operator composes a new Hamiltonian, which is unitary equivalent to the old one, because S is unitary.

3.4.4 Ground State

The Hamiltonian is

$$\mathbb{H} = -\sum_v A_v - \sum_p B_p$$

Since the Hamiltonian is a sum of commuting operators, we want to find a state with the lowest eigenvalues for each operator. We show the construction of one state with

these properties. This will show that we have a frustration free Hamiltonian. We can build at least one vacuum state which satisfies the conditions for the ground state (GS). In this section we consider only the group algebra case. The space of solutions is defined by the following conditions

$$GS = \left\{ |vac\rangle \;\middle|\; A_v |vac\rangle = B_p |vac\rangle = |vac\rangle \;\forall v, p \in \Sigma \right\} .$$

For the construction we can start from a state $|0\rangle$ called seed state. The seed state $|0\rangle$ has the identity element $e \in \mathbb{G}$ for all the links. It naturally satisfies the condition for the holonomy operator. A proposal to construct the vacuum needed is to apply all the A_v operators,

$$|vac\rangle = \prod_v A_v |0\rangle \ .$$

This state is a superposition of states, called loop gas state. We verify what is the behavior of the operators in this vacuum, we check $|vac\rangle$ belongs to the GS set:

$$B_p |vac\rangle = B_p \prod_v A_v |0\rangle = \prod_v A_v B_p |0\rangle = \prod_v A_v |0\rangle = |vac\rangle \;\; \forall p \in \Sigma ,$$
$$A_{\tilde{v}} |vac\rangle = A_{\tilde{v}} \prod_v A_v |0\rangle = A_{v_0} A_{v_1} \dots A_{\tilde{v}}^2 \dots A_{v_n} |0\rangle = \prod_v A_v |0\rangle = |vac\rangle \;\; \forall \tilde{v} \in \Sigma .$$

Here n is the total number of vertices. Note, please that the seed and the new vacuum are different, as the second is a superposition of states after all the gauge transformations. In the following formula for example, we open the n products over the vertices of the sum of N elements of $\mathbb{G}$, we define N the dimension of $\mathbb{G}$, in

$$|vac\rangle = \frac{1}{|\mathbb{G}|^n} (\mathbb{1} + A_{v_0}^{g_1} + \dots + A_{v_0}^{g_N})(\mathbb{1} + A_{v_1}^{g_1} + \dots + A_{v_1}^{g_N}) \dots (\mathbb{1} + A_{v_n}^{g_1} + \dots + A_{v_n}^{g_N}) |0\rangle \ .$$

As we are going to show the dimension of the space GS is an invariant of the surface Λ. This is invariant is related to the first homotopy group, $\pi_1(\Lambda)$. A way to calculate the dimension of ground state is to take the trace of the operator projecting into this subspace. We describe in the next paragraph this operator P_0 and how to build the tensor network associated to it.

3.4.5 Projector Operator

Consider the projector defined by $P_0 := \prod_v A_v \prod_p B_p$. The subspace created by it is non empty as we have shown one fundamental state. Its trace is proportional to the degeneracy of the ground state as proved in [31], so it is

$$GSD \propto tr(P_0).$$

When we take the trace of this tensor network, we just contract all the input arrows with the output ones, one-to-one. The result is the ground state degeneracy (GSD). Remember that for every vertex and every plaquette we integrated a factor $dim(A)$, explained in 3.4.2. The GSD is then

$$GSD = \left(\frac{1}{dim(A)}\right)^{N_v+N_p} tr(P_0) \ .$$

It is an invariant of the surface Λ and the algebra A. To prove this statement we are going to introduce transformations in the tensor network of the projector operator for different triangulations. The transformations are local limited to the interior of a 2-complex, whose boundaries aren't influenced. The transformations require a complicated tensor network of Kuperberg diagrams. We change our notation to better suited diagrams, for the presentation of the transformations.

3.4.6 Curves Diagrams

In this section we realize a more graphical notation of the Kuperberg diagrams, inspired by the Heegaard diagrams. We deal with loops with crossings. We introduce the new dictionary for the algebra maps useful later. This formalism was inspired by the Heegaard decomposition into curves, but we transformed it into something totally new.

Definition 3.4.1. The multiplication is represented as a blue circle with orientation anticlockwise. The arrows coming in are small blue circles, and the arrow going out is a small red one, 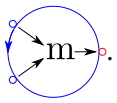

.

Definition 3.4.2. The coproduct is depicted by a red circle oriented clockwise, with a blue small circle coming in a two small circles going out, 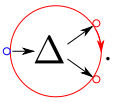

.

Definition 3.4.3. The contraction of the maps is represented with a dotted black line, between the small red circle representing the out arrow to the small blue circle representing the inward arrow, .

The composition of two products with the same orientation in 3.12 means that they can fuse together in a larger blue circle, as in

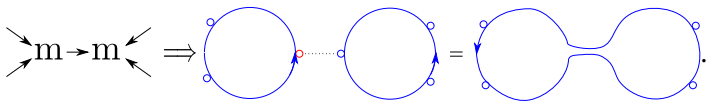

(3.12)

While if they have different orientations in 3.13 they form a loop with a crossing

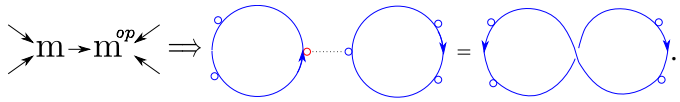

(3.13)

Composing coproducts with the same orientation in 3.14 results in a coproduct with all the input and output arrows left after the contraction, as in

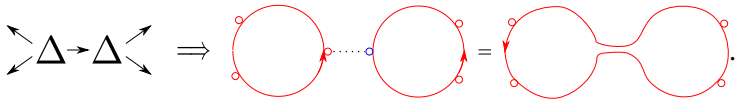

(3.14)

If the circles differ in orientation in 3.15, they form a crossing,

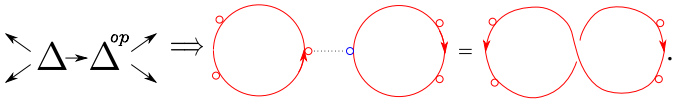

(3.15)

The contraction between the exit of the coproduct and the entry of the product can happen directly as shown in 3.16 or indirectly with the interposition of the antipode S, pictured in 3.17. We represent a zoom on the crossing between the two loops: direct with

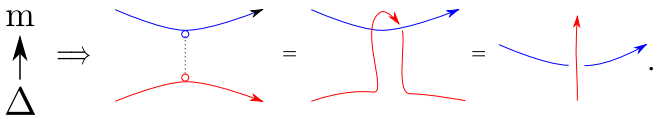

(3.16)

We have the antipode for the case of anticlockwise orientation, in

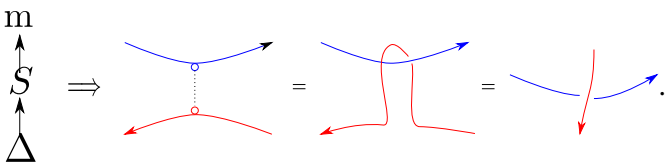

(3.17)

We present a property for the identity arrow 3.18 allowing us to write the arrow identity as the following tensor network

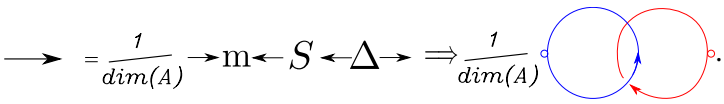

(3.18)

Using this property we can show the contraction between the exit of the product into the coproduct as shown in 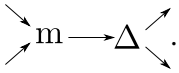

. The result is

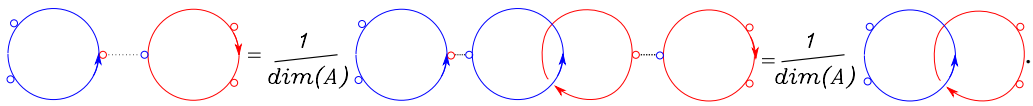

(3.19)

There are special representation for the counit ϵ, $\longrightarrow \epsilon \implies$, and the integral $\lambda \longrightarrow \implies$. The following diagram 3.20 shows the integral applied to the multiplication . The definition of the integral is

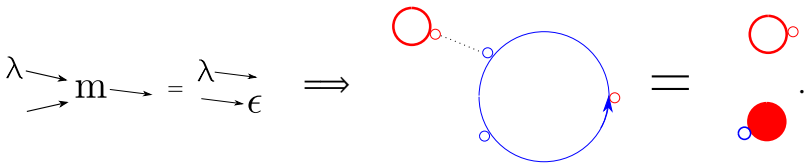

(3.20)

While the diagram 3.21 for the counit applied to the product is

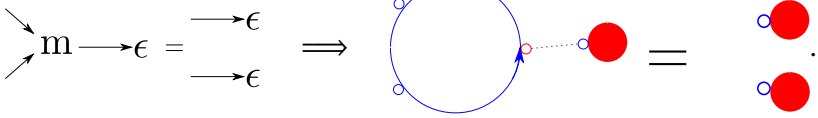

(3.21)

Beyond the contraction of tensors, there are two operations to simplify the diagrams. The first being the sliding 3.22: where a circle can enclose another circle of the same color. The right side has to be consistent with the left one; after choosing an orientation and color for the left side the right side follows. We show a general case in

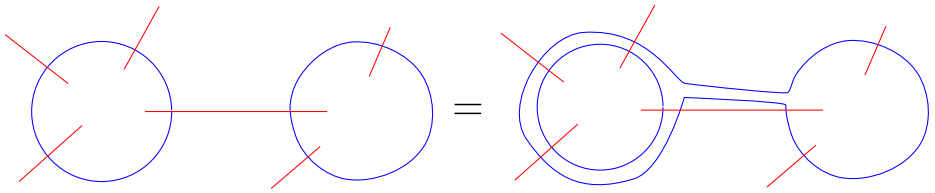

(3.22)

And the two points move 3.23, where if a curve crosses another curve with the opposite color an even number of times then you can uncross the two. The move is valid for whatever orientation and relative color of the curves. We show an example in

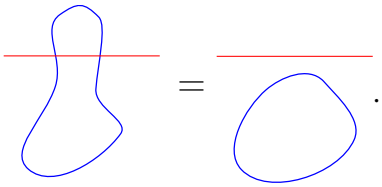

(3.23)

The proof of the equivalence of the diagrams is the sequential application of the Hopf algebra axioms realized in the curve diagrams, it can be found in [29].

Equipped with this dictionary we can derive the definition made for the operators B_p in 3.24. With this definition of the lattice 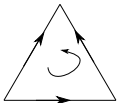 we have associated the operator

in Kuperberg diagrams 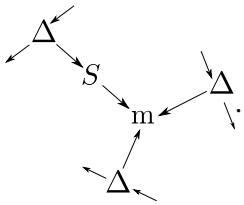

. Then the B_p operator with the circle is

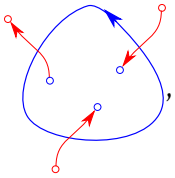
, (3.24)

the red circles are partially drawn as red oriented lines.

We can apply the operator twice, B_pB_p, in the following: we show the contraction of the coproducts at first using 3.14, then we can apply the sliding move 3.22 of the out circle into the inner one. To simplify the diagram we use the two point move 3.23 of the blue external circle over all the red curves, so we can factor out a blues circle. It results in one plaquette operator with a factor equal to the dimension of the algebra represented by a circle without small red and blue circles, as shown in

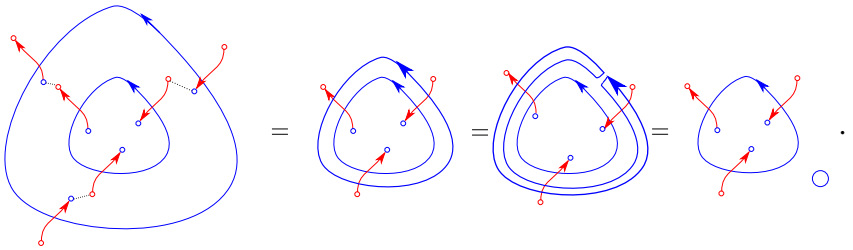

.

For the vertex operator we define our lattice as 
. The definition in the tensor diagram for the vertex operator A_v becomes 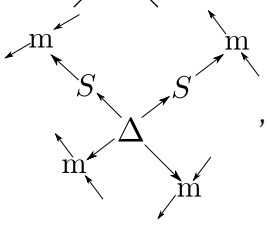

, therefore into curves the A_v is

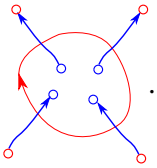
. (3.25)

As before mentioned we sometimes draw the circles with just a portion of them, just as an oriented line, to avoid a cluttered image. In this case we reduce the blue circles into

blue oriented arrows. We can then apply twice the same operator, $A_v A_v$. We perform the contraction 3.12 in the first passage. Then we apply the sliding 3.22 of the external red circle into the internal one. At last we act with the two point move 3.23 of the red external circle over all the blue arrows, we collect a disconnected red circle. The factor is equal to the dimension of the Hopf algebra A. The passages are depicted in

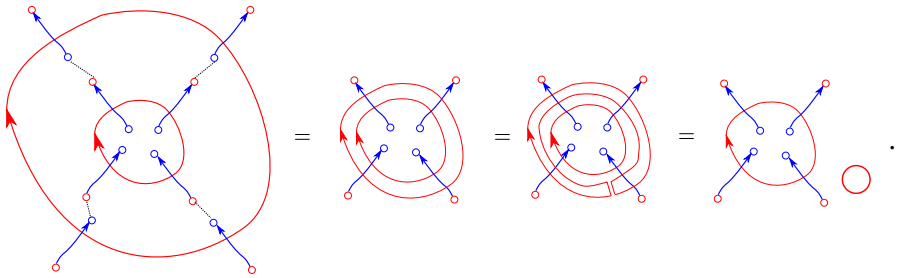

The commutation for the two operators results in the two possible realizations following the two contractions

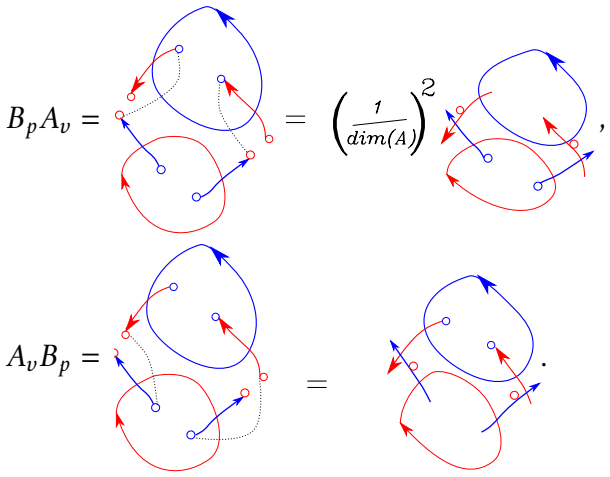

Where in the first line we use the property 3.18 twice.

We present the product of three plaquette operators of adjacent triangles, useful later. We define the lattice and its orientations 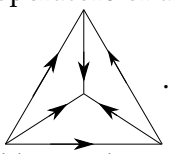 . The associated diagram for the triangles has two versions: one with the blue circles oriented anticlockwise 3.26

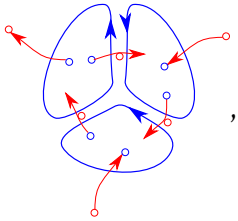

, (3.26)

the other with the blue circles in the opposite direction 3.27

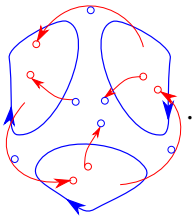

(3.27)

The two versions are the same, they generate the same tensor network, we just change the way we look at it for convenience.

We are ready now to examine the transformation in the tensor network using this diagrammatic formalism.

3.4.7 Transformation of the Tensor Network

As already stated the ground state degeneracy of the model is an invariant only dependent on: the topology of the surface in which is embedded our model, and the finite algebra associated to the links.

To demonstrate the topological nature of the model we apply transformations on the lattice allowed by the Pachner moves [6]. If two triangulations are homeomorphic there is a sequence of Pachner moves connecting them. The moves change locally a triangulation.

We are going to associate to every Pachner move a transformation M in the tensor network. Applying the transformation M, the tensor network associated to $P_0^{(1)}$ changes into the tensor network associated to $P_0^{(2)}$ of the transformed lattice.

$$\begin{array}{ccc} \text{Triangulation } T^{(1)} & \xrightarrow{\text{Pachner move}} & \text{Triangulation } T^{(2)} \\ \downarrow & & \downarrow \\ \text{Hilbert space } \mathcal{H}^{(1)} & \xrightarrow{\text{Transformation } M} & \text{Hilbert space } \mathcal{H}^{(2)} \\ \downarrow P_0^{(1)} & & \downarrow P_0^{(2)} \\ \text{Hilbert space } \mathcal{H}_0^{(1)} & \xrightarrow{\text{Transformation } M} & \text{Hilbert space } \mathcal{H}_0^{(2)} \end{array}$$

We will prove the commutation of the last square diagram above.

Theorem 3.4.4. *Each transformation M satisfies:*

$$MP_0^{(1)} \simeq P_0^{(2)} M$$

The 2D moves introduced by Pachner are the flip, the cancellation and the subdivision. In the following we define the transformation of the tensor network for every Pachner move.

Subdivision move

The subdivision D move changes the triangulation introducing three more links around a new vertex. The vertex is situated in the interior of a triangle whose boundaries are not modified by the move. The transformation between the Hilbert spaces is $D : \mathcal{H}($  $) \rightarrow \mathcal{H}($ 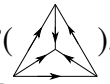 $)$. We create the curve diagram of the transformation modifying the three B_p operators presented above in 3.26 and 3.27. We contract the entries for the internal links with integrals: in this way we obtain the D transformation with three entries and six output arrows. We present two versions with anticlockwise oriented blue circle and with the opposite orientation. It results in

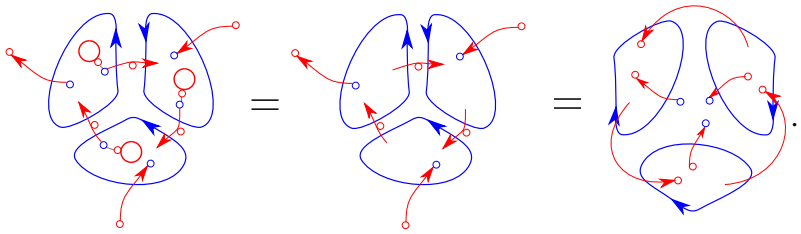

Cancellation move

In the cancellation move C the triangulation changes from three adjacent triangles whose boundaries form a larger triangle to just the external triangle. Therefore the move cancels the internal vertex and links, resulting in one triangle. The Hilbert space transformation is $C : \mathcal{H}($  $) \rightarrow \mathcal{H}($  $)$, so this move has six input arrows, while only three output ones. The diagram is built by using counits in the outputs of the three internal links, as

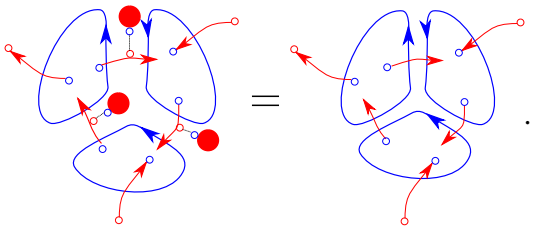

You may have noticed that the C transformation is the opposite move of the subdivision D. We are ready now to prove that the composition of them results in an operator. First we show the subdivision followed by the cancellation CD.

Theorem 3.4.5. *The composition CD is proportional to the plaquette operator applied on the external triangle*

$$\rightarrow D \rightarrow C \rightarrow \propto \rightarrow B_p \rightarrow .$$

To prove this statement we start from an Hilbert space $\mathcal{H}($  $)$, we apply the subdivision, then the cancellation. We use the curves transformations in the anticlockwise blue circles versions. The first diagram is the contraction of the outputs of D with the entries of C using 3.14. To avoid misunderstanding, we put the cancellation move more external in dashed lines and we underline real crossings between curves with black dots. In the following diagram, we already show all the contractions in place, and we start to simplify with sliding of the internal blue circles with the respective external blue circles using 3.22. Then we can use the two points moves 3.23, we disconnect three blue circle leading to factors multiplying the diagram. We proceed by sliding one blue circle over the others with 3.22, and recognizing the property of the integral 3.20 to simplify the two remaining internal blue circles. We can factor two blue circles crossing red circles. We recover a plaquette operator for the initial large triangle, with factor equivalent to the dimension of the algebra to the fifth power, in 3.28. The sequence of operations is

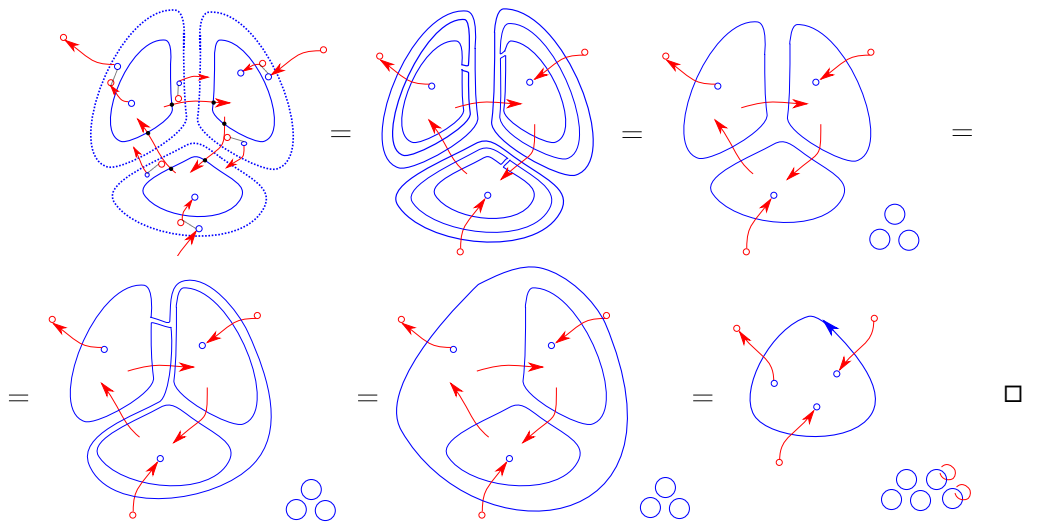

(3.28)

When we change the order: we start with the cancellation (internal diagram in the anticlockwise version) and after the subdivision (more external, clockwise version),

$\longrightarrow C \longrightarrow D \longrightarrow$, shown in

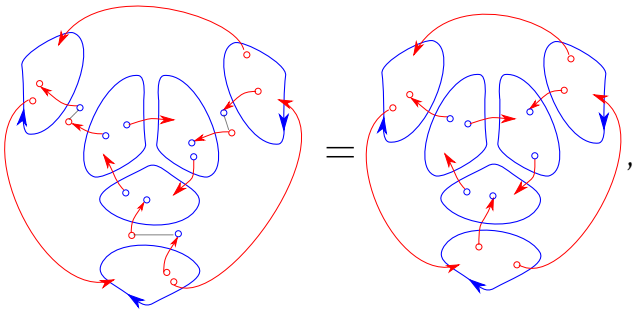

(3.29)

where we show the contraction of the exits of the C with the entries of the D transformation using 3.14.

Theorem 3.4.6. *The diagram 3.29 is equivalent to part of the projector to the ground space in* $\mathcal{H}($ 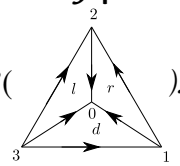

$)$. *More in specific to three plaquette operators for the three triangles, the vertex operator for the internal vertex and again three plaquette operators,* $\longrightarrow C \longrightarrow D \longrightarrow = \longrightarrow B_{p_l} B_{p_r} B_{p_d} \longrightarrow A_{v_0} \longrightarrow B_{p_l} B_{p_r} B_{p_d} \longrightarrow$, *whose curve diagram is shown in 3.30.*

In this composition we have the first three plaquette operators internal. Their outputs are connected with the vertex diagram using 3.19, whose outputs are linked to the three plaquette operators external in the clockwise version using 3.14. After contracting we have a factor $dim(A)^3$. We can proceed by applying the sliding moves 3.22 over the blue circles multiple times, until we can factor two blue circles out. In the last passage we can use the property of the integral 3.20, factoring out a blue circle crossed with a red circle. The factor made by the circles cancels out the $dim(A)^3$ in the front. We have proved that the last diagram in 3.29 is equal to the last diagram in 3.30.

$B_{p_l} B_{p_r} B_{p_d} A_{v_0} B_{p_l} B_{p_r} B_{p_d} \Longrightarrow$ 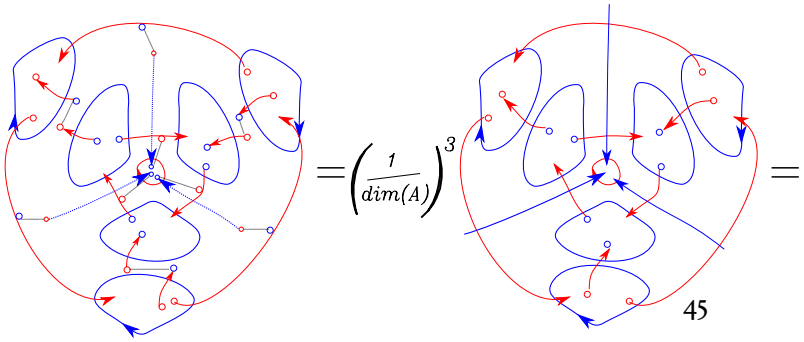

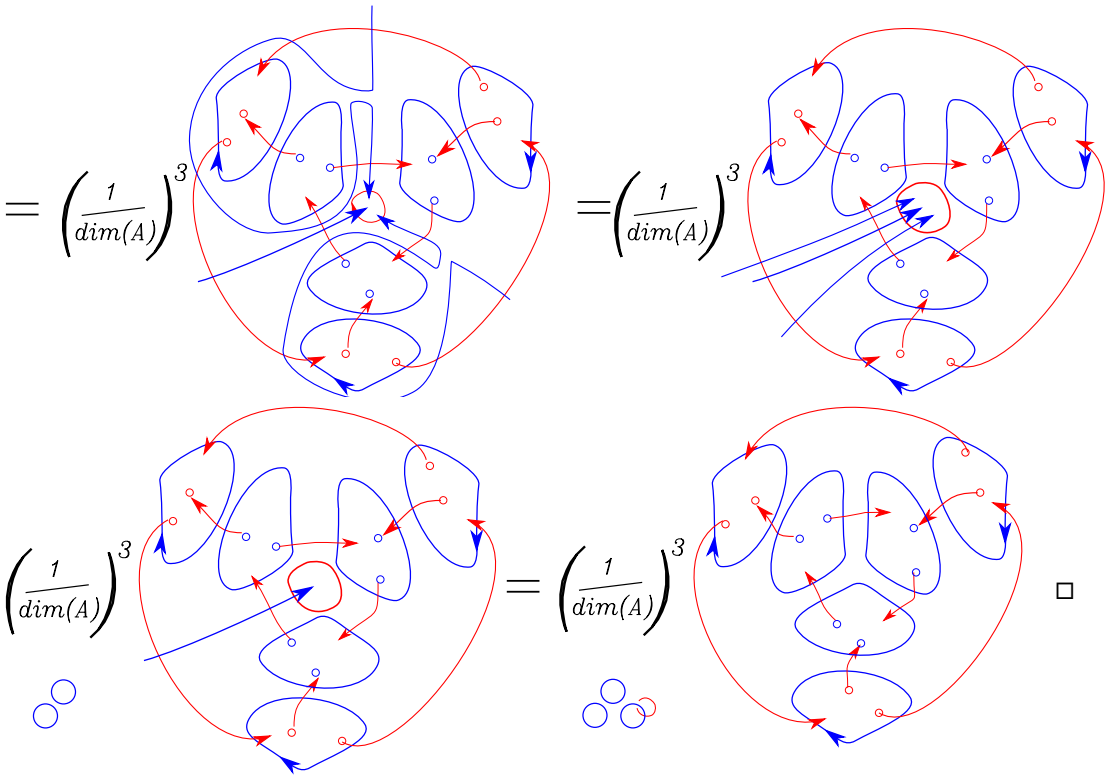

(3.30)

Flip move

The flip move F involves two adjacent triangles. In the diagrams we have numbered the vertices just to help the reader, $F : \mathcal{H}\Big($ 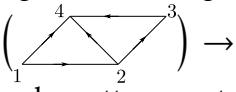 $\Big) \to \mathcal{H}\Big($ 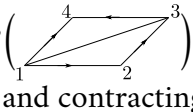 $\Big)$. We build the move as before starting from the plaquette operators and contracting the output for the link we want to cancel with the counit. We apply the integral to the input of the new link introduced. The blue circles for the starting triangles are on the left with on the right, vertically, the circles for the final triangles, as shown on the left side of 3.31. On the right side we show the same transformation with the vertical blued circles flattened into arrows. We do so to have a better view of the composition with

the opposite move we are going to need below. The transformation results in

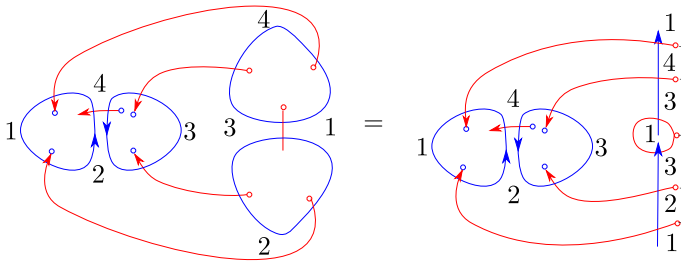

(3.31)

The transformation is its own opposite, considering a rotation.

Theorem 3.4.7. *The composition FF^{-1} is equivalent to two plaquette operators in the initial ground state space, $\rightarrow F \rightarrow F^{-1} \rightarrow\propto\rightarrow B_pB_p \rightarrow$.*

To prove it we contract the two transformation in the first line of sequence of diagrams in 3.32 using 3.14. Then we can start applying the sliding moves 3.22 over the blue circles, factoring them out. As before when a red circle crosses just one blue circle we can factor both of them out using the property of the integral 3.20. The factor is $dim(A)^6$ shown in the last diagram of the following sequence of 3.32:

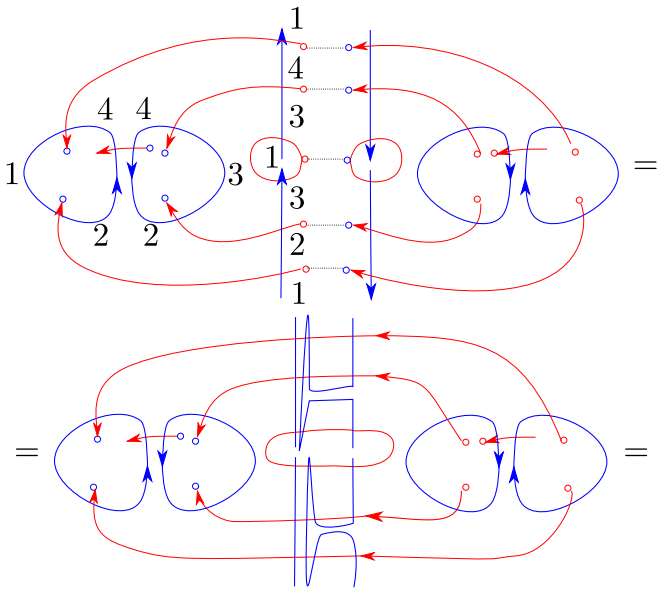

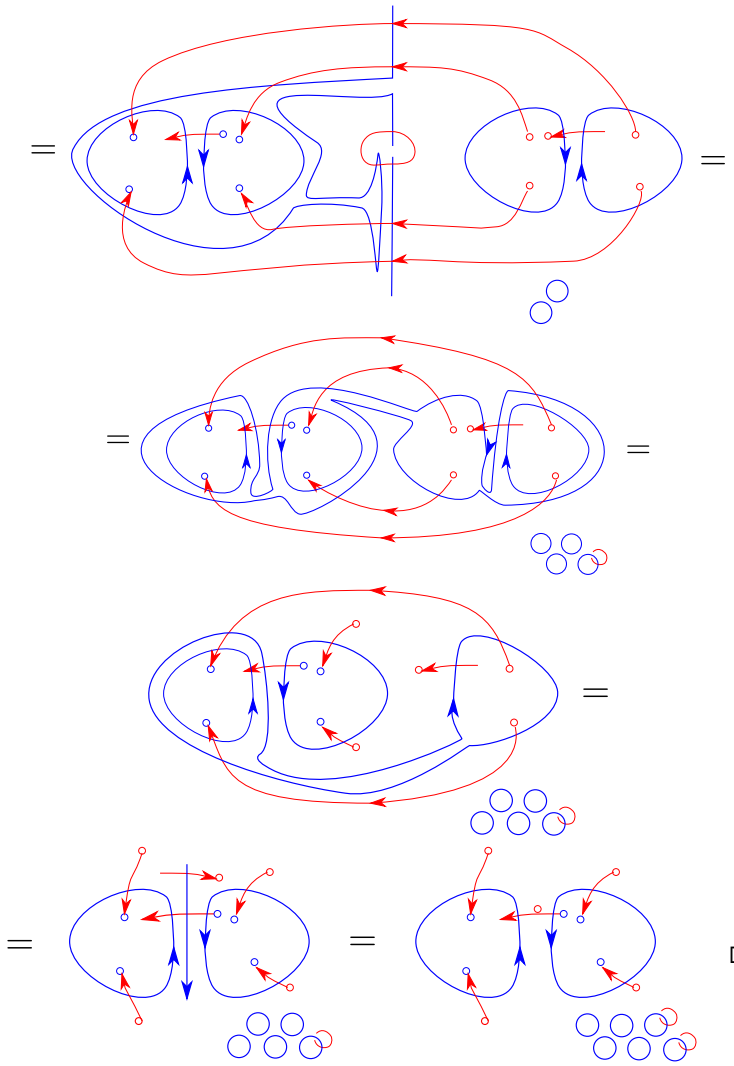

□ (3.32)

Yet we still have some work to prove that every move M satisfies the relation $P_0^{(1)} M \simeq M P_0^{(2)}$. We have only proved the following relations:

- $DC = B_{p_l} B_{p_r} B_{p_d} A_{v_0} B_{p_l} B_{p_r} B_{p_d}$
- $CD \propto B_p$
- $FF^{-1} \propto B_p B_p$.

We remember that the ground state projector is $P_0 = \prod_v A_v \prod_p B_p, \ \forall v, p \in \Sigma$. We focus only on the small region Σ_M of the triangulation, which contains the triangles modified by the Pachner move. The only operators involved are the plaquette operators

of the triangles and their vertex operators. We showed the relation of the transformations with part of the projector: we are left to consider only the vertex operators of the vertices on the boundaries of Σ_M. These operators are the ones to achieve the desired relation: $P_0^{(1)} M \simeq M P_0^{(2)}$.

We can manipulate the relation $CD \propto B_p$ of Theorem 3.4.5 applying the division move $D : \mathcal{H}^{(1)}($  $) \rightarrow \mathcal{H}^{(2)}($ 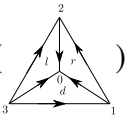 $)$ on both sides. We can then use the relation $DC = B_p^d B_p^l B_p^r A_{v_0} B_p^d B_p^l B_p^r$ of Theorem 3.4.6, to obtain

$$DCD \propto DB_p$$
$$B_p^d B_p^l B_p^r A_{v_0} B_p^d B_p^l B_p^r D \propto DB_p.$$

To complete the projector operator we multiply on the right the vertex operators of the external vertices,

$$B_p^d B_p^l B_p^r A_{v_0} B_p^d B_p^l B_p^r D A_{v_1} A_{v_2} A_{v_3} \simeq DB_p A_{v_1} A_{v_2} A_{v_3} = DP_0^{(1)}.$$

Theorem 3.4.8. *The transformation D satisfies $DA_{v_1}^{(1)} A_{v_2}^{(1)} A_{v_3}^{(1)} = A_{v_1}^{(2)} A_{v_2}^{(2)} A_{v_3}^{(2)} D$.*

To built the D move we chose the plaquette operators of three triangles and we contracted the entries of the internal links with integrals. We can consider the move in parts: we remove the integrals it results in the three plaquette operators. We already have proved that the plaquette operators commute with the vertex ones, so we perform the commutation and we are left with the integrals applied to the vertex operators. We concentrate ourselves just on one vertex operator for the proof. We show the relevant part of the vertex in $T^{(1)}$: 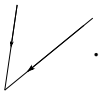 . After the subdivision move one triangle transforms into three, so there is an additional link in the vertex of $T^{(2)}$:  . We can apply the property of the integral 3.20, so we generate the new link in $T^{(2)}$, as shown in

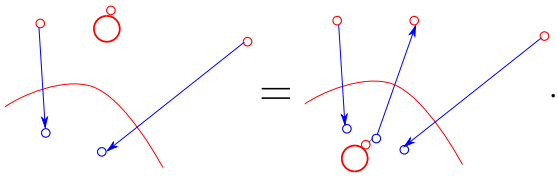

The same resolution is applied in the other direction from in $T^{(2)}$ to $T^{(1)}$, using the

same property in the opposite direction. It results in

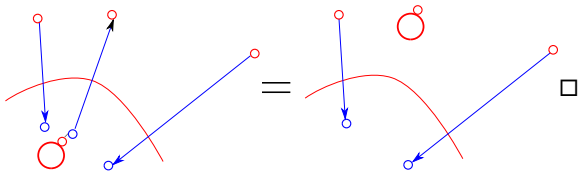

□ (3.33)

We can conclude that $P_0^{(2)} D = D P_0^{(1)}$. The proof for the other transformations, C and F, retraces exactly the same steps, to the same result.

4 Group Quantum Double Model

In the previous chapter we have prepared all the ingredients to realize the calculation for the Kuperberg invariant. In the following with the due modification we can use the path paved for the new invariant. We show the necessary steps allowing us to prove the diffeomorphism invariance with the transformation of the tensor network associated to the ground state projector and the monodromy invariance for K_H.

Topological quantum field theories (TQFTs) can be generalized by replacing manifolds by maps from manifolds to a fixed target space V. In this way we obtain homotopy quantum field theories (HQFTs). In this thesis we are interested in realizing the theory only for surfaces, connecting our model's ground state degeneracy to the K_H.

The Quantum Double Model is a family of exactly solvable lattice models proposed by Kitaev in [16], where the mathematical structure is a finite dimensional Hopf Algebras. As we have described in the previous chapter, a Hopf algebra has a self-dual structure; the self duality between algebra and coalgebra is no longer truth in the new setting. We have in the Group Quantum Double Model (G-QDM): a set of algebras, a set of homomorphisms between algebras as coproducts and a set of homomorphisms as antipodes. An extensive analysis of the algebraic properties can be found in [34].

Our aim is to construct Hamiltonian model with the maps of a finite dimensional Hopf group coalgebra. We will rely on a diagrammatic proof valid for the invariant à la Kuperberg associated to the ground state of the Hamiltonian model.

4.1 Hopf G-Coalgebra

In our model the Hilbert space is characterized by the involutory Hopf group coalgebra proposed by Turaev in [33]. A Hopf group coalgebra is a family of algebras over the field $\mathbb{C}$, denoted by $H = \{H_\alpha\}_{\alpha\in G}$ with G a finite group. The algebras have the same finite dimension, this is a consequence of being an algebra over a field of characteristic zero, like the complex numbers. H is also semi-simple, so every algebra H_α must be semi-simple, and ${H_1}^\dagger$ must be finite dimensional.

[†]With the number 1 we design the identity element of G.

Let us first introduce the formalism for the Hopf group coalgebra and its diagrammatic representation, later used in the definitions of the model. The Hopf group coalgebra is endowed with a family of algebra homomorphisms, the coproducts $\Delta = \{\Delta_{\alpha,\beta} : H_{\alpha\beta} \to H_\alpha \otimes H_\beta\}_{\alpha\beta\in G}$. An algebra homomorphism $\epsilon : H_1 \to \mathbb{C}$ is

the counit. And a family of anti-homomorphisms $S = \{S_\alpha : H_\alpha \longrightarrow H_{\alpha^{-1}}\}_{\alpha \in G}$ are the antipodes. We show in the list below all the homomorphisms, where to specify the different spaces, we label the arrows with red Greek letters:

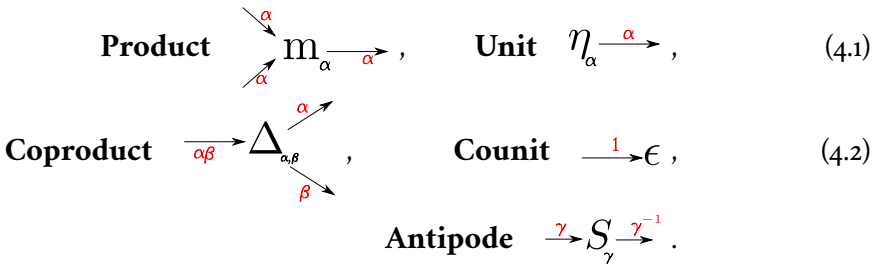

4.1.1 Algebra

Each algebra H_α is unital and associative respect to the multiplication $m_\alpha : H_\alpha \otimes H_\alpha \longrightarrow H_\alpha$, endowed with a right/left unit $\eta_\alpha : \mathbb{C} \longrightarrow H_\alpha$. We have the equation $m_\alpha(\eta_\alpha \otimes 1_\alpha) = 1_\alpha = m_\alpha(1_\alpha \otimes \eta_\alpha)$. The input elements of the product in the graphical notation have the order fixed by the anticlockwise order from the output. As an example the product $m_\alpha(v \otimes w)$ would have the element v in the uppermost arrow of the diagram in 4.1. We show the equation in diagram:

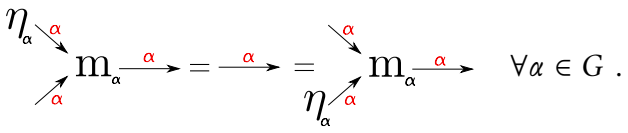

The usual definition of opposite algebra applies to H_α, therefore we can construct the opposite product m^{op}. The opposite product is realized switching the inputs, it is defined by $m_\alpha^{op}(v \otimes w) = m_\alpha(\tau(v \otimes w))$. The switching is done by the map $\tau : v \otimes w \longrightarrow w \otimes v$, $\forall v, w \in H_\alpha$. Thus, the reading order is clockwise in the opposite product.

For all $\alpha \in G$ the product satisfies the associativity: $m_\alpha(m_\alpha(v \otimes w) \otimes z) = m_\alpha(v \otimes m_\alpha(w \otimes z)) = m_\alpha(v \otimes w \otimes z) \quad \forall v, w, z \in H_\alpha, \forall \alpha \in G$. Let us see the equivalent realization in diagrams, where to underline the generality we cancel the input elements of the diagrams. The order of the input legs are respected in the last diagram of a multiple product:

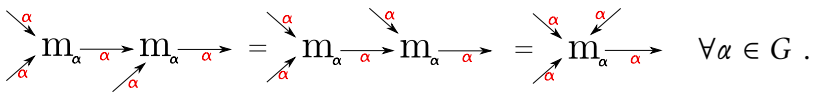

The left and right traces are considered equal. In the following definition when we show a product with just arrows pointing in, it means the exit arrow is contracted with

one input, it is a trace:

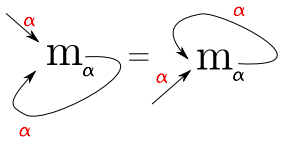

$\forall \alpha \in G$.

4.1.2 Homormophism between Algebras

The coproducts are algebra homomorphisms acting on different spaces. The compatibility is granted by combinatoric of all pairs α, β equal to the product $\alpha\beta$. The counit exists only in the H_1 algebra, this implies the following diagrams. The definition of left/right counit is $(1_{H_\alpha} \otimes \epsilon)\Delta_{\alpha,1} = 1_{H_\alpha} = (\epsilon \otimes 1_{H_\alpha})\Delta_{1,\alpha}$. In the Δ diagram the order for writing the outputs is clockwise respect to the input leg as in diagram 4.2. The contraction of the maps results in:

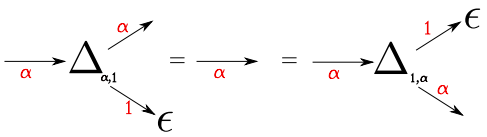

$\forall \alpha \in G$

The coproduct as well has an opposite coproduct that switches the output by the map introduced: $\Delta^{op}(v) = \tau \circ \Delta(v)$.

The coproducts obey the compatibility between different algebras to realize the equivalent of the coassociativity. Such that for all α, β, $\gamma \in G$ is $(1_{H_\alpha} \otimes \Delta_{\beta,\gamma})\Delta_{\alpha,\beta\gamma} = (\Delta_{\alpha,\beta} \otimes 1_{H_\gamma})\Delta_{\alpha\beta,\gamma} = \Delta_{\alpha,\beta,\gamma}$. The relation at the end show the general notation respecting the order of the external legs in a compact way, pictured as

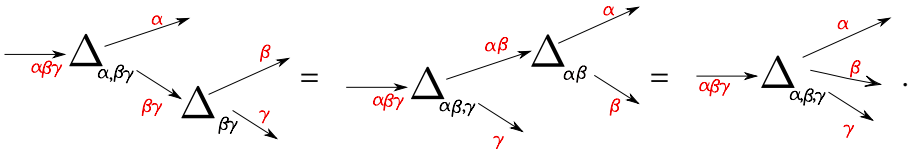

.

The cotrace left and right are equal and are described by the following diagram 4.3. Whenever we consider a coproduct with just arrows pointing out it means that the arrow pointing in is the cotrace, which only allows the identity algebra H_1 as internal cycle. The cotrace is:

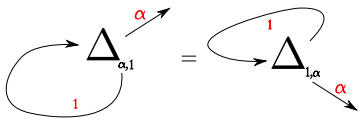

$\forall \alpha \in G$. (4.3)

4.1.3 Compatibility Axioms

The compatibility between the algebras and the homomorphisms is granted by a series of equivalences. The bialgebra axiom is the compatibility between the products and the coproduct maps. There are the same realizations of the axiom substituting the products for the opposite maps, or the coproducts for the opposite, or both in

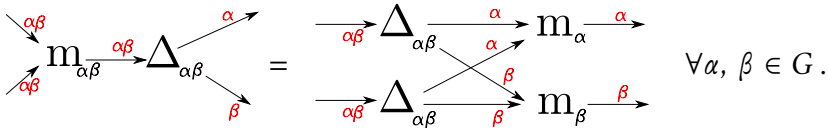

$\forall \alpha,\ \beta \in G\,.$

The compatibility between the algebras and the homomorphisms imposes also the diagrams between units and coproducts, which involves different algebras,

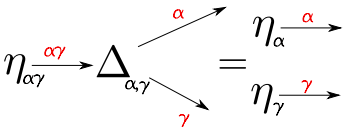

$\forall \alpha,\ \gamma \in G.$ (4.4)

The compatibility for the counit and product is possible only in the H_1 algebra, as shown in

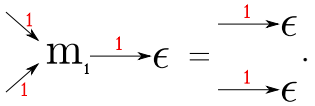

4.1.4 Antipode

The role for the anti-homomorphism S_α is played by a homomorphism between algebras labeled by the opposite element of G. The antipode axiom is valid for every H_α, the position for the map in the internal leg is irrelevant. The axiom expression is $m_\alpha\left(S_{\alpha^{-1}} \otimes 1_{H_\alpha}\right)\Delta_{\alpha^{-1},\alpha} = \eta_\alpha \epsilon = m_\alpha\left(1_{H_\alpha} \otimes S_{\alpha^{-1}}\right)\Delta_{\alpha,\alpha^{-1}}$. While in diagram it is:

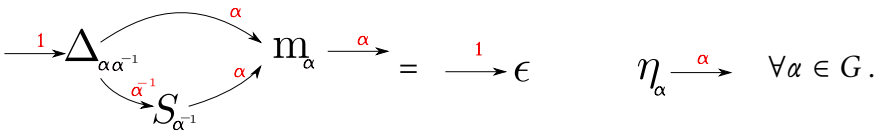

An important property is the compatibility of the antipode maps with the multiplications. For each algebra γ the property is: $m_{\gamma^{-1}}(S_\gamma \otimes S_\gamma) = S_\gamma \circ m_\gamma \circ \tau\ \forall \gamma \in G$. Its realization in diagram is 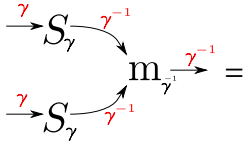

$=$ 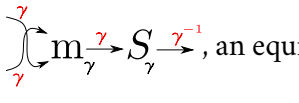

, an equivalent property is valid for the coproduct.

The antipode applied to the output of the unit cancels out with a change in the algebra, $\eta_\alpha \xrightarrow{\alpha} S_\alpha \xrightarrow{\alpha^{-1}} = \eta_{\alpha^{-1}} \xrightarrow{\alpha^{-1}}$.

When the antipode is applied to the counit, it can be canceled $\xrightarrow{1} S_1 \xrightarrow{1} \epsilon = \xrightarrow{1} \epsilon$

4.1.5 Integrals

The Hopf G-coalgebra has a right/left G-integral Λ_α for every algebra H_α. In contrast it is endowed with a right/left integral only for the algebra H_1. They are unique in the Hopf G-coalgebra, to prove this statement we modify the proof of Kauffman and Radford to adapt it with the labels [49, 34]. The definition for the left G-integral is $(\Lambda_\alpha \otimes 1_\beta)(\Delta_{\alpha,\beta}) = \Lambda_{\alpha\beta}\eta_\beta$, while in diagram results in

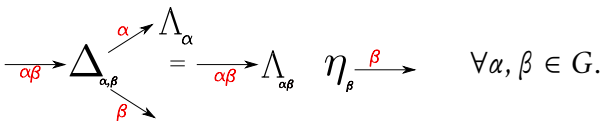

For the right G-integral the outputs are switched $(1_\alpha \otimes \Lambda_\beta)(\Delta_{\alpha,\beta}) = \Lambda_{\alpha\beta}\eta_\alpha$, so it results in

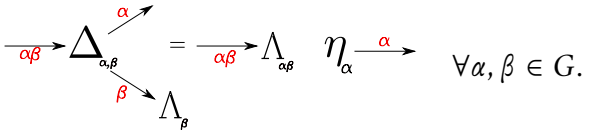

For the left integral we have the following definition: $m_1(\lambda_1 \otimes 1_1) = \lambda_1\epsilon_1$, in diagram $\lambda_1 \xrightarrow{1}$, $1 \xrightarrow{}$ $m_1 \xrightarrow{1} = \xrightarrow{1} \epsilon \quad \lambda_1 \xrightarrow{1}$. The right integral realizes $m_1(1_1 \otimes \lambda_1) = \lambda_1\epsilon_1$, which is pictured as $1 \xrightarrow{}$, $\lambda_1 \xrightarrow{1}$ $m_1 \xrightarrow{1} = \xrightarrow{1} \epsilon \quad \lambda_1 \xrightarrow{1}$.

The proof for the uniqueness of the integrals needs a step ahead, the Ladder Lemma:

Lemma 4.1.1 (Ladder Lemma). *The diagrams*

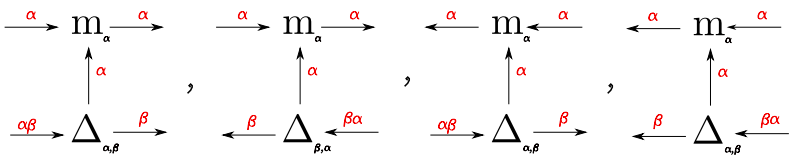

have an inverse diagram which composed with them results in their input arrows diagram. The inverse diagrams are a copy of the original ones with an antipode in the internal arrows

from the coproduct to the multiplication. The inverses are

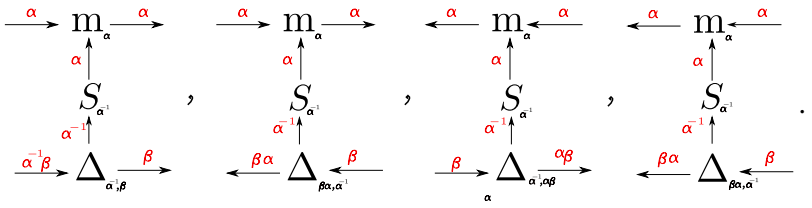

An equivalent realization takes place when there are maps like m^{op}, Δ^{op} or both of them.

The proof for the uniqueness of the G-integral and integral starts from the bialgebra axiom where we apply the integral and G-integral. After that we apply the proper definition of integrals. To arrive at the 4.5, we just wrote the first diagram in a more clear way. After that we apply repeatedly on both sides the inverse diagram needed to cancel out parts of the left side diagram.

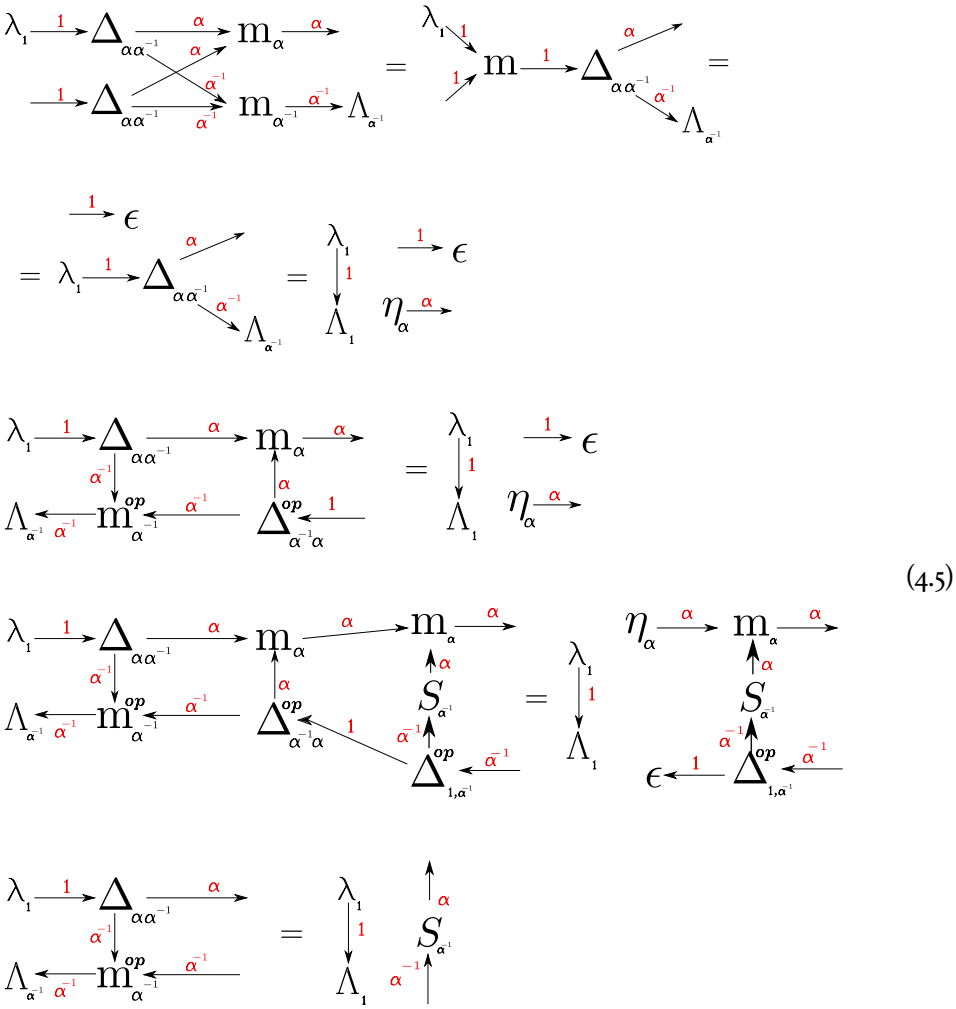

(4.5)

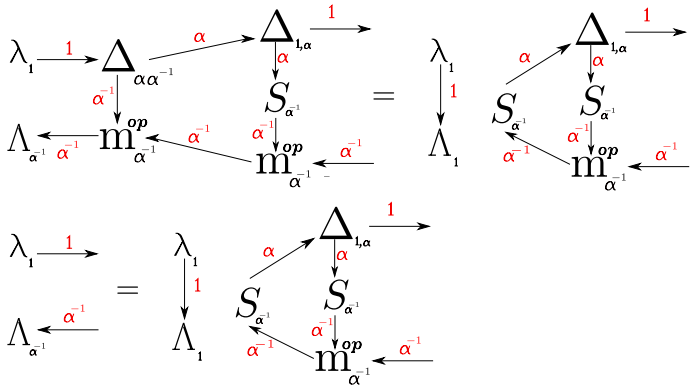

(4.6)

The result finds the relation of proportionality between the cointegral and the trace, calculating its numerical factor. In our Hopf group coalgebra the proof is valid in every H_α algebra. The trace rotates in the clockwise direction for the right integral and the opposite direction for the left integral. The cointegral is:

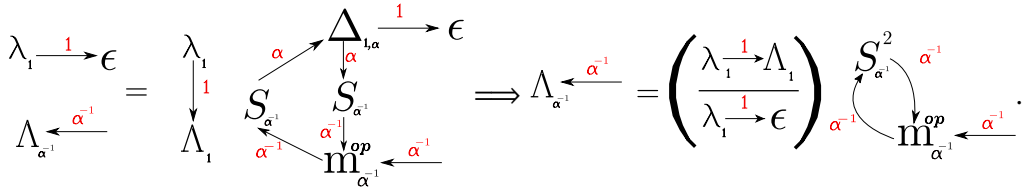

The same sequence of diagrams 4.6 proves also the relation of proportionality between the cotrace and the integral. The integral exists just in the H_1, but the proportional factor for the cotrace depends on the algebra H_α. The rotation in the cotrace depends if we choose in the first diagram to use the left or right integral. A similar proof can be done for the right integral resulting in the opposite direction for the internal loop in the cotrace. The integral is:

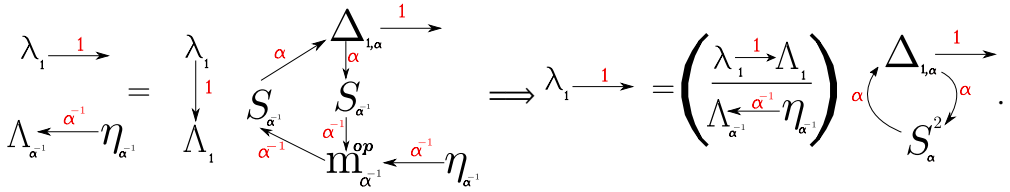

(4.7)

Let's try to make sense of this factors using another identity. In the proof below at first we use the identity 4.4, then the proper definition of the G-integral. Thus, the two contractions $\Lambda_\alpha(\eta_\alpha)$, $\Lambda_1(\eta_1)$, are equal:

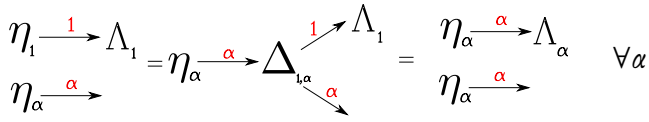

To fix the value of the other factor we need to introduce an equivalence for involutive algebras, knowing that for every α: $S_\alpha^2 = 1_\alpha$, its trace is the dimension of the algebra H_α,

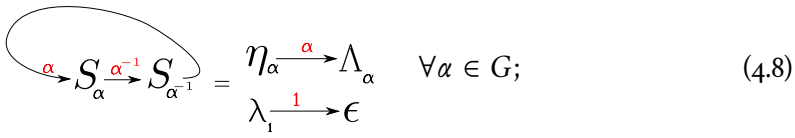

$\forall \alpha \in G;$ (4.8)

so the late fixes $\epsilon(\lambda) = dim H_1$.

4.1.6 Hopf Algebra

Only H_1 possesses all maps to be a Hopf algebra. Just as a curiosity we mention that we can recover a full finite Hopf algebra by a direct sum of all the algebras, as G is a finite group $\overline{H} = \bigoplus_\alpha H_\alpha$. It is naturally endowed with the following maps $(\overline{H}, \overline{m}, \overline{\eta}, \overline{\Delta}, \overline{\epsilon}, \overline{S})$. Where the multiplication is restricted to one algebra, the counit is unique, the other maps are sums over the algebras:

$$\overline{m}|_{H_\alpha \otimes H_\beta} = \delta_{\alpha,\beta} m_\alpha\,, \quad \overline{\eta} = \sum_{\alpha \in G} \eta_\alpha,$$
$$\overline{\Delta}|_{H_\alpha} = \sum_{\alpha=\beta\gamma} \Delta_{\beta,\gamma}\,, \quad \overline{\epsilon}|_{H_\alpha} = \delta_{1,\alpha}\epsilon,$$
$$\overline{S} = \sum_{\alpha \in G} S_\alpha.$$

The dimension of $\overline{H}$ is the sum of the dimensions $|\overline{H}| = \sum_\alpha |H_\alpha|$.

4.2 Hamiltonian Model

The definition of the model is dependent on the detail of the surface: its discretization and orientation of the lattice. More generally we can specify the surface discretization by a simplicial complex Σ constituted by a set of ordered vertices $\mathcal{K}_0$, a set of links connecting all of them $\mathcal{K}_1$. The links' orientations are derived by the order of the vertices. Every $\mathcal{K}_1$ element is boundary of an oriented 2- simplex, whose set is $\mathcal{K}_2$. To simplify our notation we consider a squared lattice in the following for its regularity. To construct the model we choose for every link of the lattice of an algebra H_α of H: we color the lattice. To have an inner product well defined we require that every H_α is equipped with a map $* : H_\alpha \to H_\alpha, a \to a^*$. We have then the inner product defined as $< h, k >= h^* k, \forall h, k \in H_\alpha$. In this manner we have the algebra H_α as a local Hilbert space $\mathcal{H}_l$. The degrees of freedom are independent so the total Hilbert space is defined

by the tensor product. This time it is a 'colored' version, as every local space has a different algebra:

$$\mathcal{H} = \otimes_{l\in\Sigma}\mathcal{H}_l.$$

We are going to define operators for the Hamiltonian $\mathbb{H}$ using the diagrammatic notation. We do so as it is much simpler in manipulating the great number of maps involved. The Hamiltonian is the sum of local operators commuting between each other, which are idempotent:

$$\mathbb{H} = -\sum_v A_v - \sum_p B_p.$$

As presented for the QDM, we present the operators into the Hamiltonian as tensor networks. Our aim is to build the tensor network of the projector operator to the vacuum and take its trace to calculate the degeneracy of the ground state. let us see the realizations for the operator as a tensor network first.

4.2.1 Vertex Operator A_v

The vertex operator acts on the links around a vertex, it is derived by the lattice: its orientation and the algebras associated to every link. We specify our vertex in consideration to define the graphical version of the operator using the Hopf group coalgebra. In the definition is straightforward to see that links pointing outward the vertex acquire an antipode when connected to the central coproduct. For this definition of the vertex the operator is

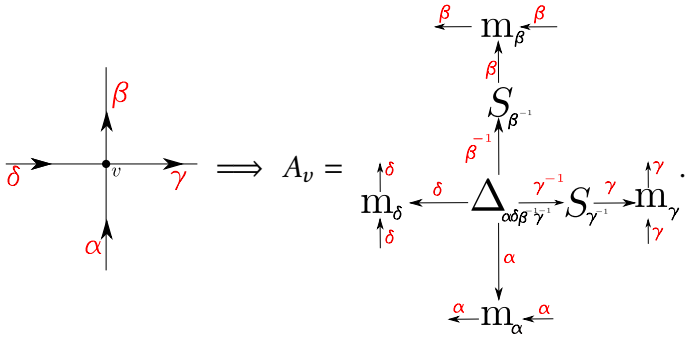

This operator gives to the model a condition of monodromy along the vertex. This happens because the definition of the operator has a cotrace nested inside of the coproducts, which forces the identity $\alpha\delta\beta^{-1}\gamma^{-1} = 1$.

Let us show how two vertex operators behave when applied on the same vertex, A_vA_v. In 4.10 we use the definition of the associativity for the external products, then

we move the antipodes towards the external legs.

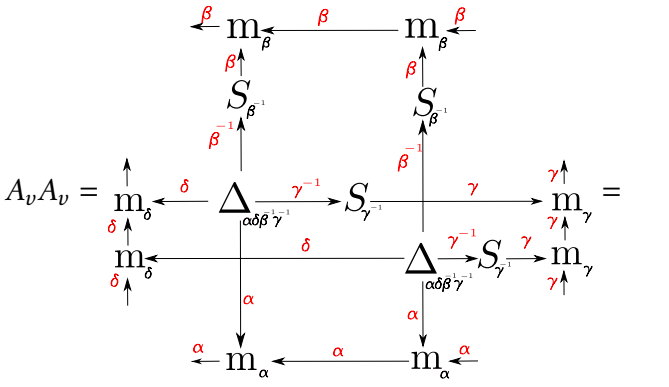

(4.9)

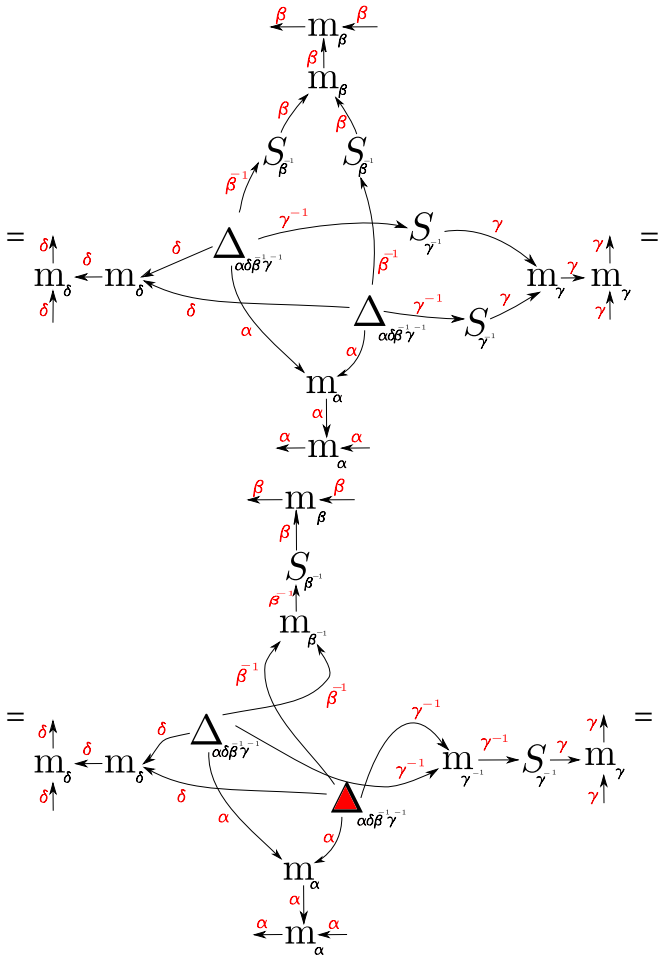

(4.10)

For the following passage we color one coproduct to identify the order when displaying the tensor network in a useful fashion in 4.11. We are ready to apply the compatibility

axiom three times until in 4.12 we have the cotrace applied to the product.

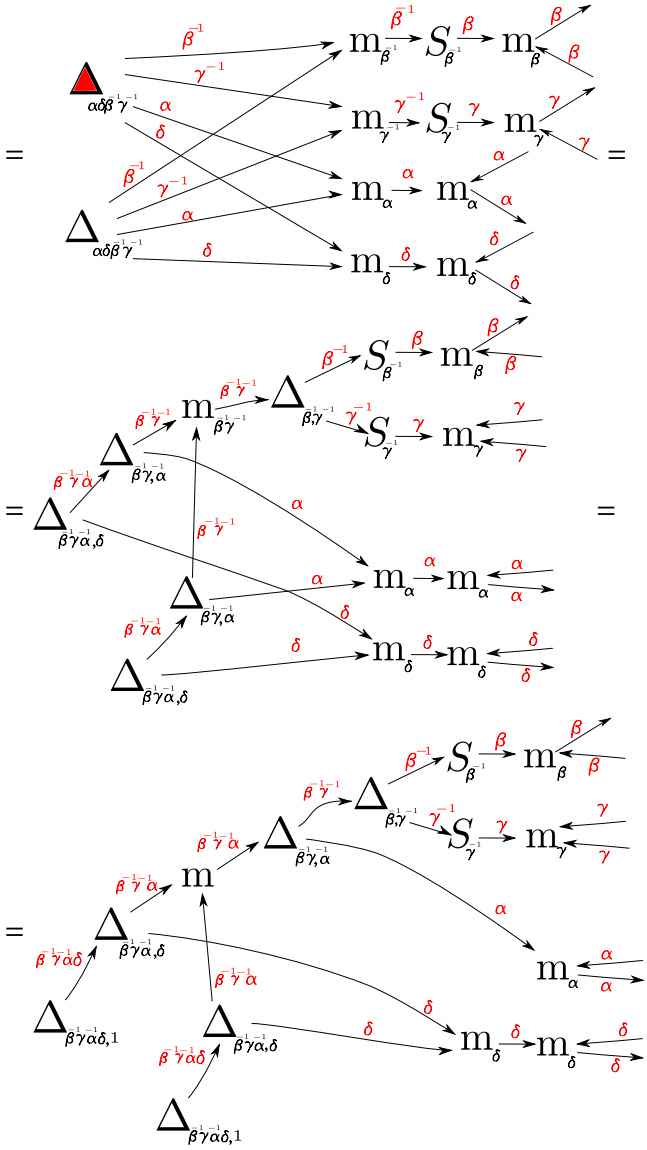

(4.11)

Remembering the definition of the integral in 4.7, we can extract a factor resulting in the proper definition of one A_v. The factor is exactly $\epsilon_1(\lambda_1) = dim H_1$, discussed in 4.8.

To have an idempotent operator we need to factor it out, $A_v A_v = (dim H_1) A_v$.

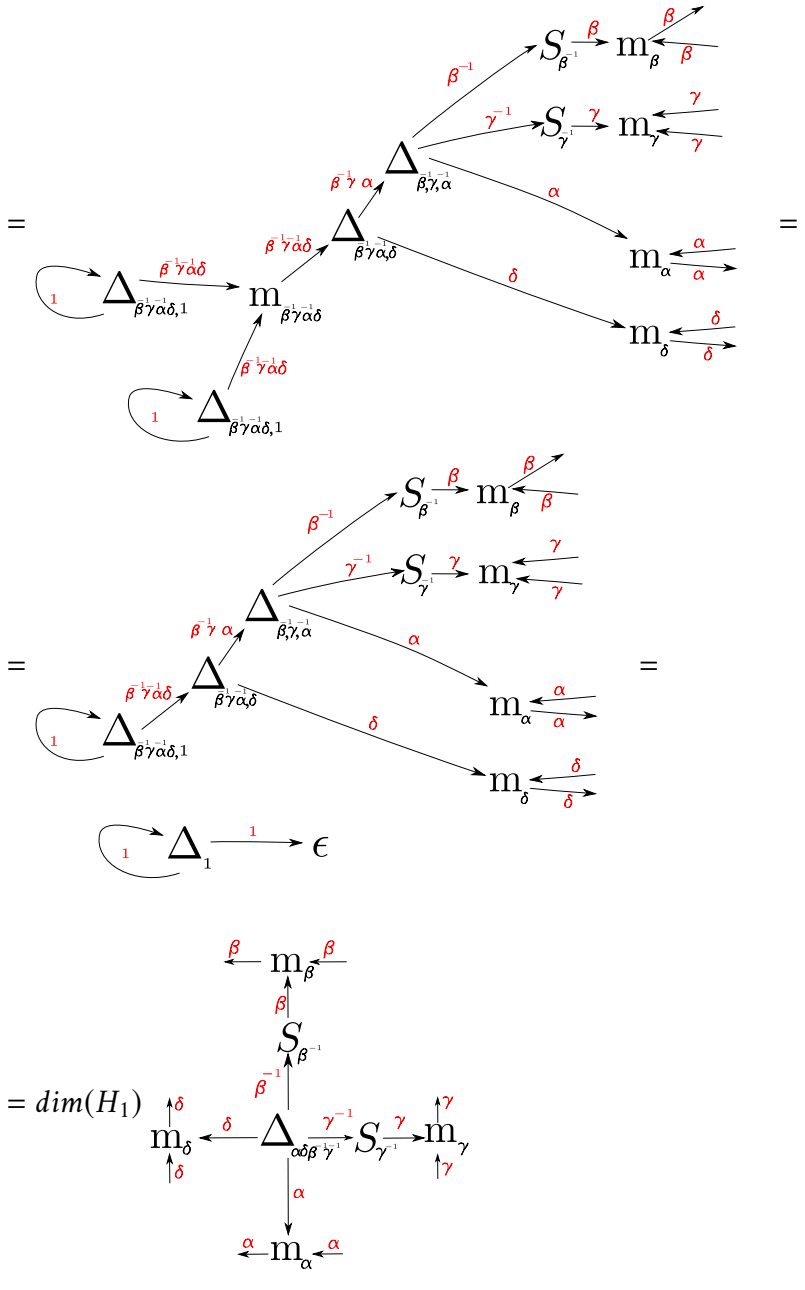

(4.12)

4.2.2 Plaquette Operator B_p

The operator is performed around a plaquette, the coproduct homomorphisms transforms the elements in each link to the corresponding element in the H_1 algebra.

The plaquette operator acts upon the links around a plaquette, it is derived by the orientation of the plaquette and links. The links with opposite orientation respect to the plaquette are multiplied by the antipode with the first leg of the coproducts. Defining the plaquette and the algebras for the links, the operator is

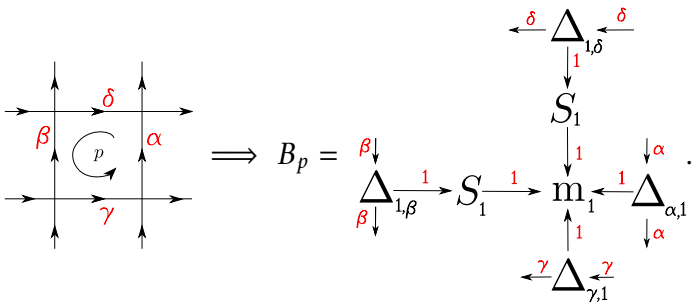

(4.13)

We now proceed with the product $B_p B_p$, where we spare a much similar calculation as presented in 4.9. The same factor appears, so for both operators we have the same factor as correction:

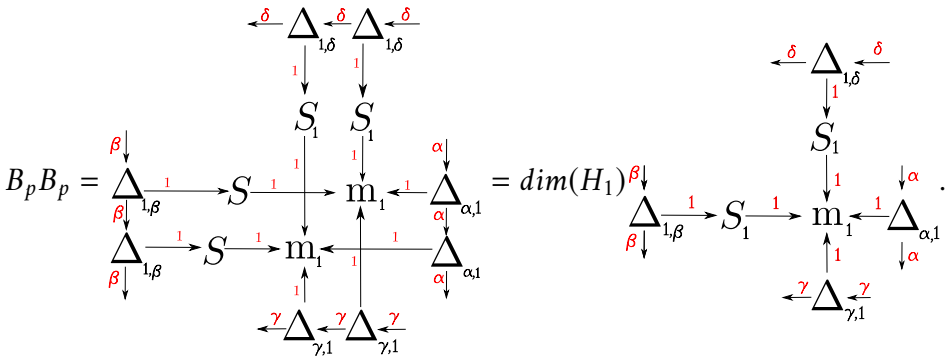

Let now see how the two operators behave with each other, $B_p A_v$. They interact in just two adjacent links indexed by the elements $\alpha, \delta \in G$. We show just the part of the tensors relevant for the interaction 4.14. We can use the compatibility axiom at the upper and lower part in 4.15.

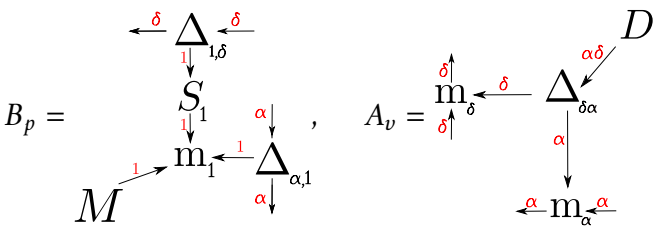

(4.14)

$B_p A_v =$ 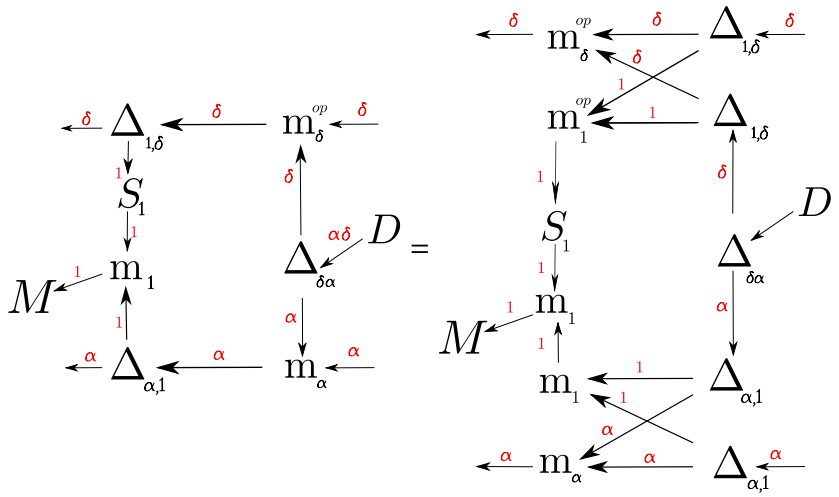 (4.15)

Then the antipode can be moved through the multiplication, so the antipode axiom can be performed in 4.16. The last step is just to rewrite in a cleaner way, to recognized the swapped operators in 4.17.

= 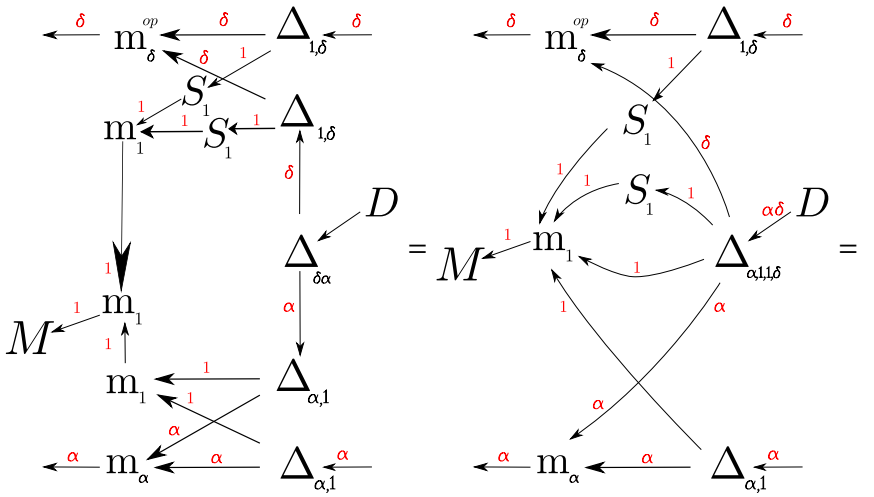 (4.16)

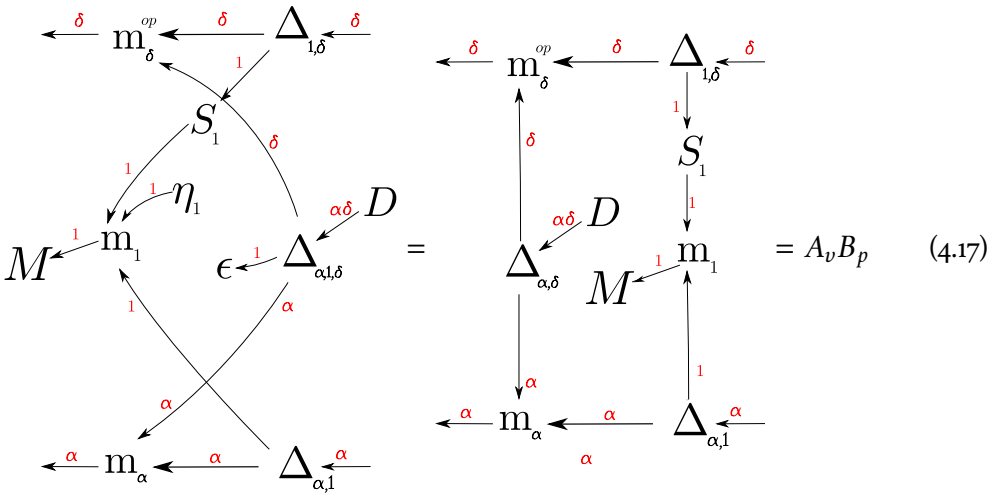

$$= A_v B_p \qquad (4.17)$$

We are ready now to build the tensor network for the projector operator $P_0 = \prod_v A_v \prod_p B_p$.

4.2.3 Unitary Equivalence

Now we compare two Hamiltonians related by a unitary transformation. The simplest one is to switch the orientation of the link. In this example shown below we switch the orientation of the link with parameter α. We want now to verify that a different orientation in the lattice generates a different operator $\widetilde{B}_p$. The Hilbert space for the link associated changes the label accordingly with the inverse element, as in 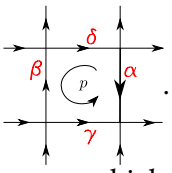 .

The new operator is the original operator conjugated by the antipode maps, which being involutive is a unitary map. This new operator composes a new Hamiltonian, which is unitary equivalent to the old one 4.13, as proved below

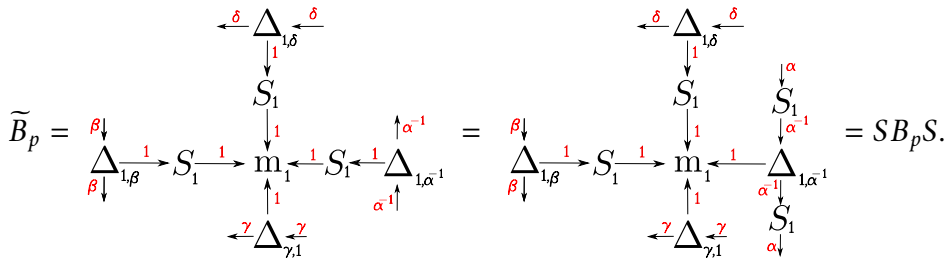

$$= SB_pS.$$

sectionGround State The invariant associated to the degeneracy of the ground state is constructed insensible to the lattice. We change the triangulation using the Pachner moves, consequently we transform the tensor network associated to the projector

operator P_0. In this effort we modify the transformation in order to consider the external gauge field, so to cancel out the dependency of our results on our arbitrary choices.

4.2.4 Curves Diagrams with External Gauge Parameter

We modified the curve diagrams introduced, specifying the algebra for the links they are acting upon.

Definition 4.2.1. As the product belong just to one algebra, we label the blue circles with the corresponding Greek index, 

.

Definition 4.2.2. The coproducts act as interpolation maps between the algebras, so we label the entries and exits, while the crossing have the corresponding label of the blue circle, 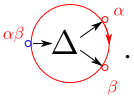

.

We show below the two moves to manipulate the diagrams. The sliding changes the algebra associated to the copied circle as shown in 4.18

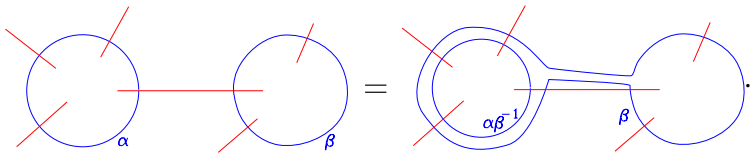

. (4.18)

The two points move is modified as in 4.19

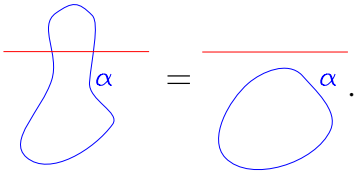

. (4.19)

We can resume the two way of connecting the circles for the crossing as the direct one 4.20:

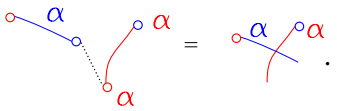

. (4.20)

And the indirect one 4.21

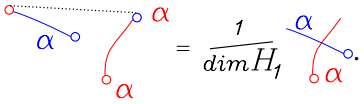

. (4.21)

Having specified the lattice and its orientation we can associate to it the tensor network of the operators. We then look at the tensor network in the curve diagram's formalism to better manipulate it. We fix the lattice and its algebras 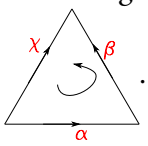

. The plaquette operator is then

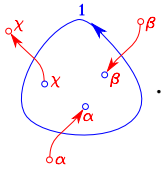

.

The algebras around the vertex are fixed 

. The vertex operator is

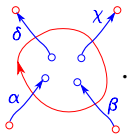

.

The integral applied to the product is defined by the property 4.22, it is only existent in the H_1 algebra as the counit ϵ_1. We remember that the integral is proportional to the cotrace. It results in:

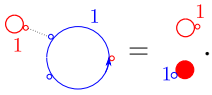

. (4.22)

We can now introduce the transformation in the external parameters done around a plaquette, which multiplies the algebras living in the links by a common new parameter.

4.3 Gauge Transformation in the Parameters

The gauge transformation in the external gauge parameters changes one lattice coloration to another. The change is done changing the labels of the links, we change the algebras associated to them. As the compatibility condition limits the possible local labels for the algebras, it proves the invariance of the ground space under this local transformation. We can swap between different models in the same class defined by the monodromy.

In the ground state space we can transform the parameter in the links around a plaquette. Pictorially it is if with a red loop of label ϵ we could change the labels around

a face, as in 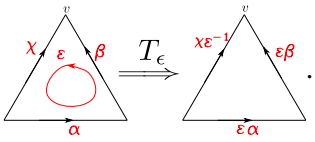

. The operator doing the transformation is

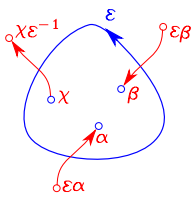

(4.23)

You can notice that the transformation T_ϵ of the algebras is done in a consistent way as to satisfy the compatibility condition at every vertex. Preserving the compatibility condition around each corner it changes to another admissible coloration for the lattice. The transformation does not change the homotopy classes $[\gamma]$, it conjugate their value by the element ϵ.

For each coloration C we have a map $\phi_C : \pi_1(\Lambda) \longrightarrow G$, or in the elements $[\gamma] \longrightarrow \phi_C(\gamma)$. We have defined $\phi_C(\gamma)$ as the monodromy of the dual path. Its value around vertex v at the beginning is $\phi_C = \chi^{-1} \cdots \beta^{-1}$. While after the transformation with coloration C' it is $\phi_{C'} = \epsilon\chi^{-1} \cdots \beta^{-1}\epsilon^{-1}$.

The equivalence classes of Hamiltonian are respected by these transformations presented, only interested in local information as the orientation and the algebras associated. These transformations only modify the algebras associated and the operators defined from them. To prove that the classes of Hamiltonians have the same ground space characterized by the monodromy we need to modify the lattice. The ability to change the specifics of the lattice is to be invariant under the number of constituents, and enable us to confront models from different lattices.

4.4 Transformation of the Tensor Network with the External Gauge Parameter

To prove the invariance of the model under changes in the triangulation T, we have modified the moves introduced by Pachner to address the different parameters sets C coloring the links. We can perform the transformation in the triangulation only when the links involved have parameter identity. We need to act with a gauge transformation of the parameter first to change the local G-connection. The Pachner moves only consider a small portion of the lattice, like three or less links and consequently only theirs Hilbert spaces $\mathcal{H}$ are altered. We are interest in the tensor network of the projector operator to the ground state, so in its Hilbert space $\mathcal{H}_0$. We introduce the transformation of the tensor network M associated to every Pachner move.

$$\begin{array}{ccc}
\text{Triang. } T^{(1)}\text{, Par. set } C^{(1)} & \xrightarrow{\text{Pachner move + Gauge tran.}} & \text{Triang. } T^{(2)}\text{, Par. set } C^{(2)} \\
\downarrow & & \downarrow \\
\text{Hilbert space } \mathcal{H}^{(1)} & \xrightarrow{\text{Transformation } M} & \text{Hilbert space } \mathcal{H}^{(2)} \\
\downarrow P_0^{(1)} & & \downarrow P_0^{(2)} \\
\text{Hilbert space } \mathcal{H}_0^{(1)} & \xrightarrow{\text{Transformation } M} & \text{Hilbert space } \mathcal{H}_0^{(2)}
\end{array}$$

We will prove the commutation of the last square diagram above.

Theorem 4.4.1. *Each transformation of the tensor network M satisfies:*

$$MP_0^{(1)} \simeq P_0^{(2)}M$$

The transformation of the tensor network are three: the flip, the subdivision and the cancellation.

4.4.1 Flip Move

The move involves two adjacent triangles, with a link in common in a triangulation $T^{(1)}$: 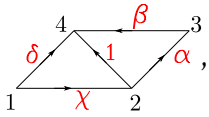

, and Hilbert space $\mathcal{H}^{(1)}$. The move cancels the common link and creates another between the opposite vertices, going to a triangulation $T^{(2)}$: 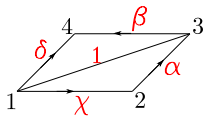

and Hilbert space $\mathcal{H}^{(2)}$. We show that it is a transformation between the ground space: $F : \mathcal{H}_0^{(1)} \longrightarrow \mathcal{H}_0^{(2)}$.

The condition imposed by the parameter on the vertices only allows us to flip a link with parameter equal 1, the identity in G. To achieve this result we simply start applying an external gauge parameter transformation 4.23 on one triangle with the inverse element of the link's parameter. In the representation of part of the lattice in 4.24 we show first the changing of the parameters as a result of 4.23 then the result of the flip:

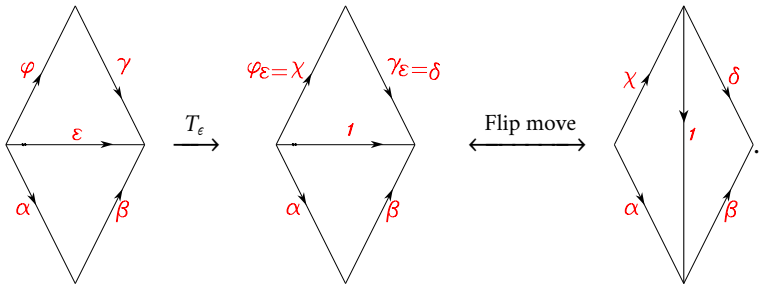

(4.24)

We show the transformations of the tensor network in 4.25. However we manipulate the circle version of the transformation after. The tensor networks are:

$F =$ 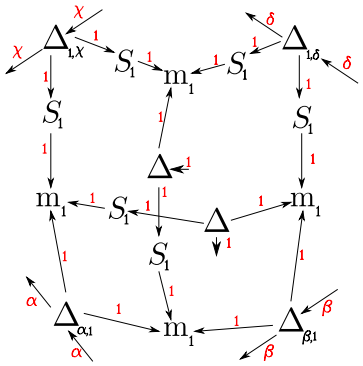 ; $F^{-1} =$ 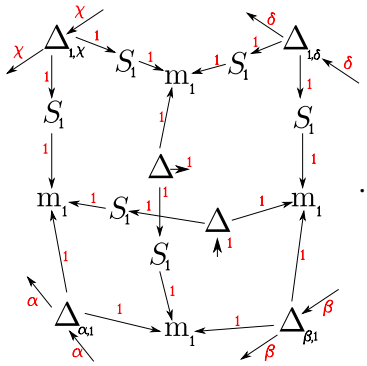 . (4.25)

We can now introduce the transformation with the circles maps. It looks like four coupled plaquette operators: for the first two initial triangles on the left and the final ones vertical on the right. The second version of the right side of the equivalence 4.26 we depict the triangles on the right as vertical lines.

The transformation is

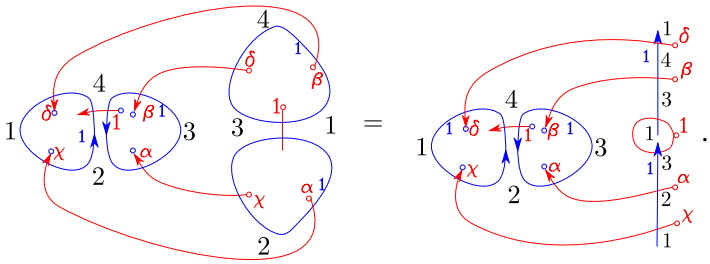 (4.26)

Theorem 4.4.2. *The composition of the flip transformation and its reverse is proportional to the plaquette operators of the initial triangles.*

Proof. Applying the flip and its reverse we end up into two plaquette operators of the initial triangles, as shown in 4.28. The first operator on the left is the forward flip F, while the second on the right is the reverse F^{-1}. We contract the two diagrams in the first line of the sequence of diagrams using 4.20. After we apply the sliding 4.18 of the vertical triangles, which are piled up as factors in 4.27, in the following sequence of

diagrams.

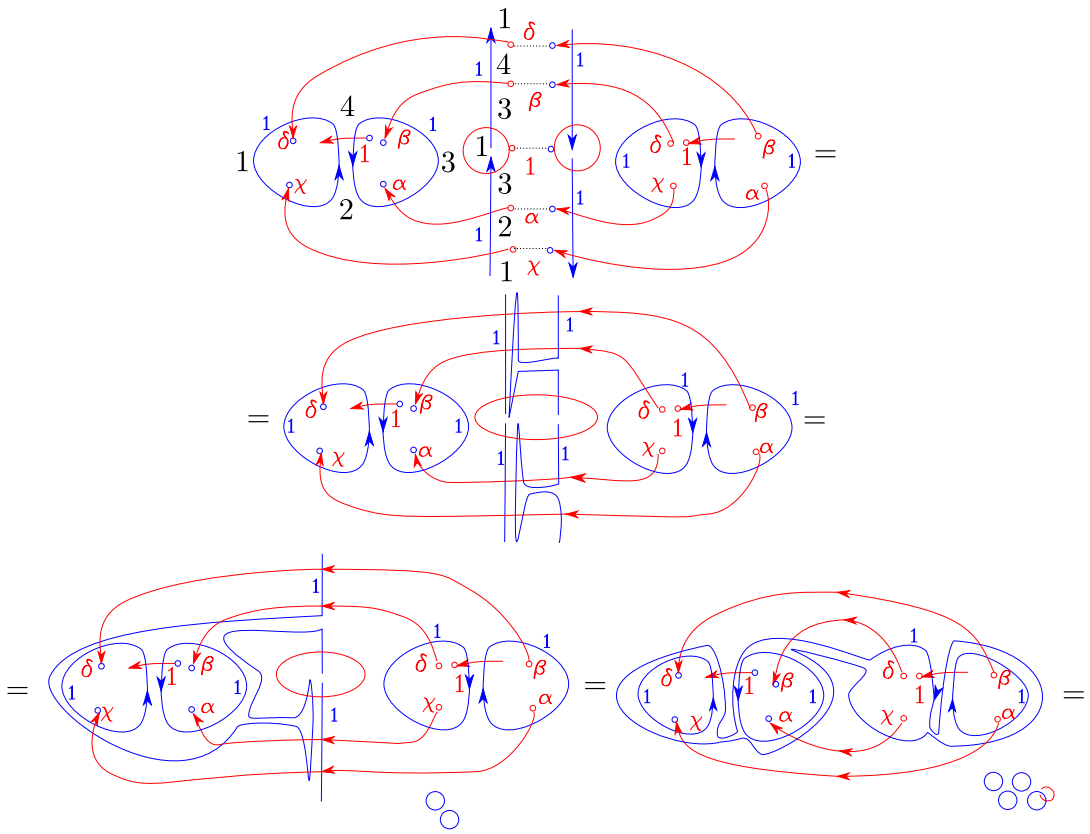

(4.27)

When we are left with a red circle connected to just one blue circle we apply the integral equivalence 4.22 factoring a red circle crossed with a blue one out. We proceed by the sliding moves on the blue circles, all with the identity element associated. At last we can use the equivalence of the diagram associated to the crossing rule, to then apply the integral equivalence 4.22. The result are two plaquette operators in the triangulation $T^{(1)}$.

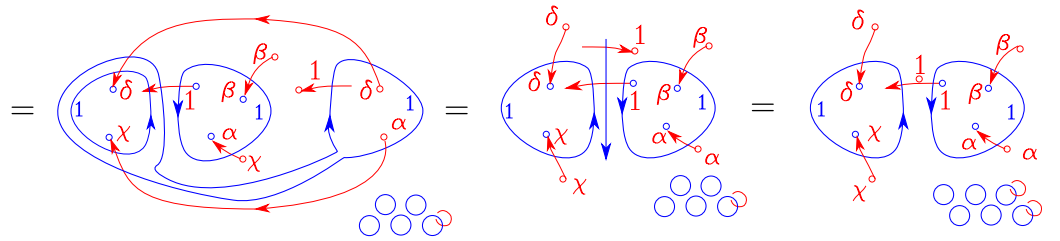

(4.28)

We have proved the relation: $FF^{-1} \propto B_p^{(1)} B_p^{(1)}$. The factor is $(dim H_1)^6$.□

4.4.2 Subdivision Move

The subdivision is a transformation of one triangle into three new triangles enclosed by the boundary of the original triangle, having the external boundary unaltered. We are shifting from a triangulation $T^{(1)}$: 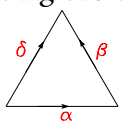 and Hilbert space $\mathcal{H}^{(1)}$ to a smaller triangulation $T^{(2)}$: 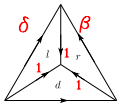 and larger Hilbert space $\mathcal{H}^{(2)}$. The process does not require transformation in the parameters. The links introduced can only have parameter identity of G, as shown by the tensor network in 4.29.

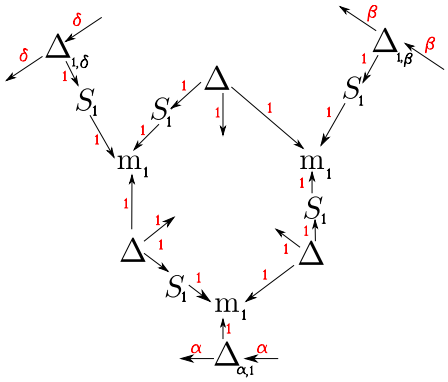

(4.29)

The equivalent diagram operator has three edges as entry while six states coming out. The new states introduced naturally satisfy the flatness conditions over the three final triangles. We can achieve the following diagram adding to the three plaquette operators an integral in the entries of the internal links. We show the two versions of the operator: with the m circles in the anticlockwise direction and the opposite one in 4.30

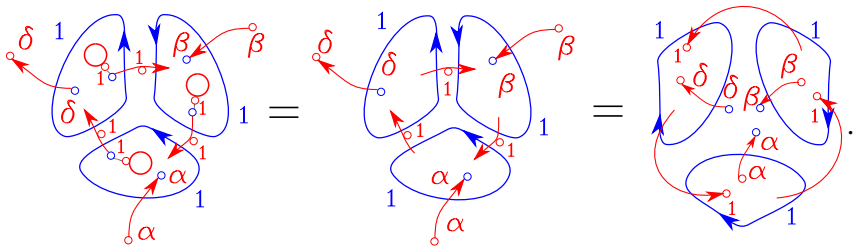

(4.30)

4.4.3 Cancellation Move

Starting from three triangles in $T^{(2)}$: 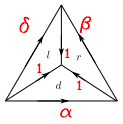 whose borders form a triangle, we can cancel the three links in the inside to obtain a triangle in $T^{(1)}$: 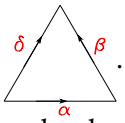 . The transformation is the inverse move of the subdivision. It can be performed only when the internal parameters' links are equal to the identity. This is guarantee applying the parameter transformation 4.23 multiple times over the internal triangles, pictured in

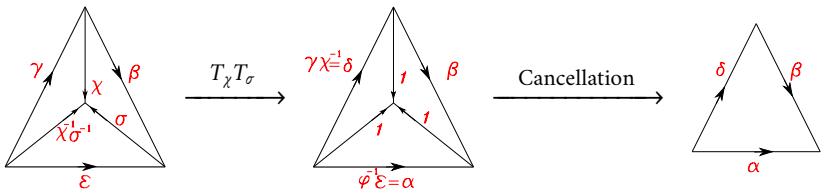

For the realization with maps in the Hopf G-coalgebra we can construct an operator with the internal coproduct without the exiting arrows. It means we enter the operator with six states of the corresponding edges, while only the external edges survive, which are copied in the output, as in the tensor network

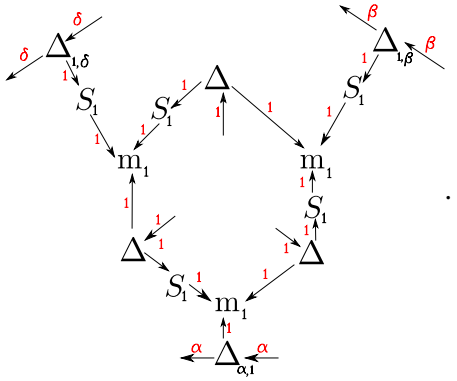

Below we represent the cancellation move with the curve diagrams, already with the internal links in the H_1 algebra. Their exits are connected to counits:

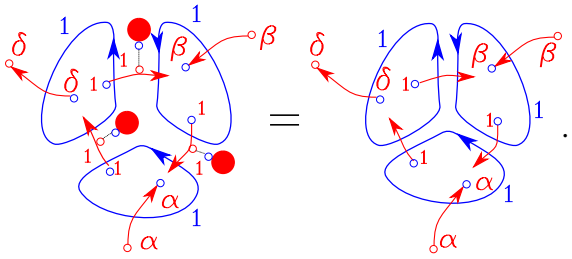

We are now equipped with all four modified moves: they all are possible with local transformations in the external gauge parameters. As a result before the move the transformation in the parameters must push the information of the connection outside the interested region. They represent the invariance of the model for the different discretizations.

Theorem 4.4.3. *The composition of the Subdivision followed by the Cancellation is proportional to the plaquette operator of the initial triangle.*

Proof. To prove this statement we first draw the two diagrams one inside the other with the subdivision internal. We underline a real crossing with a black dot when it can be misunderstood. The composition is direct 4.20 and we can proceed with multiple sliding moves 4.18, until we can apply the integral equivalence 4.22, pictured in 4.31.

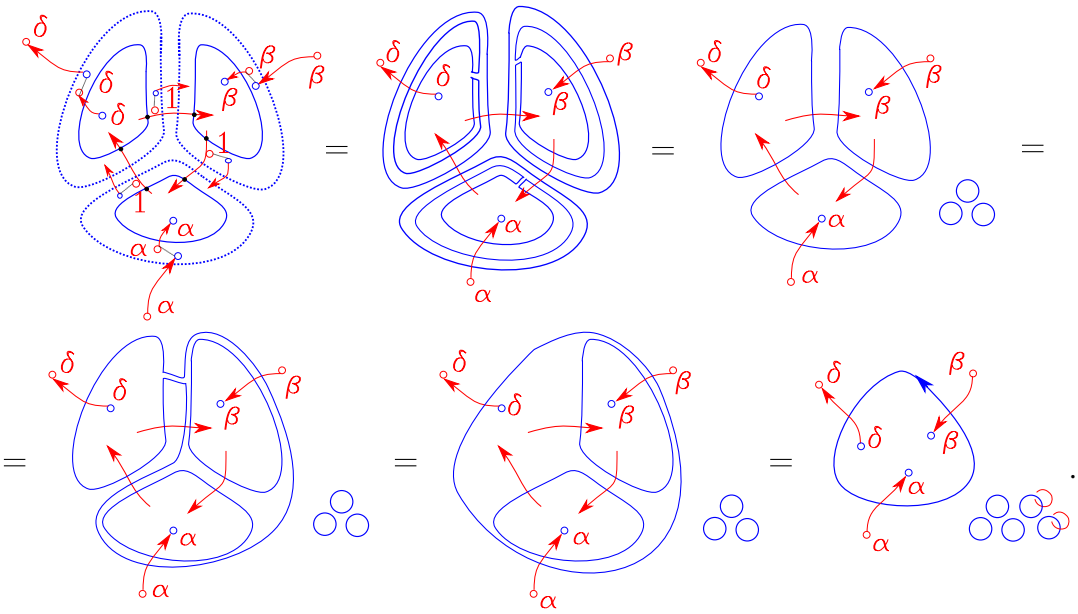

(4.31)

The result is $CD \propto B_p^{(1)}$.□

Theorem 4.4.4. *The composition of the Cancellation followed by the Subdivision is proportional to the composition of three plaquette operators followed by the vertex operator of the internal vertex , followed by three plaquette operators.*

Proof. To draw the composition of the transformation, we insert the subdivision

external in the clockwise direction, shown in

$DC \Longrightarrow$ 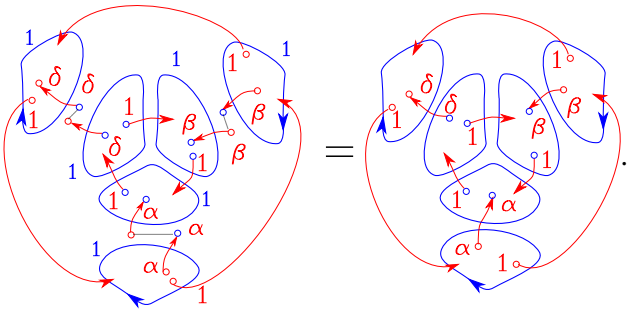 . (4.32)

This diagram is equal to the composition of the B_p for the three triangles followed by the A_v for the central vertex and again the three plaquette operators. The composition is shown in the sequence of diagrams 4.33. In the first row appears the dimension of the H_1 algebra as the contraction between the vertex operator and the external plaquette operators is indirect 4.21. We apply the sliding 4.18 of the blue lines multiple times, until we can factor out the internal red loop with the integral equivalence 4.22. The factors cancel out with the initial factor in the denominator, resulting exactly as in 4.32. The sequence of simplification is:

$B_{p_l}B_{p_r}B_{p_d}A_{v_0}B_{p_l}B_{p_r}B_{p_d} \Longrightarrow$ 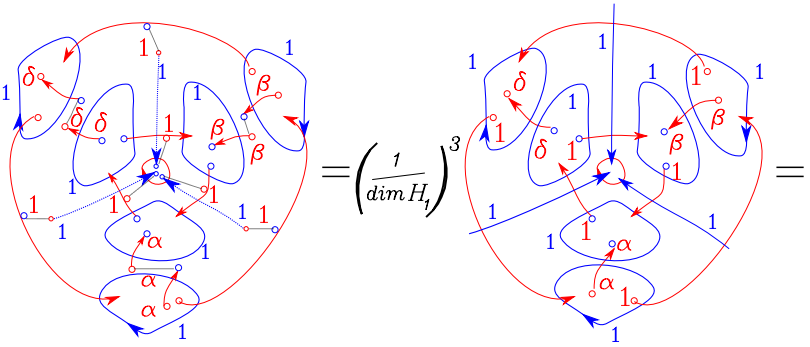

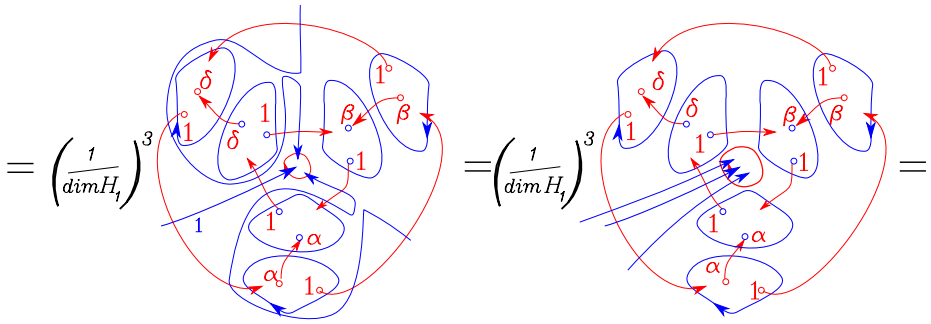

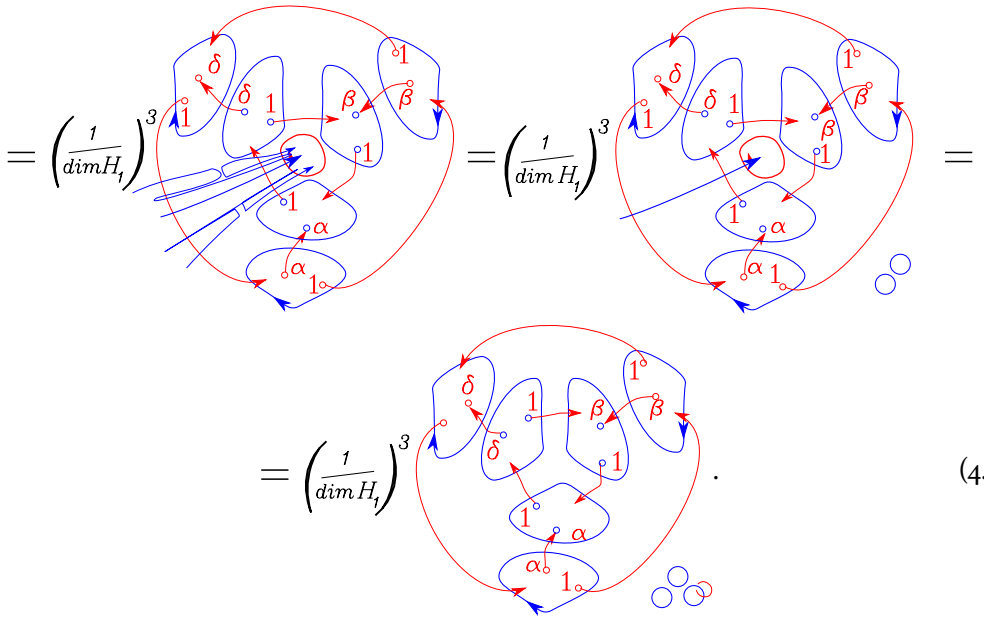

(4.33)

This proves that $DC = B_{p_l} B_{p_r} B_{p_d} A_{v_0} B_{p_l} B_{p_r} B_{p_d}$.□

We are now presenting the last step to complete the proof that each modified transformation M, altering a small number of triangles in Σ_M. The transformation between the tensor network of the ground space of models on different triangulations is $M : \mathcal{H}_0^{(1)} \to \mathcal{H}_0^{(2)}$. As already stated the composition of the move and the opposite map is equivalent to part of the projector P_0, i.e. $MM^{-1} \subset P_0$. The proof really follows the one presented extensively in 3.33, we just show the appropriate coloring to consider the different algebras.

Theorem 4.4.5. *The transformations of the tensor network satisfy the relations with the vertices on the boundary of the small region considered Σ_M. The relation is $MA_v^{(1)} = A_v^{(2)} M$.*

Proof. We just consider um vertex and its vertex operator. We show part of the vertex operator for the $T^{(1)}$: 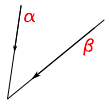 and for the vertex in $T^{(2)}$: 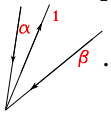 . The relation of the vertex operator $A_v^{(1)}$ and the integral result in a vertex operator$A_v^{(2)}$, applying the property of the integral 4.22. As shown in

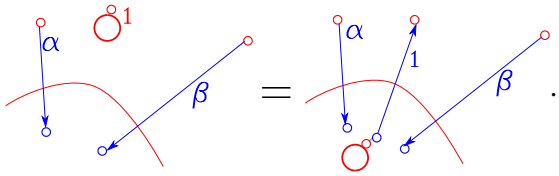

(4.34)

If we start from the triangulation $T^{(2)}$ and operator $A_v^{(2)}$, we apply the integral to the operator input we recover $A_v^{(1)}$, proper of triangulation $T^{(1)}$. This is the reverse of 4.34 pictured as

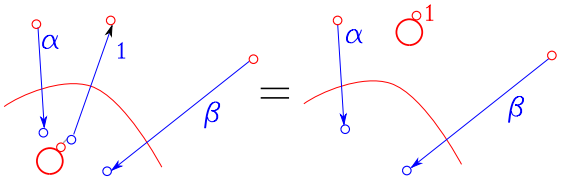

The same process is applied on every vertex, so we have achieved to show that the moves shift from the ground state space of the two triangulations.□

We are ready to use what we have learned to an example where we can calculate the invariant numerically.

4.5 Example

In order to construct our example we use a simpler version of a Hopf group coalgebra. We consider copies of a Hopf algebra, a group algebra A, indexed by elements of a finite group G, therefore they are H_g. Therefore we interpret H as a sum of subspaces $H = \sum_{g \in G} H_g$. We have the set of algebra $\{H_g\}$, with a family of products $\{m_g\}$ and one for the units $\{\eta_g\}$. The algebra have all the same dimension and are isomorphic.

To better understand the particular structure, we introduce an equivalent expression for the diagrams, using an isomorphism 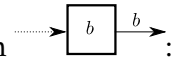 : $A \to H_b$. The multiplication is then realized with the inverse isomorphism on the entry states, it is applied the multiplication in A and on the exit state is applied the isomorphism. The spaces and maps are well defined, following the compatibility conditions already presented. The realization of the product is:

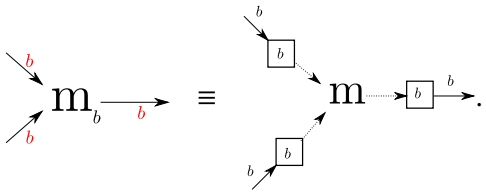

Every unit has the isomorphism between the spaces. We have the diagrams:

A particular feature of this model is the presence of an action, by an element of the group over the one of the group algebra. The first appearance is in the coproduct: the label of the second leg acts over the first leg. Here it is the graphical realization of the coproduct:

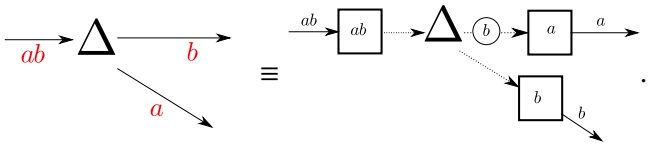

The counit can just live in the algebra indexed by the identity element. The action applied over the identity is trivial:

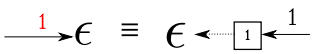

The antipode presents again the action on one leg of the A element. The behavior of the antipode with the action is presented by the two diagrams. The move to pass through is $S(a^{-1} \triangleright x) = a \triangleright S(x)$, $x \in H$, $a \in G$, or graphically

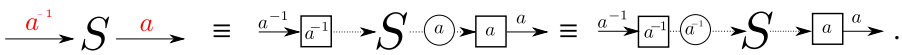

Let us now verify all the properties to grant us dealing with the Hopf group coalgebra previously presented. The unit, in relation with the multiplication, contracts resulting in the identity arrow for the algebra H_b. The result is the same on the other leg:

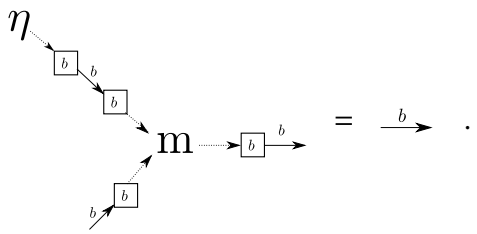

When the counit is contracted with the coproduct, it results in the identity arrow. The action on the counit is ineffective: $\epsilon(a \triangleright x) = a \triangleright \epsilon(x) = \epsilon(x) \quad \forall a \in G,\ x \in A$, as shown in

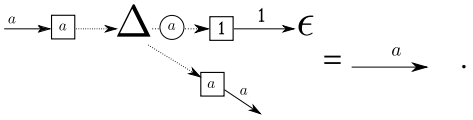

Now that we have presented all the maps for our example, we revisit the relations already presented at the beginning of this chapter. The proof for the associativity is valid in the A algebra, we just color the external legs using the isomorphisms. For its simplicity we skip to the more interesting proof for the coassociativity. When we combine more coproducts we collect different actions, so we show how to dislocate them through the coproducts. First when there is only one action and after how they are composed:

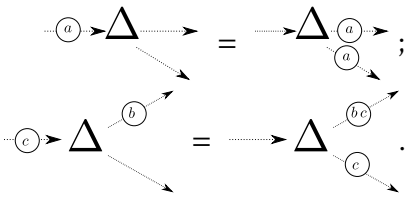

To prove the coassociativity in diagrams we have equal final and initial algebras, and we use the properties for the actions presented above. It results in

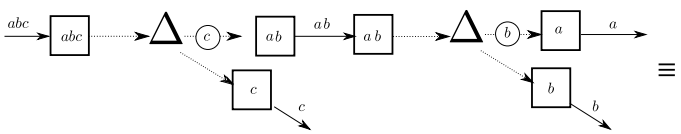

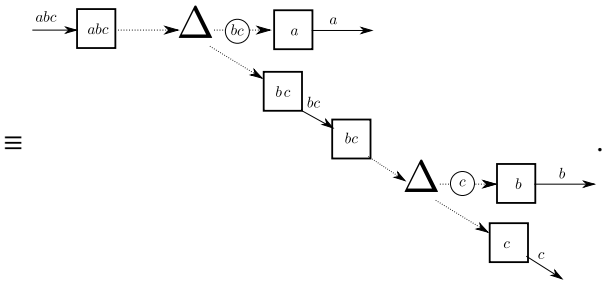

An important sequence used to define later the operators is the closed circle of coproducts, which can be written closing the sequence of Δs with a cointegral. The proof for the integrals can be found in [49]. This gives the condition of compatibility on the algebras expressed by the delta:

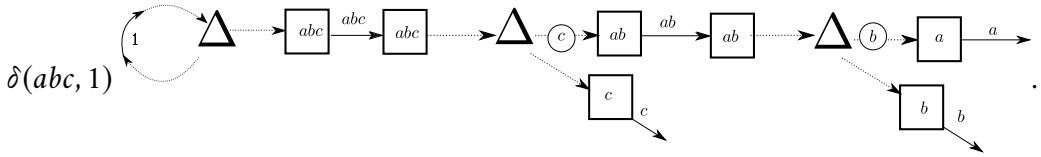

As regards to the circle of products we use an integral, with no additional condition, so we don't show it here. More fundamental in the following analysis, we present the compatibility between product and coproduct. Where we show how the action behave with the multiplication, it can be pass through as shown in the last passage.

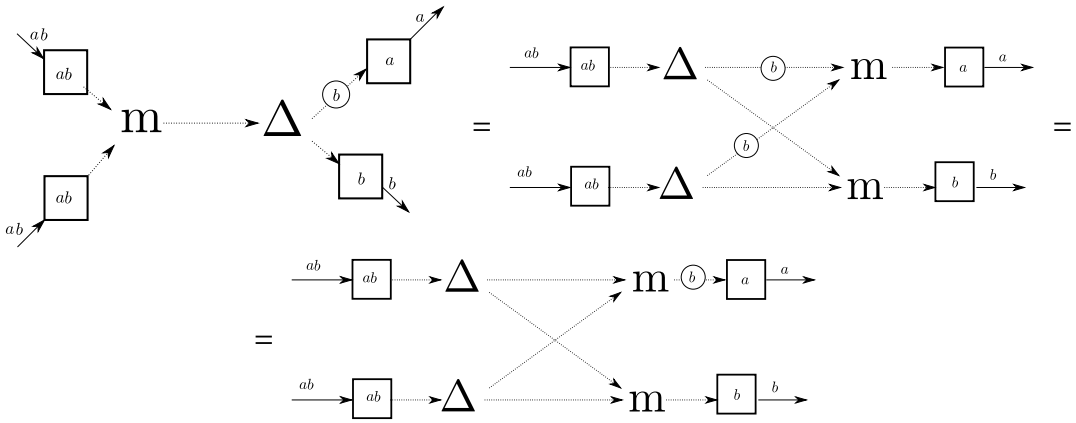

Let us see the antipode axiom, where we see how the counit behaves with the action. We have already eliminated the isomorphisms and inverse for the internal arrows. In the first diagram, the first arrow of the internal circle would have the a label, while the second the a^{-1} label appearing as action on the first leg. We can shift the action through the antipode gaining a a^{-1} on the second leg as well: next we shift them passing the delta to act on the input leg in H_1. Therefore, once we solve the core of the diagram

the action is applied to the counit, but it results in just the counit.

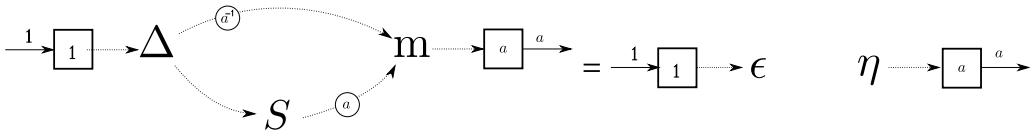

If we apply the antipode on the first internal line the actions cancel each other, we can pass one on the other side of the antipode gaining the opposite element a^{-1}.

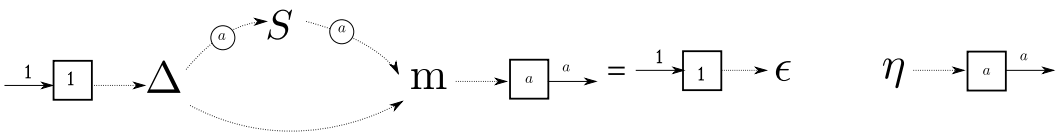

We have proven that our example satisfies every diagram needed to be a Hopf group coalgebra. The action introduced must be a homomorphism, so we have pointed out few properties.

Hamiltonian Model

We introduce the operators in the Hamiltonian with the new definition for our example. We show before the squared lattice version to compare with the one presented in 4.2, but adding the actions. The vertex operator is

$A_v =$ 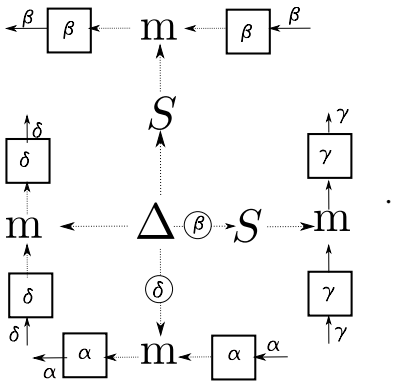 .

In the vertex operator we have the constraint $\beta^{-1}\gamma^{-1}\alpha\delta = 1$, therefore the actions on the inside are simplified with the ones for the antipodes. The resulting ones are shown

in the first diagram. The plaquette operator is

$B_p =$ 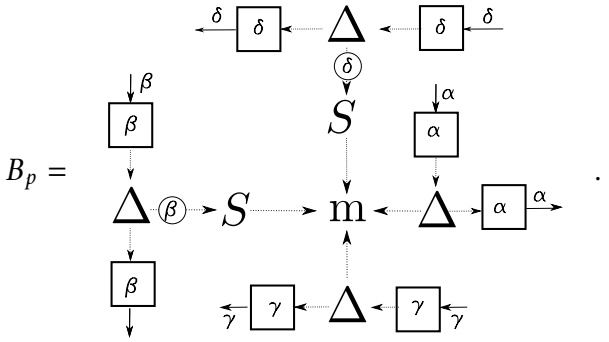

In the plaquette operator the internal arrows have only the identity label, so the only actions are the ones on the first legs of the deltas on top and on the left.

The calculation of the invariant is made on a torus as explained in 3.4.5. We are calculating the trace of the Projector operator on a squared plaquette with identified opposite links. To calculate the projector we grow for each vertex a vertical link to obtain a 3D cube with opposite faces identified 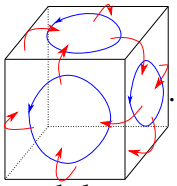 . Therefore the result have three faces and three links for the three spatial dimensions, as shown in the simplification realized below in 4.35. On a torus there are only two different possible non trivial flat connections. We put the generic label $a, b \in \mathbb{C}[G]$. The cube is pictured flat on a plane with the six faces. The numbers were introduced to signalize the continuity of the red circles. For example starting in the 1 we follow the arrow through the 5, then the sequence restarts from the 5 to the 3. Followed by 3 to 6, and at last 6 to 1, to reconnect to the start. When we identify the faces we can simplify the red circles too, so we obtain the final figure with only three blues circles representing the faces.

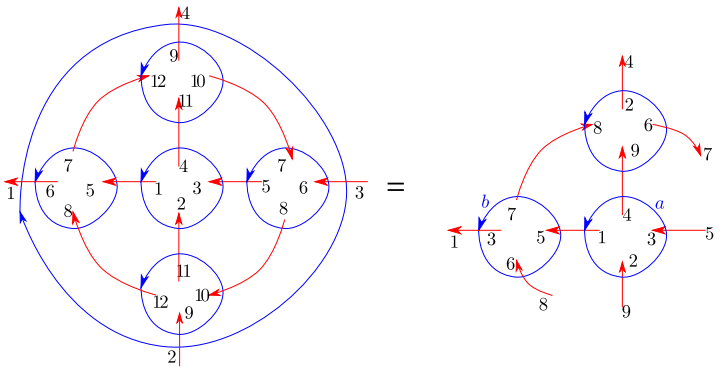

(4.35)

The tensor network associated for this curves diagram is expressed below in 4.36. The non trivial connections color two products, the compatibility conditions are realized

on the Δs, so we have the condition $aba^{-1}b^{-1} = 1$. We have colored the Δs just to distinguish into the forest of arrows. There are no loose arrows, they are all contracted, so we don't have any isomorphisms left. For the products the labels are just to remind of the faces they come from.

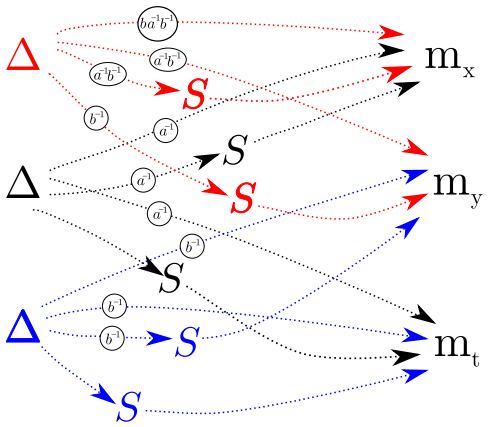

(4.36)

In the following we use this tensor network 4.36 to calculate explicitly the GSD with different group algebras A.

Calculations of GSD

We consider two calculations where we show the different degeneracy for the ground state depending on the G-connection. The calculations are made: one with an Abelian group and one non Abelian.

- The first example is realized with the group algebra $A = \mathbb{Z}_4$, we consider the group $\mathbb{Z}_2$ as external gauge field to color the lattice. The action is required to be a morphism $\triangleright : \mathbb{Z}_2 \times \mathbb{Z}_4 \longrightarrow \mathbb{Z}_4$. We choose for the components the realization $-1 \triangleright \pm 1 = \pm 1$, while $-1 \triangleright \pm i = \mp i$.

  The model with monodromy $a,\ b = 1$ is a toric code with group $\mathbb{Z}_4$ on the links. The degeneracy of the ground state is sixteen, $GSD = |\mathbb{Z}_4|^{2g} = 16$. We show the states in figure Fig. 4.1(a). The pictures are schematized tori, opposite sides are identified. We consider the first state with value $|1\rangle$ in every link, pictured just as a blank space. The states are the first representative of the superposition of states as in the loop gas description of the toric code. The superposition of states is achieved by applying $\prod_v A_v$ to the state represented. In the other pictures the red line indicates a line of successive links $|-1\rangle$ around a non-contractible circuit. For the values $|\pm i\rangle$ we add a green line, but the orientation in the characterization of the states doesn't play a role.

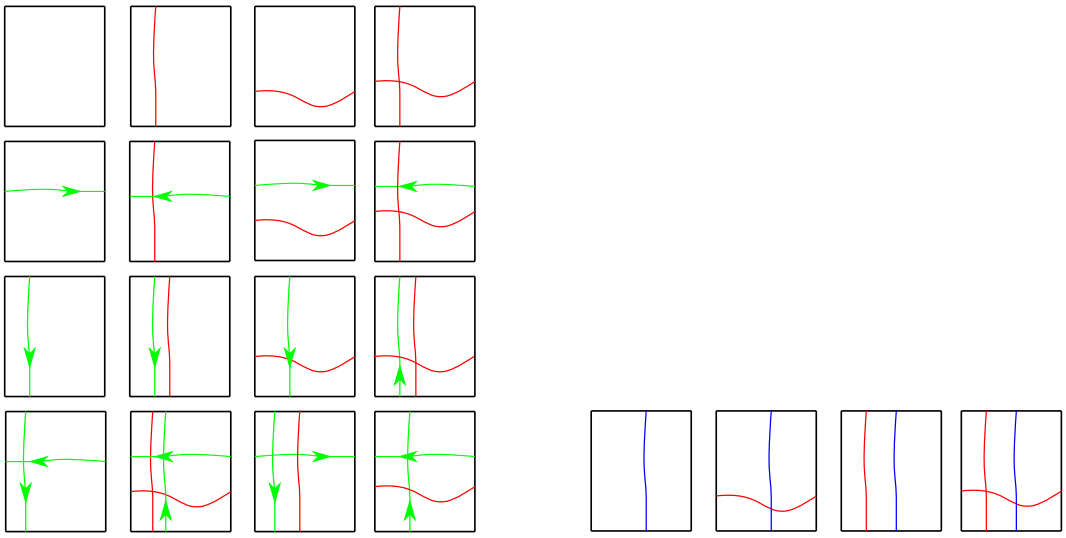

(a) $GSD = 16$ for the monodromy $= 1$ (b) $GSD = 4$ for the monodromy $= -1$

Figure 4.1: Ground states for the $H = \{\mathbb{C}[\mathbb{Z}_4]_g\}_{g\in\mathbb{Z}_2}$ model.
Color line code: (i) red= links line of value $|-1\rangle$, (ii) green= oriented links lines for values $|\pm i\rangle$, (iii) blue= $\mathbb{G}$-connection line of value -1.

The monodromy can add lines in the lattice as links with external parameters -1. For the vertex compatibility condition the line has to be closed, but it can wrap in a non contractible way our surface. In our surface there are two possible monodromy lines. The ground state degeneracy for the presence of one or two lines is reduced to four, $GSD = 4$. We show the states in figure Fig. 4.1(b). The presence of one or two lines with $a,\ b \neq 1$ prevents the appearance of loops of links with value $|\pm i\rangle$.

- In the second example we calculate the invariant for the non-Abelian case, we opted for the $H = \{\mathbb{C}[S(3)]_g\}_{g\in S(3)}$. The degeneracy in this case is always eight, $GSD = 8$, for all the possible monodromies on the torus.

We present now the program used to calculate the invariant, i.e. the degeneracy, in the first calculation.

Program calculating the GSD for the $H = \{\mathbb{C}[\mathbb{Z}_4]_g\}_{g\in\mathbb{Z}_2}$

The program runs in python 2 or 3. The program was made for the manifold $S^1\times S^1\times S^1$ calculating the projector operator:

$$Z = \sum_{a,b,c\in Z_4} m_x(a,b,c)m_y(a,b,c)m_t(a,b,c).$$

We use the tensor network 4.36. We chose to identify the opposite faces of the cube, for the faces the holonomy h is the product of the link's value considering its orientation, $h = abc^{-1}d^{-1}$. In our case we consider the monodromy with $\alpha,\ \beta,\ \gamma \neq 1_G$, so we have the action of the group $\mathbb{Z}_2$ over some links. There exist three possible values for the monodromy $\alpha, \beta, \gamma \in \mathbb{Z}_2$, one for each S^1 of the torus. They are associated to the dual links, as the three axes of the cube. Since one S^1 is not physical, it is the trace of the P_0 projector, we fix γ to be 1.

The $m_x(...)$, $m_y(...)$ e $m_t(...)$ are the weight/tensors associated to every face. They have value 1 if the modified holonomy is identity or value 0 otherwise. We deal with the group as additive, so we use mod 4 (or 2). The *rho(r, a)* function implements the action of $\mathbb{Z}_2$ over $\mathbb{Z}_4$. The *for* circle at the end looks all the possible values of $\mathbb{Z}_4$ labeling the cube's links. The variable *trace* is the trace of the projector operator: the value of the GSD multiplied by the group order.

You can modify the value for *alpha, beta* to calculate the projector for different monodromies.

```
from itertools import product
from math import log

N = 4 \sharp Z_N  # gauge (dynamic)
M = 2 \sharp Z_M # gauge (background)

# (r -> a) = rho(r, a)
#table for the values resulting from the action
#
#   r\a    0 1 2 3   = 1  i -1 -i
#   0      0 1 2 3
#   1      0 3 2 1

def rho(r, a):
if (r % M) == 0:
return a
else:
if (a == 2)|(a == 0):
return a
else:
if a==3:
a=a-2
return a
```

```
else:
a=a+2
return a

def m_x(alpha,beta, a, b):
   s= rho(alpha+2*beta, a)+rho(alpha,b)-rho(alpha+beta,a)-rho(alpha,b)
    if s % N == 0:
        return 1
    else:
        return 0

def m_y(alpha,beta, a, c):
    s= rho(alpha+beta,a)+rho(beta, c)-rho(beta,a)-rho(beta,c)
    if s % N == 0:
        return 1
    else:
        return 0

def m_t(alpha, beta,b, c):
    s =  rho(alpha, b) + rho(beta, c)-b-c
    if s % N == 0:
        return 1
    else:
        return 0

#Here you can change the value for the $\G$-connection
alpha, beta, gamma in Z_M,
REMEMBER gamma always =0
alpha= -1
beta = 0
gamma= 0

trace = 0
for a, b, c in product(range(N), repeat=3):
print(a,b,c)
trace += m_x(alpha, beta, a, b)*m_y(alpha, beta, a, c)*m_t(alpha, beta, b, c)

print(trace/N)
```

5 Conclusions

In this present thesis we began by revisiting the QDM. We prove its topological invariance of the ground state degeneracy with a new method, it can be find in 3.4.7. The proof is based on a new formalism that allows us to recompute the tensor network when the triangulation is locally modified by a Pachner move. We realized the new proof using curves inspired by the Heegaard decomposition. In the sequence we introduce the G-QDM with the external gauge field coloring of the lattice. We construct its tensor network associated to the ground state projector. The trace of the projector is an invariant for small modification of the lattice and a specific class of transformations in the parameters coloring the lattice. The proof of the invariance was realized modifying the one presented in the QDM to include the information of the G-connection in the G-QDM.

The scalar invariant of the G-QDM is topological in the sense that it is invariant under transformation in the triangulation realized with the Pachner moves 4.4. They grant us local transformations from one triangulation to another, hence the model is insensitive to the specifics of the lattice. The invariant is invariant also under transformations of the external gauge parameters with the transformation presented in 4.3. It is a local transformation that changes the flat G-connection over the surface, but it can not change the monodromy. Therefore it switches between Hamiltonians within the same class.

We can now have a look at different classes, what does it change when the monodromy is different? Considering the examples we have calculated when the monodromy is labeled by the identity element in G, we have the complete degeneracy allowed by the topology: recovering the QDM. In this case the GSD is encoded in the scalar invariant proposed by Kuperberg. Otherwise when the monodromy is not trivial the degeneracy is restricted, evaporating some ground states to excitations.

In the analysis we switch through different formalism better suited to describe the calculations presented. However this may be in detriment of the accessibility of the content. We proposed the new formalism justifying the steps taken, in a sequential way, being self contained in the knowledge required, to familiarize the reader.

The family of model proposed realizes gapped models, with degenerate ground state, which present highly entangled ground states. We are exploring the field beyond topological order. The study of G-QDM ground state reveals a degeneracy dependent

on the global information encoded in the external gauge field coloring the lattice. The coloring imposes a Hamiltonian, however there are classes of Hamiltonians equivalent under local transformations in the external gauge field. These transformations can not change the monodromy of the lattice.

5.1 Publications

The first two publications are not directly related to this work.

- J. P. Ibieta-Jimenez and M. Petrucci and L. N. Queiroz Xavier and P. Teotonio-Sobrinho, Topological Entanglement Entropy in d-dimensions for Abelian Higher Gauge Theories, Journal of High Energy Physics [50].

  The topological term in topological entanglement entropy (TEE) is considered as an indicator of topological order, at least in $2D$ [51], but not much is known in higher dimensions. There are some speculations about its nature, yet only for the toric code. My research group developed an exact calculation for the topological term in the TEE for a class of models generated by the AHGT [36] for d dimensions.

- J. P. Ibieta-Jimenez and L. N. Queiroz Xavier and M. Petrucci and P. Teotonio-Sobrinho, Fracton-like Phases from Subsystem Symmetries, Physical Review B [37].

  We built general models for the fracton phases, a new type of order with highly degenerate ground state and excitations with restricted mobility.

- M. Petrucci and P. Teotonio-Sobrinho, Group Quantum Double Model, to appear in 2020.

  The result of my thesis research.

Bibliography

[1] L. Landau. Theory of Phase Transformations I. Phys. Z. Sowjetunion, 11(26), 1937.

[2] L. Landau. Theory of Phase Transformations II. Phys. Z. Sowjetunion, 11(545), 1937.

[3] R. B. Laughlin, Phys. Rev. Lett., 50, 1395 (1983), "Anomalous Quantum Hall Effect: An Incompressible Quantum Fluid with Fractionally Charged Excitations"

[4] D.J. Thouless, "Quantized hall conductance in a two-Dimensional periodic potential", *Physical Review Letters*, vol.49, pp.405-408, (1982)

[5] Michael Atiyah, "Topological quantum field theories", *Publications Mathématiques de l'Institut des Hautes Études Scientifiques*, pp.175–186, vol. 68, (1988)

[6] Udo Pachner, "P.L. Homeomorphic Manifolds are Equivalent by Elementary Shelling", *European Journal of Combinatorics*, vol.12, pp.129-145, (1991)

[7] Edward Witten, "Topological quantum field theory", *Communications in Mathematical Physics*, pp.353–386, vol.117, (1988)

[8] Xiao-Gang Wen, "Quantum field theory of many-body systems: from the origin of sound to an origin of light and electrons", *Oxford University Press*, (2004)

[9] Albert Schwarz, "Topological quantum field theories", arXiv:hep-th/0011260, (2000)

[10] C. Blanchet and V. G. Turaev, "Quantum Invariants of 3-manifolds", *Quantum*, pp.1-17, (2005)

[11] John B. Kogut, "An introduction to lattice gauge theory and spin systems", *Rev. Mod. Phys.*, vol.51, pp.659-713, (1979)

[12] R. Oeckl, "Discrete Gauge Theory: From Lattices to TQFT", *Imperial College Press*, (2005)

[13] Ohtsuki Tomotada,"Quantum invariant: A study of knots, 3-manifolds and their sets", *Series on Knots and Everything*, vol.29, (2001)

[14] Xiao-Gang Wen, "Zoo of quantum-topological phases of matter", *Reviews of Modern Physics*, vol.89, (2017)

[15] Alexei Kitaev and Chris Laumann, "Topological phases and quantum computation", *Lecture Notes of the Les Houches Summer School*, vol.89, (2009)

[16] A. Kitaev, "Fault tolerant quantum computation by anyons", *Annals Phys.*, vol.303, pp.2-30, arXiv: quant-ph/9707021, (2003)

[17] Chetan Nayak and Steven H Simon and Ady Stern and Michael Freedman and Sankar Das Sarma, "Non-Abelian anyons and topological quantum computation", *Reviews of Modern Physics*, pp.1083", vol.80, (2008)

[18] Jiannis Pachos, "Introduction to topological quantum computation", *Cambridge University Press*, (2012)

[19] Gavin K Brennen and Jiannis K Pachos, "Why should anyone care about computing with anyons?", *Proceedings of the Royal Society A: Mathematical, Physical and Engineering Sciences*, pp.1-24, vol.464, (2007)

[20] D. J. Thouless and M. Kohmoto and M. P. Nightingale and M. den Nijs, "Quantized Hall Conductance in a Two-Dimensional Periodic Potential", *Phys. Rev. Lett.*, pp.405-408, vol.49, (1982)

[21] A. Kitaev, "Anyons in an exactly solved model and beyond", *Annals of Physics*, pp.2-111, vol.321, arXiv: cond-mat/0506438, (2006)

[22] Oliver Buerschaper and Miguel Aguado, "Mapping Kitaev's quantum double lattice models to Levin and Wen's string-net models", *Physical Review B*, vol.80, (2009)

[23] Masaki Oshikawa and T. Senthil, "Fractionalization, Topological Order, and Quasiparticle Statistics", *Phys. Rev. Lett.*, vol.96, (2006)

[24] Ady Stern, "Anyons and the quantum Hall effect—A pedagogical review", *Annals of Physics*, vol.323, pp.204-249, (2008)

[25] Robbert Dijkgraaf and Edward Witten, "Topological gauge theories and group cohomology", *Communications in Mathematical Physics*, pp.393-429, vol.129, (1990)

[26] G. Kuperberg, "Involutory Hopf algebras and 3-manifold invariants",*International Journal of Mathematics*, vol.02, pp.41-66, arXiv: math/9201301, (1991)

[27] Mark Hennings, "Invariants of Links and 3-Manifolds Obtained from Hopf Algebras", *Journal of the London Mathematical Society*, vol.54, pp.594-624, (1996)

[28] D.N. Yetter, "Topological quantum field theories associated to finite groups and crossed G sets", *J. Knot Theor. Ramifications*, vol.1, pp.1-20, (1992)

[29] Miguel Jorge Bernabè Ferreira, "Teorias de Campos Discretas e Modelos Topológicos", Master's thesis in Physics USP , *https://www.teses.usp.br/teses/disponiveis/43/43134/tde-03052012-082048/pt-br.php*, (2012)

[30] Miguel Jorge Bernabè Ferreira, "Teorias de gauge e modelos topológicos", PhD's thesis in Physics USP, *https://teses.usp.br/teses/disponiveis/43/43134/tde-14092016-234644/pt-br.php* , (2017)

[31] Miguel Jorge Bernabé Ferreira and Pramod Padmanabhan and Paulo Teotonio-Sobrinho, "2D quantum double models from a 3D perspective", *Journal of Physics A: Mathematical and Theoretical*, vol.47, pp.375204, arXiv: cond-mat.str-el/1310.8483, (2014)

[32] Hudson Kazuo Teramoto Mendonça, "Teorias de 2-gauge e o invariante de Yetter na construção de modelos com ordem topológica em 3D", PhD's thesis in Physics USP, *https://www.teses.usp.br/teses/disponiveis/43/43134/tde-01082017-155641/pt-br.php*, (2017)

[33] V.G. Turaev, "Homotopy Quantum Field Theory", *European Mathematical Society*, (2010)

[34] Alexis Virelizier, "Algebraic properties of Hopf G-algebra", *Appendix in Homotopy quantum field theory by Turaev*, (2010)

[35] Alexis Virelizier, "Graded Quantum Groups and Quasitriangular Hopf Group-Coalgebras", *Communications in Algebra*, vol.33, pp.3029-3050, (2005)

[36] R Costa de Almeida and J. P. Ibieta-Jimenez and J. Lorca Espiro and P. Teotonio-Sobrinho, "Topological Order from a Cohomological and Higher Gauge Theory perspective", arXiv:1711.04186, (2017)

[37] J. P. Ibieta-Jimenez and L. N. Queiroz Xavier and M. Petrucci and P. Teotonio-Sobrinho, "Fracton-like phases from subsystem symmetries", *Phys. Rev. B*, vol.102, pp.045104, arXiv: cond-mat.str-el/1908.07601, (2020)

[38] Boye Buyens and Jutho Haegeman and Frank Verstraete and Karel Van Acoleyen, "Tensor networks for gauge field theories", *Proceedings, 33rd International Symposium on Lattice Field Theory (Lattice 2015): Kobe, Japan, July 14-18*, arXiv: hep-lat/1511.04288, (2016)

[39] Román Orús, "A practical introduction to tensor networks: Matrix product

states and projected entangled pair states", *Annals of Physics*, vol.349, pp.117-158, (2014)

[40] Louis Crane and Louis H. Kauffman and David N. Yetter, "State-Sum Invariants of 4-Manifolds I", *Journal of Knot Theory and Its Ramifications*, vol.6, arXiv: hep-th/9409167, (1994)

[41] Edwin E. Moise, "Affine Structures in 3-Manifolds: V. The Triangulation Theorem and Hauptvermutung", *The Annals of Mathematics*, vol.56, pp.96, (1952)

[42] Edwin E. Moise, "Geometric topology in dimensions 2 and 3", *Springer-Verlag*, (1977)

[43] Tibor Radó, "Über den Begriff der Riemannschen Fläche", *Acta Szeged*, pp.101-121, (1925)

[44] A. Hatcher, "Algebraic Topology ", *Cambridge University Press*, (2002)

[45] Sorin Dascalescu and Constantin Nastasescu and Serban Raianu, "Hopf algebras. An introduction", *Dekker*, (2001)

[46] R.G. Underwood, "An Introduction to Hopf Algebras", *Springer*, (2011)

[47] Oliver Buerschaper and Martin Mombelli and Matthias Christandl and Miguel Aguado, "A hierarchy of topological tensor network states", *Journal of Mathematical Physics*, vol.54, (2010)

[48] M. D. Gould, "Quantum double finite group algebras and their representations", *Bulletin of the Australian Mathematical Society*, vol.48, pp.275-301, (1993)

[49] Louis Kauffman and David Radford, "On Two Proofs for the Existence and Uniqueness of Integrals for Finite-Dimensional Hopf Algebras", *Contemp. Math.*, vol.267, (1999)

[50] J. P. Ibieta-Jimenez and M. Petrucci and L. N. Queiroz Xavier and P. Teotonio-Sobrinho, " Topological Entanglement Entropy in d-dimensions for Abelian Higher Gauge Theories", *J. High Energ. Phys.*, vol.167, arXiv: cond-mat.str-el/1907.01608, (2020)

[51] Alexei Kitaev and John Preskill, "Topological entanglement entropy", *Physical Review Letters*, pp.4-7, vol.96, arXiv: hep-th/0510092, (2006)